From the Department of Molecular Medicine and Surgery
Karolinska Institutet, Stockholm, Sweden

Avidity-guided Radionuclide Therapy for Thyroid Cancer

Joachim Nilsson

Karolinska Institutet

Stockholm 2022

Cover image: Grupp VI, nr 9. Evolutionen, Hilma af Klint, 1908
© Stiftelsen Hilma av Klints Verk

Previously published papers were reproduced under the Creative Commons Attribution 4.0 International licence.

Published by Karolinska Institutet.
Printed by Universitetsservice US-AB, 2022
© Joachim Nilsson, 2022
ISBN 978-91-8016-681-2

Avidity-guided Radionuclide Therapy for Thyroid Cancer

Thesis for Doctoral Degree (Ph.D.)

By

Joachim Nilsson

The thesis will be defended in public at Karolinska University Hospital, Rehabsalen, Eugeniavägen 27, Solna, 09:00 on the 30th of September, 2022

Principal Supervisor:
Associate Professor Catharina Ihre Lundgren
Karolinska Institutet
Department of Molecular Medicine and Surgery

Co-supervisors:
Jonathan Siikanen, PhD
Karolinska Institutet
Department of Oncology-Pathology

Christel Hedman, PhD
Karolinska Institutet
Department of Molecular Medicine and Surgery

Per Grybäck, PhD
Karolinska Institutet
Department of Molecular Medicine and Surgery

Opponent:
Professor Frederik A. Verburg
Erasmus Medical Centre
Department of Radiology and Nuclear Medicine

Examination Board:
Professor Eva Forssell Aronsson
University of Gothenburg
Department of Radiation Physics

Associate Professor Robert Bränström
Karolinska Institutet
Department of Molecular Medicine and Surgery

Associate Professor Mikael Lantz
University of Lund
Department of Clinical Sciences

"To see what is in front of one’s nose needs a constant struggle."

George Orwell

Popular Science Summary

Over a lifetime, thyroid cancer is found in about 1% of people, usually first appearing as a lump on the neck. While it is rare for patients to die from thyroid cancer, some patients develop life-threatening metastases long after the discovery of their tumour. Finding such metastases can require long follow-up, and the fact that life-threatening thyroid cancer is rare requires adaptation of the treatment to the risk for each individual patient.

Thyroid cancer is usually treated by removing the thyroid gland surgically. In cases of large tumours of the most common type of thyroid cancer, nearby lymph nodes are also removed. After the operation, patients are often treated with radioactive iodine. This is a targetted radiation treatment for both normal thyroid cells and thyroid cancer cells. It exploits the fact that thyroid cells are the only place in the body where iodine is concentrated in large amounts. The concentration of iodine depends on a biochemical machinery that pumps iodine from the blood stream. In the thyroid, iodine is transported into storage pools called follicles, where it is used as a chemical component in thyroid hormones.

Radioactive iodine treatment can effectively kill thyroid cancer cells if they are iodine avid, that is, if they still transport and concentrate iodine somewhat like normal thyroid cells. However, the cellular machinery in thyroid cancer cells is more focussed on survival and growth, and less on the finely tuned hormone and iodine balance of normal cells. This causes radioiodine treatment to be much less effective in some tumours. Why some tumours behave this way is not yet fully understood, but may be investigated with microscopic and genetic analysis of the tissue. Since the primary tumour is almost always removed with surgery, this inner cellular machinery of the removed tumour can be studied and its results used to guide the next treatment.

The research in this thesis studied iodine avidity in a new way, by measuring iodine content in tumours that were surgically removed. The measurements add new detailed information on iodine avidity and its relation to other factors. Some of those microscopic and genetic factors have previously been linked to iodine avidity by other researchers, while others were reported for the first time. Previous links have only been suggested by imaging studies of metastases still present in the body,

while the tissue samples collected in this thesis enabled study of both avidity and microscopic factors in the same tumour tissue. This work also aimed to suggest uses for that information, in order to better inform which treatment is best for the individual patient.

The results show that the presence of thyroglobulin, a thyroid-related protein, in tumour tissue is a strong sign that any metastases of that tumour are iodine-avid. It was also shown that a measure of the rate of division of tumour cells, Ki-67 index, was closely connected to the degree of iodine avidity. Both of these measures were much better signs of iodine avidity than the size of the original tumour, a measure which is often used today to guide treatment. If the tumour cell walls had detectable levels of the protein responsible for pumping iodine into the cells, NIS, the tumour was highly iodine-avid. However, even tumours without NIS in the cellular walls were found to be able to accumulate iodine.

Further, genetic profiling of tumour tissue was found to be useful in separating iodine-avid tumours from others. The results showed that mutations in a gene called *BRAF* (genes are written in italics) and mutations in a segment that controls the reading of a gene called *TERT* signified tumour tissue with low iodine avidity. This effect was more pronounced if the mutations were detected in lymph node metastases.

The results also showed that if the initial tumour in the thyroid is iodine-avid, it is very likely that any metastases from that tumour will also be avid - a good sign for those patients.

Lastly, calculations in this work showed that very small tumours, below 2 mm in diameter, can be more difficult to treat with radioactive iodine, due to the radiation escaping from the tumour. If the surroundings make the tumour grow in a compressed way, this may also diminish the effect of the treatment.

In conclusion, this work has shown that intelligent use of more detailed analysis of tumour tissue can help fine-tune the treatment, enabling *avidity-guided* treatment of thyroid cancer.

Abstract

The treatment of differentiated thyroid cancer has three main modalities: surgery, hormone suppression and radioiodine therapy. Effective radioiodine therapy requires cancer cells to be iodine avid, i.e. exhibit relatively functional iodine transport and retention. The iodine avidity is often unknown at the time of initial treatment and the range has not been quantified in detail.

To find the true range of iodine avidity in papillary and poorly differentiated thyroid cancer, a unique prospective study was designed. Tissue samples were collected directly after surgery in order to estimate iodine concentrations following a pre-operative injection of radioactive iodine. Clinical, molecular and genetic parameters were studied in relation to the iodine avidity observed in the tissue samples. Furthermore, computer modelling using Monte Carlo simulations was performed to establish the impact of target geometry and size.

The results show that iodine avidity was correlated to the proportion of tumour cells that express thyroglobulin (correlation coefficient r = 0.50) and the tumoural Ki-67 index (r = -0.49). Avidity was found to be seven-fold higher in favourable histological subtypes of PTC. High patient age was also found significantly correlated with low iodine avidity (r = -0.35). No strong connection between avidity and tumour size or TNM staging was found, despite TNM being the current main guiding parameter in radioiodine treatment strategy selection. Furthermore, links between low iodine avidity and mutations in *BRAF* (18-fold lower avidity) and the *TERT* promoter (10-fold lower avidity) were found, if mutations were observed in lymph node metastases. Expression of the iodine-transporter NIS was found to indicate high iodine avidity (40-fold higher avidity), but only when localised at the plasma membrane, which appears to be rare in thyroid cancer cells.

Follow-up studies showed that the iodine avidity estimated in primary tumours and lymph node metastases at initial surgery predicted uptake in persistent metastases well (both regional and distant metastases). This confirms that knowledge gathered from the initial surgical specimens can reliably help guide treatment targetting subsequent metastases.

The Monte Carlo simulations showed that for small targets, both size and shape of the target tissue has an impact on radioiodine therapy, with up to a three-fold lower effectiveness for compressed targets at the size-threshold for micrometastases. However, the effect was dwarfed by the much larger variation in iodine avidity observed in the prospective material.

Data from this work has strengthened the link between iodine avidity and many readily available parameters, that can guide treatment. A shift to avidity-guided therapy for high-risk patients is proposed to better adapt the radioiodine strategy to expected effect than was previously possible.

List of Scientific Papers

I. **Nilsson, J.N.**; Siikanen, J; Ihre Lundgren, C; Ardenfors, O.
Dosimetric Dependences on Target Geometry and Size in Radioiodine Therapy for Differentiated Thyroid Cancer
Physica Medica **2022**, *99*, 68–72,
doi:10.1016/j.ejmp.2022.05.010

II. **Nilsson, J.N.**; Siikanen, J.; Hedman, C.; Juhlin, C.C.; Ihre Lundgren, C.
Pre-Therapeutic Measurements of Iodine Avidity in Papillary and Poorly Differentiated Thyroid Cancer Reveal Associations with Thyroglobulin Expression, Histological Variants and Ki-67 Index
Cancers (Basel) **2021**, *13*, 3627,
doi:10.3390/cancers13143627

III. **Nilsson, J.N.**; Siikanen, J.; Jatta, K; Saini, R; Hedman, C.; Ihre Lundgren, C.; Juhlin, C.C.
BRAF and *TERT* Promoter Mutations Pinpoint Thyroid Cancers with Reduced Iodine Avidity Quantified by *ex vivo* Measurements

Manuscript

IV. **Nilsson, J.N.**; Grybäck, P.; Juhlin, C.C.; Hedman, C.; Ihre Lundgren, C.
Primary Tumour Iodine Avidity Predicts Uptake in Metastatic Disease in Papillary and Poorly Differentiated Thyroid Cancer

Manuscript

Contents

List of Abbreviations

Abbreviation	Meaning
AIC	Akaike information criterion
BRAF	B rapidly accelerated fibroblastoma
ddPCR	Digital droplet polymerase chain reaction
DHGTC	Differentiated high-grade thyroid cancer
FDG	Flourodeoxyglucose
FNAC	Fine needle aspiration cytology
FOXE1	Forkhead box E1
FTC	Follicular thyroid cancer
HHEX	Hematopoietically-expressed homeobox
hTERT	Human telomerase reverse transcriptase
MACIS	Metastasis, (patient) age, completeness of resection, (local) invasion and (tumour) size
MAPK	Mitogen activated protein kinase
NKX2-1	NK2 Homeobox 1
NIS	Sodium-iodide (Na^+/I^-) symporter
PAX8	Paired box 8
PCR	Polymerase chain reaction
PDTC	Poorly differentiated thyroid cancer
PET	Positron emission tomography
PPARγ	Peroxisome proliferator-activated receptor γ
PTC	Papillary thyroid cancer
RAS	Rat sarcoma virus
RET	Rearranged during transfection
Tg	Thyroglobulin
TNM	Tumour, (lymph) node and metastasis
TPO	Thyroid peroxidase
TSH	Thyroid stimulating hormone, thyrotropin
TSHR	Thyroid stimulating hormone receptor
SPECT	Single photon emission computed tomography

List of Units

Symbol	Name [SI units]	Quantity
Bq	Becquerel [s^{-1}]	Radioactivity
Ci	Curie [$3.7 \cdot 10^{10}$ s^{-1}]	Radioactivity
eV	Electron volt [$1.602 \cdot 10^{-19}$ J]	Energy
Gy	Gray [$J \cdot kg^{-1}$]	Absorbed dose
Sv	Sievert [$J \cdot kg^{-1}$]	Effective dose
man·Sv	Man-sievert [$J \cdot kg^{-1}$]	Collective dose

1 Prologue

Do we need another PhD thesis? On thyroid cancer, of which almost no one dies? About a treatment that has been around for almost a century?

These questions are not lost upon this PhD student.

Obviously, if you are in the field of therapeutic nuclear medicine, thyroid cancer is near at hand. But I normally find myself uncomfortable in areas crowded with footprints left by those of greater ability. Despite this, I realised that I was gravitating towards an impressive multidisciplinary collaboration around thyroid cancer at our institution. Treatment decisions were based on rational arguments and thorough scientific knowledge in surgery and pathology. It seemed to me that there was a void in the nuclear medicine and physics part of it. Scientific guidance on how to best think about radionuclide therapy was lacking, now that it had been terribly outpaced by advances in molecular medicine. Especially for patients that were succumbing to their disease.

There was also a gaping contradiction. My undergraduate studies taught me how to do precise theoretical calculations of absorbed doses that would guide the rational treatment of patients. Then the clinical reality, where robust and simple methods are required for broad adoption and high standards of care. Dosimetry was nowhere to be found.

I thought I might have found something clever there, hiding right under my nose. Irresistible. I began, thinking, "This will be *easy*".

2 Introduction

Radioactive substances can deliver precise localised radiation therapy by means of charged particle emission. The study of such treatments was sparked in the 1930's by fundamental insights into nuclear physics, the construction of the first cyclotrons, and the fusion of physics and medicine. It was discovered that by pairing a radioactive substance to a specific physiological uptake mechanism in the body, systemic yet targetted treatment could be provided. Such use of radioactive iodine in treating thyroid cancer was first described in 1942, when Albert Keston et al. observed accumulation of radioactivity in a bone metastasis of thyroid cancer, using mainly ^{130}I provided by physicists Ernest Lawrence and Robley Evans [1]. Successful treatment of metastatic thyroid cancer was first reported in 1946 by Seidlin et al., using both ^{130}I and ^{131}I, with lasting clinical improvement and pain-relief in bone metastases [2].

2.1 Thyroid Cancer

Thyroid cancer arises from cells in the thyroid gland. In the body, hormones produced by differentiated thyroid follicular cells are essential to regulation of metabolism, heart rate and fetal development. Cancers arising in these cells are often categorised into the differentiated types of papillary (PTC) and follicular thyroid cancer (FTC). Tumours in these categories, despite their names, all originate as follicular cells. The respective type is characterised by histological growth patterns, and each type can be further divided into subtypes [3]. Overall, patients with differentiated thyroid cancer have excellent prognosis [4,5]. The outcome is dependent on tumour stage, degree of differentiation, type (PTC or FTC), patient age and sex, and surgical completeness [6,7]. PTC has characteristic growth patterns in papillary structures, micro-calcifications, and nuclear features including enlargement, pseudo-inclusions, grooves and chromatin clearing, displayed in Figure 1. FTC typically grows in an encapsulated structure, and malignant growth is defined as penetration through the capsule, evident only upon histological examination. The clinical management of PTC and FTC are discussed in detail in national and international guidelines [8–11].

The histological subtypes of PTC have been studied in terms of aggressiveness and prognosis [12–15]. More aggressive subtypes have been identified, including tall cell subtype, insular subtype, hobnail subtype and diffuse sclerosing subtype, all named for their histological characteristics [16]. However, to the present date, guidelines do not recommended different management on the basis of histological subtype of PTC. While patients with PTC enjoy a favourable prognosis, the risk of recurrence is relatively high, reported between 10 and 30% [17–19]. It has been argued that a large proportion of what has been reported as recurrent disease in PTC may be persistent disease, detectable on ultrasonic examination or serum thyroglobulin (Tg) assays throughout [20]. Perhaps somewhat surprisingly, the discovery of lymph node metastases at disease presentation is not clearly associated with worse overall survival [21]. Recurrent disease can manifest many years after initial surgical and radioiodine treatments, suggesting need for long follow-up to maintain good disease control [22]. PTC commonly present as multiple foci in the thyroid gland, even in both lobes; multi-focal growth does not appear to translate to a worse prognosis [23].

Distant metastases from PTC are uncommon, reported in a few percent of patients both at disease presentation and during follow-up [24,25]. While rare, metastases are most often seen in lungs, more rarely in bone, and only occasionally in other sites, as illustrated in Figure 2. These cases of distant metastases constitute the majority of disease-related deaths in the PTC population.

Other types of thyroid cancer include oncocytic thyroid cancer, which has a slightly worse prognosis than PTC and FTC [26]. Another type called differentiated high-grade thyroid cancer (DHGTC), introduced in the 2022 World Health Organisation classification, comprises tumours that have high levels of mitoses and necrosis, but still retain a differentiated grown pattern [3,27]. They behave more aggressively than PTC and FTC. However, some thyroid cancers undergo further molecular and genetic transformation from differentiated types and shed many thyroid-specific characteristics. They are then classified as poorly differentiated thyroid cancer or as the even further de-differentiated anaplastic thyroid cancer. The prognosis for poorly differentiated thyroid cancer (PDTC) is worse than for the differentiated types, but the disease can still respond to radioiodine therapy [28,29].

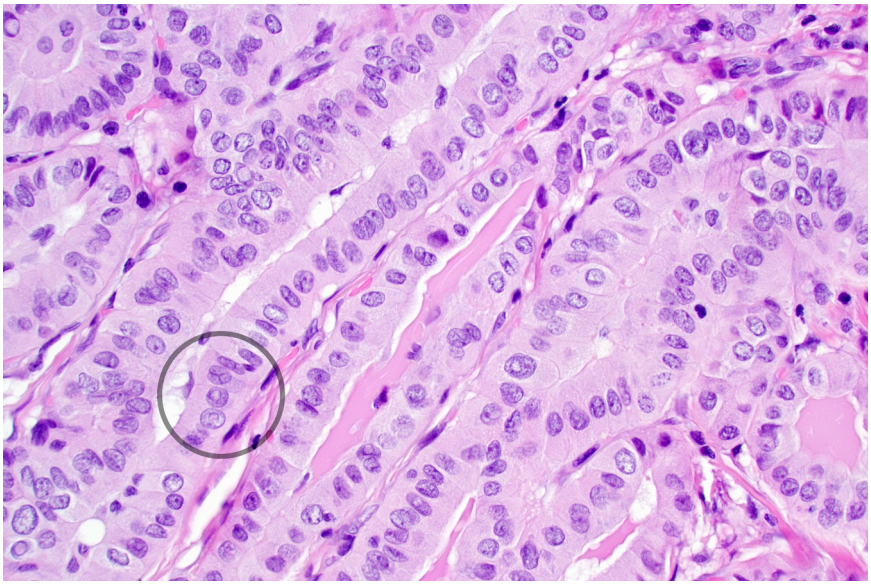

Figure 1: Histological cross-section of PTC, stained with hematoxylin and eosin. The darker purple (hematoxylin) makes cell nuclei easily visible, while the lighter pink (eosin) displays the extent of the cytoplasm. The crowded growth pattern in papillae is typical of PTC, as opposed to follicular structures in healthy thyroid tissue. The highlighted area has examples of enlarged nuclei, nuclear grooves and pseudo-inclusions. Furthermore, predominant growth in elongated cellular arrangement seen here (height > 3·width) is the criterion for diagnosis of tall cell subtype PTC.

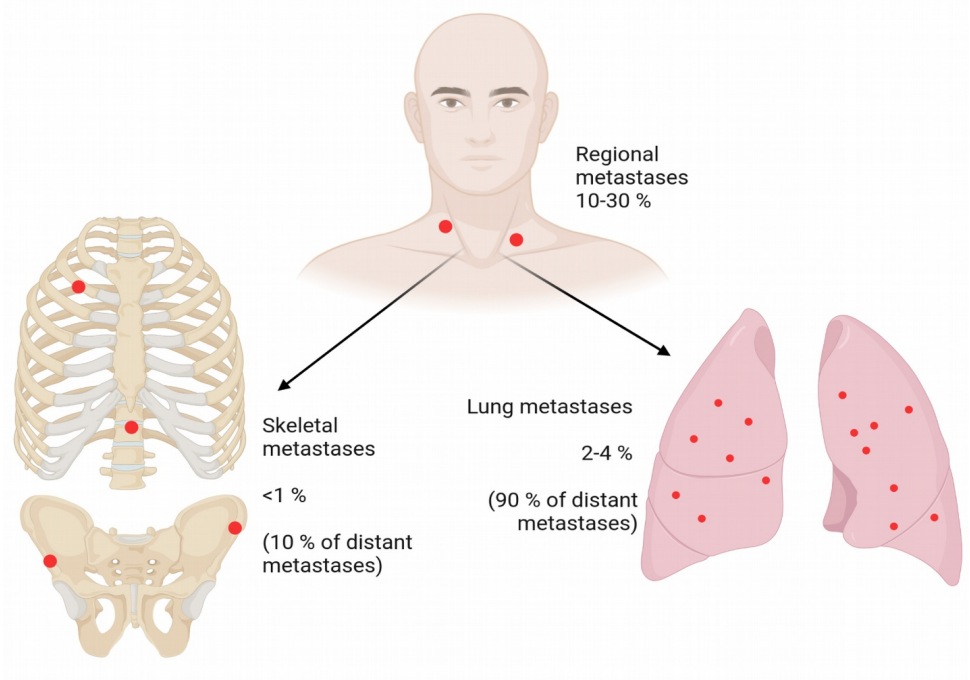

Figure 2: Common metastatic sites in PTC. The frequencies are approximate for the whole patient population.

Anaplastic thyroid cancer (ATC) occurs very rarely, in only 1-2% of all thyroid cancers, but is one of the most aggressive and deadly of all cancers, with a median survival of only a few months [30]. These tumours have lost any resemblance of functional iodine transport and cannot be treated with radioiodine [31]. Combined, PDTC and ATC account for more than 50% of all deaths from thyroid cancer [29,32].

Medullary thyroid cancer arises from C-cells in the thyroid gland and behaves very differently from cancers that originate in follicular cells. They are not treated with radioiodine and are similarly to anaplastic thyroid cancer not discussed further in this thesis.

In the follow-up and surveillance of thyroid cancer, measurements of Tg in serum is central [33]. It is not useful prior to surgical and radioiodine treatment because the healthy thyroid tissue present also produces Tg [34]. After completed initial treatment, however, the presence of Tg in blood is a strong indicator of persistent disease, and is linked to higher risk of recurrence [35,36]. If Tg antibodies are present in blood, the assessment of tumour presence by use of serum concentrations of Tg may be incorrect. These antibodies are relatively common in patients with thyroid cancer, present in approximately 20% of patients [37]. Still, in absence of serum Tg, the levels and trends of Tg antibodies can be a useful proxy for tumour burden [38,39].

Ultrasonography is used both to identify the primary tumour and to map any cervical lymph node metastases prior to surgery [40]. It also has an important role in detecting recurrent and persistent disease after completed initial therapy [41]. Ultrasonography-guided fine needle aspiration cytology (FNAC) can be used as well, to confirm any suspicious findings [42].

Post-therapeutic imaging using the therapeutic activity of ^{131}I is useful in the localisation of regional lymph node metastases, and enables assessment of disease extent and monitoring of distant metastatic disease [43]. The use of SPECT/CT in addition to whole body scintigraphy has been shown to increase the accuracy of diagnosis and enables the detection of non-iodine-avid lesions in lungs [44,45]. It also enables post-therapeutic dosimetry to be performed [46,47]. For diagnostic scanning with the purpose of risk-evaluation and metastasis localisation, SPECT/CT using ^{123}I is another option [48]. ^{123}I has a shorter half-life and more beneficial emissions for purely diagnostic purposes. For both diagnostic and dosimetric

imaging, ^{124}I is another relevant isotope, as its positron emissions enables superior imaging with PET/CT [49]. PET/CT imaging using [^{18}F]-FDG is a useful diagnostic modality in case of elevated serum Tg or suspicious anatomical lesions that do not accumulate iodine [50].

2.2 Thyroid Cancer Genetics

Several landmark genetic discoveries have provided a more precise understanding of the mechanisms that enable, and may disable, successful radionuclide therapy in thyroid cancer. The central molecule for transport of iodine into the thyroid follicular cells, the sodium-iodide symporter (NIS) protein, was characterised and cloned in 1996 [51]. Research on NIS has established its molecular structure and function, the regulation of its cellular location and many mutations that can affect its function [52]. It is also known that the *PAX8, NKX2-1, FOXE1* and *HHEX* genes all encode proteins that function as thyroid specific transcription factors [53]. Expression of these transcription factors are essential to the formation of thyroid follicles and the transcription of genes for central thyroid-related molecules such as TPO, Tg, NIS and TSHR.

Extensive genetic profiling of papillary thyroid cancer has shown several mutations to be predominant [54,55]. The *BRAF* gene encodes the protein B-raf, which is a central signalling protein in the MAPK pathway. This pathway controls cellular differentiation and proliferation. The *BRAF* V600E mutation, common in PTC, causes the B-raf protein to be constitutively activated, thereby causing abnormal proliferation and de-differentiation from the thyroid phenotype [56,57]. There are some indications that iodine avidity is lower in tumours with the *BRAF* V600E mutation and some studies have suggested the mutation predicts worse clinical outcome, while others have found no difference in outcome [58–61].

Another important gene in thyroid cancer progression is *TERT,* whose transcription results in telomerase activity that in turn enables continuous cellular proliferation. It has been shown that mutations in the promoter region of the *TERT* gene (C228T and C250T) are associated with worse clinical outcome [62]. Furthermore, the presence of these mutations is a predictor of poor iodine avidity, and they may even have a negative synergistic effect on avidity, as well as prognosis, when present along with *BRAF* V600E mutations [63,64]. Genetic aberrations of *TERT* have diagnostic impact in thyroid cancer as well. Mutations, copy number gain and

promoter hyper-methylation have been shown to be telling of malignant potential in follicular tumours [65].

Other impactful genetic aberrations in thyroid cancer include *RET/PTC* and *PAX8/PPARγ* rearrangements, and *RAS* mutations [66]. *RET/PTC* rearrangements cause chimeric versions of *RET* and uncontrolled activation of MAPK, among other pathways, promoting proliferation and inhibiting apoptosis [67]. Tumours with *RET/PTC* rearrangements seem to not down-regulate *NIS* or *TPO* expression, nor drive de-differentiation, as much as *BRAF* V600E mutations do [68]. Interestingly, the RET/PTC rearrangement appears to be more common in radiation induced thyroid cancers, studied in detail following the fallout near the Chernobyl nuclear reactors [69]. *PAX8/PPARγ* is common in FTC, where fusion of a part of *PAX8* with *PPARγ* causes high levels of their chimeric protein that seem to drive malignant transformation [70]. *RAS* mutations can similarly to *BRAF* alter signalling in the *MAPK* pathway, that may also drive malignant transformation [71]. *RAS* and *BRAF* alterations are rarely seen in the same tumours, indicating that they are independent driver mutations in thyroid cancer [72]. The distinction between *RAS*-like and *BRAF*-like PTC has been suggested to be useful, considering the tendency for worse prognosis and lower iodine avidity in *BRAF*-like tumours [54]. *TERT* promoter mutations and *TP53* mutations are rare in differentiated thyroid cancer (10% and <3% respectively). In the more aggressive PDTC and ATC, they are much more common, and *TP53* mutations can be found in up to 70% of ATC [73].

2.3 Radioiodine Therapy

Radionuclide treatment with iodine isotopes, often called radioiodine therapy, are most commonly given orally in fixed amounts of ^{131}I, usually in multiples of 37 MBq (1 mCi). While the knowledge of thyroid cancer has advanced considerably during the eight decades since its first use, radioiodine therapy remains standard treatment for patients with thyroid cancer. It improves survival and disease control in high-risk patients, and enables efficient follow-up for low-risk patients [74]. Radioiodine therapy has three distinctly different aims:

1. The ablation of thyroid remnant tissue in the thyroid bed following a total thyroidectomy.
2. Adjuvant treatment of microscopic disease in patients with larger tumours or lymph node metastases at disease presentation.

3. Systemic treatment of distant metastases or gross residual primary tumour.

The ablation of thyroid remnants is done in order to facilitate efficient follow-up for patients of low risk of recurrence [75]. In such low-risk patients, there is no survival benefit to be gained from radioiodine therapy [76]. However, ablating all thyroid tissue allows for a blood assay of Tg in serum, along with post-therapeutic scintigraphic imaging and ultrasonic examination, to be used to succinctly conclude follow-up in many patients that are cured of their cancer. The activity levels used for thyroid remnant ablation is commonly between 1.1 and 3.7 GBq of ^{131}I, with strong evidence suggesting similar outcomes between the two activities [77]. On the basis of such results, most guidelines have lowered the activities recommended for ablation in the last decades. Studies have found that remnants requires absorbed doses between 50 and 300 Gy for successful ablation [78,79]. Furthermore, the completeness of surgery influences the success rate of radioiodine ablation [80,81].

Adjuvant treatment is given to patients after surgery of larger tumours or macroscopic lymph node metastases, with the aim of lowering the risk of recurrence. If this is of a substantial clinical benefit to patients remains under debate, but for higher disease stages and higher patient age, the adjuvant treatment with radioiodine treatment appears to be more beneficial [82–85]. Activities given in the adjuvant setting is higher than in thyroid remnant ablation; commonly 3.7 GBq and sometimes higher, with the rationale that cancer tissue in general has lower avidity than thyroid remnants.

Treatment of distant metastases and loco-regional gross disease with radioiodine rests on evidence from large study materials. Such analyses has shown that radioiodine treatment increases overall survival and disease-specific survival for patients with distant metastases and locally extensive tumours [86,87]. Persistent iodine accumulation in metastatic sites is strongly associated with better overall survival [88–90]. It is known that achieving absorbed doses to metastatic sites in excess of 40-80 Gy is associated with better treatment response [79,91,92]. Image-based lesion dosimetry is sometimes used to guide treatment for metastatic disease [93–96]. However, many centres give a standard activity of 7.4 GBq, which is then repeated if required.

The treatment effect of ^{131}I is achieved by means of β^- emission and subsequent energy deposition in the target tissue. ^{131}I decays into stable ^{131}Xe with a half-life of 8 days, as illustrated by the decay scheme in Figure 3. The predominant β^- emission of

^{131}I has a yield of 89% and mean kinetic energy of 192 keV, corresponding to a mean range in water of approximately 0.4 mm [97]. This is similar to the size of an average human thyroid follicle and the distance across at least a dozen thyroid follicular cells. As is shown in Figure 4, these geometric relations allows for irradiation of both cells neighbouring any intra-cellular concentration of ^{131}I as well as from colloid to nearby cellular arrangements. While colloid is present in much smaller amounts in thyroid cancer than in normal thyroid tissue, the particle range allows irradiation and treatment of nearby structures even if not all cells accumulate iodine. It also means that in lesions below a certain size, many of the β^- particles will deposit their energy outside the target, decreasing the effectiveness of treatment.

Production of ^{131}I is usually done through neutron irradiation of natural tellurium, or by nuclear fission of uranium, through the nuclear reactions:

$$^{130}Te(n,\gamma)^{131}Te \xrightarrow[\beta^-]{25min} {}^{131}I$$

$$^{130}Te(n,\gamma)^{131m}Te \xrightarrow[\beta^-]{30h} {}^{131}I$$

$$^{235}U(n,f)^{131}I + {}^{101}Y + 4n$$

Both these production pathways are possible, but the ^{131}Te method is more efficient than ^{235}U in terms of reaction yields [98]. The respective yields are 96% for the ^{130}Te pathway (the nuclear cross-section and production yield for ^{131}Te is much higher than for ^{131m}Te), while ^{131}I is only produced in approximately 3% of ^{235}U fission reactions [99]. The fission reaction is an example of one out of many reactions that can produce ^{131}I from uranium.

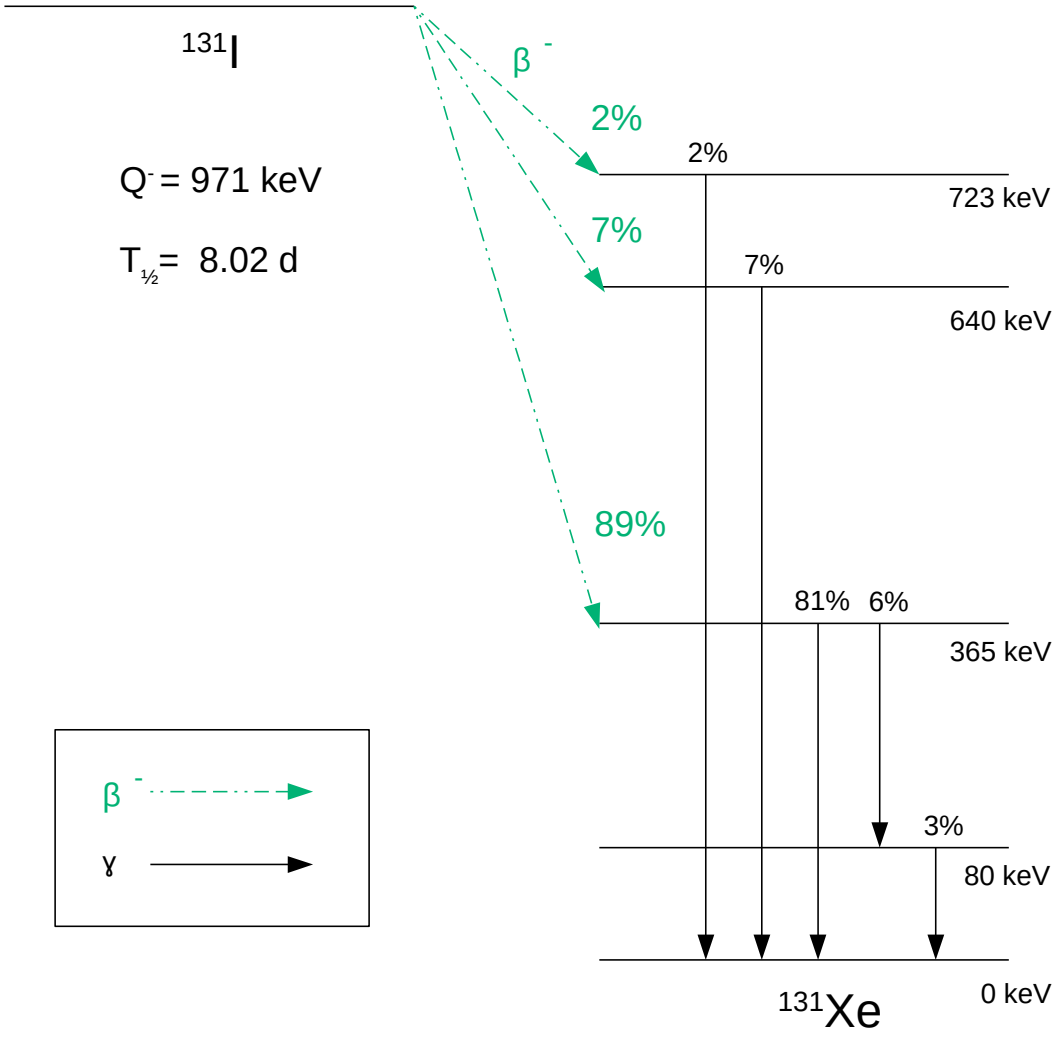

Figure 3: Decay scheme for ^{131}I to the ground state of ^{131}Xe. Only β^- and γ transitions and associated energy states with yields greater than 1% are shown. The 89% β^- emission with maximum energy 606 keV (mean 192 keV) is the dominant therapeutic emission and the subsequent γ emission with 365 keV of 81% yield is most commonly used for imaging of ^{131}I. Yields are shown as per decay.

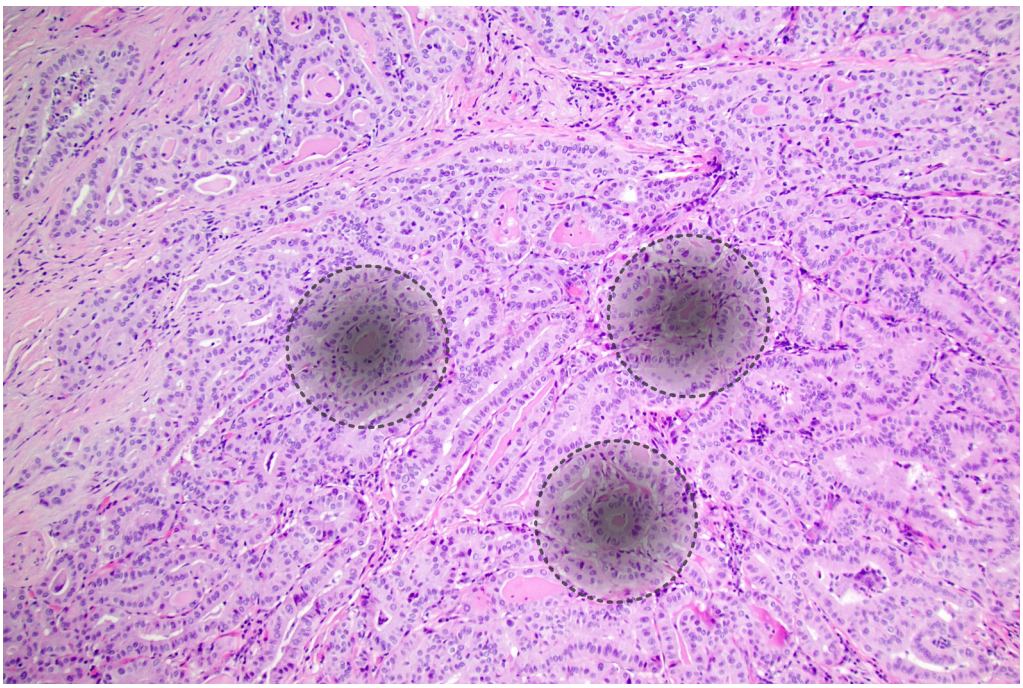

Figure 4: Illustration of energy deposition from ^{131}I in thyroid cancer tissue, stained with hematoxylin and eosin. The circles (dashed grey line) are intended to show the enclosure of the mean β^- particle range (0.4 mm) and average energy deposition (shaded grey) from three separate emission points. The particle range means that adjacent structures will be irradiated by radioactive iodine accumulated in any one cell.

There is no generally accepted limit on the amount of activity that can be administered in a single treatment. It is considered good practice to keep absorbed doses to blood below 2 Gy per treatment [100]. This threshold can be transgressed if administering high empirical activities in elderly patients with impaired renal function [101]. Higher thresholds than 2 Gy have been studied. Results from treatments using administered activities in excess of 25 GBq have been reported, in a treatment setting where 3 Gy to bone marrow was the guiding dosimetric target [102]. The activities were reported as safe with a predictable thrombocytopenia and leukopenia nadir at 3 to 5 weeks post administration and no bone marrow failure. Such an aggressive approach may be warranted in patients with life-threatening distant metastases that retain some iodine avidity.

There are however side-effects associated with radioiodine therapy that can outweigh the benefit patients receive. Sialadenitis and xerostomia are common when high cumulative administered activities are given, which is caused by NIS-mediated radioiodine uptake in salivary glands [103]. For female patients, radioiodine treatments can cause transient amenorrhoea lasting up to one year, but

no general effect on fertility has been observed [104]. The potential of inducing secondary primary cancers has been studied thoroughly. This is of concern since a single radioiodine treatment can result in effective doses of approximately 200-1300 mSv, depending on administered activity. Increased risk of developing some cancers have been reported after diagnostic administrations or treatment of hyperthyroidism, but no overall increased risk of cancer was found [105,106]. For treatment of thyroid cancer, studies have similarly reported increased risk of some cancers, such as sarcomas and lymphomas, but not for cancer overall [107]. In patients with thyroid cancer, the risk of other malignancies is already higher than in a healthy control population, but the risk does appear to be increased by high cumulative activities of radioiodine [108,109]. It is also known that exposure to ^{131}I during childhood, extensively studied in the Chernobyl fallout area, is clearly linked in an increased risk for thyroid cancer with a dose-response correlation [110]. Considering the generally accepted linear no-threshold model of stochastic effects of radiation, no radioiodine treatment can be considered completely harmless, despite mild side effects in most patients.

2.4 Iodine Avidity

In this work, the concept of iodine avidity is defined as the ability of tissue to concentrate and retain iodine. As noted in the previous sections, iodine avidity is a crucial property of cancer tissue for effective treatment with radioiodine. The exceptional iodine avidity in thyroid tissue has been known for a century [111]. Mathematically, the concept can be described by the integral of the concentration-time curve in the tissue of interest. It is this definition of iodine avidity that has been the object of study in this thesis, since it is directly related to the absorbed dose per administered activity [Gy/GBq] in radioiodine therapy. In previously published research, thyroid cancer iodine avidity has mostly been evaluated by post-therapeutic scintigraphic imaging. Such studies have used the image signal intensity in a lesion at a single time-point as a proxy for iodine avidity. While multiple imaging time points are required to assess the iodine kinetics of the individual patient more closely, it is more expensive and can be cumbersome for patients, in part explaining its low clinical use.

Well-functioning transport and incorporation of iodine into thyroid cells relies on several factors. In order to be able to pump iodine against a negative concentration gradient, the NIS protein transports one I^- anion together with two Na^+ cations. This

is possible due to a lower concentration of sodium inside follicular cells [112]. For the iodine transport to be effective, NIS must be located on the plasma membrane of the follicular cell. Both the expression and plasma membrane translocation of NIS is dependent on thyroid stimulating hormone (TSH) simulation [113].

This dependence is exploited in radioiodine therapy, where the TSH level prior to treatment is elevated. The elevation is achieved either by withdrawing thyroid hormone supplement for several weeks, stimulating endogenous TSH production, or by recombinant human TSH injections [114]. Both these methods can produce adequate iodine avidity for treatment and imaging, but exogenous TSH simulation produces less side effects [115]. The methods affect the kinetics of iodine differently; hormone withdrawal appears to reduce renal function, which can cause higher whole body radiation doses during radioiodine treatment [116,117]. If these differences in kinetics have clinical implications is still under debate. Thyroid hormone withdrawal may have advantages in treatment of distant metastases [118,119]. However, no differences in outcome has been observed for ablation and adjuvant therapy [120–124].

The plasma level of iodine itself can inhibit uptake of iodine in thyroid tissue, known as the Wolff-Chaikoff effect [125]. Since plasma concentration of iodine is highly dependent on dietary intake, recommending patients to shift to a low-iodine diet can cause a measurable decrease in plasma iodine levels [126]. In a literature review, two out of six studies suggested that a pre-therapeutic low-iodine diet has a modest improved effect on thyroid remnant ablation success rate [127,128]. The effect of low-iodine diet has only been studied with regards to thyroid remnant ablation. Most guidelines recommend some kind of limit on dietary iodine in preparation for radioiodine therapy, regardless of treatment aim.

Iodinated contrast agents used in radiology has a well established effect of transiently lowering the iodine avidity of thyroid tissue. This phenomenon has been presumed to be caused by a component of free iodine in the contrast agent inducing a Wolff-Chaikoff effect, and most guidelines recommend a delay of radioiodine therapy of at least four weeks after contrast agent administration. This appears a sufficient time period to normalise urinary iodine concentrations [129–131]. Interestingly, there is recent research suggesting that the mechanism may in part be explained by the contrast agent itself (i.e. not only free iodine) dysregulating NIS expression [132,133].

Exposure of both normal and cancerous thyroid tissue to ionising radiation can lower iodine avidity temporarily. This phenomenon has been termed thyroid stunning and has been widely studied and debated [134]. It has been observed clinically in the case of pre-therapeutic imaging using presumably sub-therapeutic activities of ^{131}I [135]. The effect seems to depend on absorbed dose and radionuclide, and may be mediated through a loss of *NIS* mRNA expression [136]. However, it has been argued that the stunning observed is in fact a partial therapeutic effect of ^{131}I, where one would expect a lower uptake of iodine after cell killing in a lesion. This may be supported by data showing that a therapeutic administration of radioiodine itself changes the kinetics of cancer tissue during irradiation [137].

A major limitation on the effectiveness of radioiodine therapy is the loss of iodine avidity in many distant metastases. It has been reported that approximately 30% of patients with distant metastases at presentation have non-avid disease [88]. Additionally, many patients eventually develop non-avid disease despite initial avidity. The therapeutic options of progressive metastatic disease that has lost iodine avidity have historically been limited, but have improved in recent decades [138]. Drugs developed to inhibit tyrosine kinases have been approved for use in patients with radioiodine-refractory metastatic disease [139,140]. These drugs can improve progression-free survival for patients, but may also cause side-effects that limit their long-term use. It is also common for tumours to develop resistance to these drugs. However, the use of drugs specifically targetting BRAF or MAPK have been shown to restore iodine avidity in many previously refractory patients [141,142]. Restoration of iodine avidity has also been reported after treatment with NTRK inhibitors, in patients with EML4-NTRK3 gene fusions [143,144]. While such fusions are rare in thyroid cancer, this suggests that multiple avenues are available to restore iodine avidity [145]. This enables a novel treatment option, where a short-term redifferentiation treatment can be given to potentiate radioiodine therapy [146–148]. The treatments seem to be able to restore avidity in 40 to 80% of radioiodine refractory patients. To date however, no survival benefit has been proven in the small studies that have been published.

3 Research Aims

Two major factors determine the absorbed dose from radionuclide therapy. The first is the absorbed dose from each decay, which depends on the atomic and nuclear properties of the radionuclide as well as the size and geometry of the target. Some aspects of this was studied in Paper I. The second is the total number of decays in the target, in thyroid cancer loosely summarised in the concept of iodine avidity; different aspects of this was studied in Papers II, III and IV.

Paper I aimed to find out the impact of target size and geometry on the absorbed dose delivered from ^{131}I.

In **Paper II**, the aim was to find and quantify correlations between tumoural iodine avidity and several clinical and histopathological parameters such as tumour size, histological subtype, Tg and Ki-67 expression, and age.

Paper III describes further studies on tumoural iodine avidity. The paper aimed to establish the quantitative impact on iodine avidity of mutations in *BRAF* and the *TERT* promoter. The extent to which NIS expression and localisation predicts iodine avidity was also explored.

In **Paper IV**, analyses of clinical progression and persistent disease in the cohort aimed to verify the clinical relevance of the findings in paper II and III.

4 Methodological Considerations

4.1 Measuring Radioactivity and Iodine Avidity

Iodine avidity in this work was estimated by a single time point measurement of the activity concentration in tissue at approximately 48 hours post injection, detailed in Figure 5. Patients were asked to follow a low-iodine diet for a week prior to intravenous injection of 5 to 10 MBq of [^{131}I]-NaI. The activity range was selected to enable accurate quantification of iodine in tissue samples, but is low enough to avoid any potential stunning of the thyroid tissue; a highly avid tissue concentrating 0.01 IA·g^{-1} (injected activity per gram tissue) would receive approximately 0.8 Gy, given an administration 10 MBq ^{131}I and an effective half life of 50 h. This was deemed acceptable considering that at least two months would pass before any radioiodine treatment, that cancer tissue would be expected to have much lower concentrations, and the low reported uptake-inhibitory effect of such absorbed doses delivered by ^{131}I. Most evidence also suggest that pre-therapeutic diagnostic scans do not change the clinical outcome in terms of recurrence or ablation success [136,149,150].

Patients underwent thyroidectomy and lymph node dissection, as indicated in the individual case. Rapid handling of surgical specimen allowed for radioactivity quantification to be performed before formalin fixation and paraffin embedding, with an estimated mean time from surgery to fixation of 3 hours.

At the pathology grossing lab, representative samples were taken of primary tumour, lymph node metastases and normal thyroid tissue, as shown in Figure 6. They were dissected by an endocrine surgical pathologist or a pathology assistant experienced with thyroid tissue handling.

There are many ways of measuring radioactivity. Ionisation in gases or excitation in scintillation crystals are the most widely used physical interactions by which to detect and quantify radiation originating from radioactive material [151].

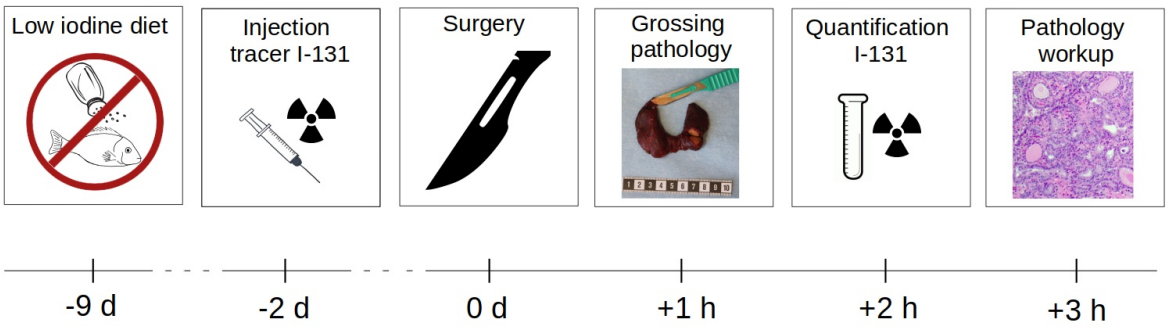

Figure 5: Schematic of preparation and handling of tissue samples in Paper II, III and IV.

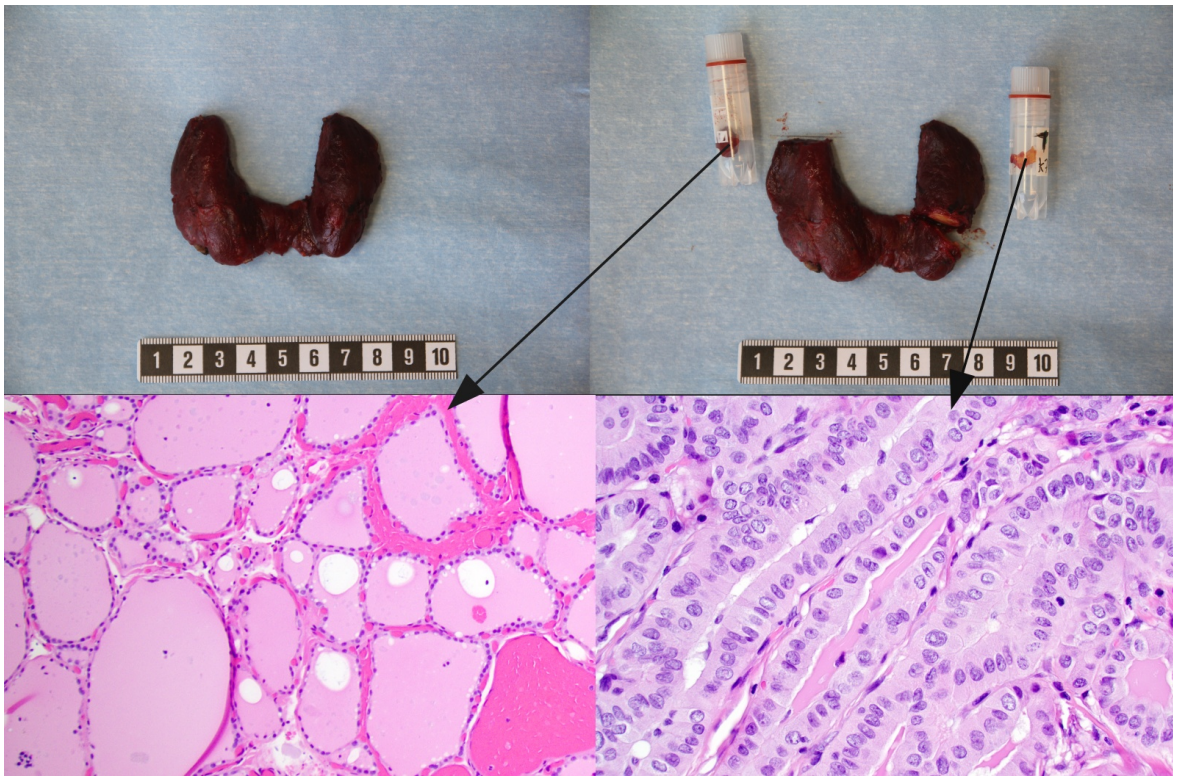

Figure 6: Tissue handling in Paper II, III and IV. (a) Fresh sample from surgery. (b) Dissection of representative tissue samples of normal thyroid, primary tumour and lymph node metastases (not shown) were performed. Histological verification of tissue representativity for (c) normal thyroid and (d) primary tumour.

In Paper II, III and IV, a scintillation well detector was used, enabling accurate quantification of sub-Bq activity levels. The detector had a sensitivity of 0.445 cps/Bq for ^{131}I, and the minimal detectable activity was determined to 0.17 Bq for the acquisition protocol used, according to the method described by Blue et al. [152].

This translates to an ability to detect normalised iodine concentrations down to $5 \cdot 10^{-6}$ IA·g^{-1} with the acquisition protocol used. Any concentrations below this level would be erroneously estimated by the detector system. This was considered an acceptable lower limit of quantification, as any such concentration levels are unlikely to be clinically significant.

The detector had a linear response for activities up to 50 kBq, where dead-time and pile-up effects became substantial. For a typical normal thyroid tissue sample of 250 mg taken in this work, this would correspond to decreased accuracy (biased towards underestimation of avidity) at normalised concentrations of 0.04 IA·g^{-1} or higher; this was considered above the range where accurate quantification of tumoural avidity was relevant in the project. Iodine concentrations were normalised to the injected activity and the mass of the tissue, IA·g^{-1}, in order to be comparable between study participants and tissue samples. All values were decay corrected to the time of surgery. All primary tumour and lymph node metastasis concentrations were adjusted for competing uptake in normal thyroid tissue, according to Equation 1:

$$C_{corr} = \frac{C_{meas}}{1 - C_{thy} \cdot m_{thy} / A_{inj}} \quad (1)$$

Where C_{corr} denotes the corrected activity concentration, C_{meas} denotes the measured activity concentration in a tumoural tissue, C_{thy} denotes the activity concentration measured in normal thyroid tissue, m_{thy} denotes the mass of the normal thyroid, and A_{inj} denotes the activity injected. If it was not possible to measure directly, m_{thy} was calculated by subtracting the estimated mass of the primary tumour, by volume and density approximation, from the total gland mass. This adjustment means that measured tumour concentrations will be increased two-fold if total thyroid uptake was 50% and four-fold if thyroid uptake was 75%. The aim was to make the results more similar to the therapeutic situation, since in this work, any ^{131}I trapped by the normal thyroid tissue would not be available for accumulation in tumour tissue.

In addition to surgical specimens, venous blood was collected after injection of ^{131}I (minimum delay 3 min) and during surgery. This was done in order to enable analysis of and correction for availability of iodine in the blood pool, which may influence the iodine concentration in tumoural tissue. Analyses of estimated glomerular filtration rate (eGFR) were also performed, with the same purpose.

Another consideration in estimating iodine avidity in this pre-therapeutic way is that TSH stimulation was present only in the euthyroid state that the patients presented in. It is well established that TSH binding to TSHR on thyroid cells, among other things, increases *NIS* transcription and translocation of NIS to the plasma membrane [153,154]. This causes an increase in iodine avidity, which is exploited therapeutically [115,155]. TSH stimulation prior to thyroidectomy was deemed hazardous in this work, as it could increase the risk of surgical complications. It also cannot be disregarded that short-term TSH stimulation could have an yet unproven, tumour-stimulatory effect. TSH stimulation would almost certainly have increased the concentrations reported in this thesis, as TSHR is still expressed in many differentiated thyroid cancers [156,157]. TSH values vary between patients after endogenous and exogenous stimulation, and achieving equal stimulation across patients is difficult. Contrary to a TSH stimulated study population, the euthyroid state of the participants in this work may therefore warrant a more equal comparison of iodine avidity. However, the absence of TSH stimulation restricts any direct extrapolation of concentrations from this work to absorbed doses in the clinical situation.

4.2 Estimating Iodine Avidity from a Single Time-Point Measurement

Using iodine concentrations at 48 hours as a proxy for iodine avidity relies on the assumption that activity measured at a single time-point is proportional to the integral of the time activity curve.

It has been shown that the integral of a mono-exponential activity or concentration curve can be approximated within 10% by a single uptake measurement, given that the measurement time is within a factor 0.8 and 2.5 of the effective half-life, see Equation 2 [158].

$$\tilde{A} = \int_0^\infty A(t)\,dt \approx A(T)\frac{2 \cdot T}{\ln 2} \quad \text{given} \quad 0.8 \cdot T_{eff} < T < 2.5 \cdot T_{eff} \tag{2}$$

Where $\tilde{A}$ denotes the cumulated activity in the target, A denotes activity in the target, t denotes time after injection, T denotes the single-measurement time point and T_{eff} denotes the effective half-life. This relationship means that the activity at a carefully selected time point, multiplied by some proportionality coefficient c_i is approximately equal to the absorbed dose that would be delivered by a treatment:

$$\widetilde{A} \simeq c_i(T)\,A(T) \tag{3}$$

Where $\tilde{A}$ denotes the cumulated activity in the target, A denotes activity in the target, T denotes the single-measurement time point and c_i denotes a proportionality coefficient, specific for a curve shape i (in the case of the mono-exponential in Equation 2: $c_i = 2 \cdot T/\ln 2$). This enables an approximate calculation of the iodine avidity in tissue, by using images or *ex vivo* measurements. Such approximations were central to the work in this thesis, and their support is therefore explored in some detail here.

As shown in Equation 2, this has been proven mathematically and experimentally for mono-exponential functions, given constraints on the measurement time [158,159]. However, the activity curve of ^{131}I in thyroid cancer tissue is not a perfect mono-exponential function; activity accumulates over time after having been absorbed through the gastrointestinal tract and transported via blood to tumour cells. The curve might be better described by multiple components for the initial and later kinetic phases. A single time-point measurement does not allow for estimation of parameters in such complex models, and the approximation cannot be assumed to hold for all curve shapes. A set of plausible curve shapes are described in Equation 4 to 6 using sums of exponential functions:

$$\tilde{A}_{mono} = \int_0^\infty a_1 e^{-k_1 t}\,dt \tag{4}$$

$$\tilde{A}_{bi} = \int_0^\infty a_1 e^{-k_1 t} + a_2 e^{-k_2 t}\,dt \tag{5}$$

$$\tilde{A}_{tri} = \int_0^\infty a_1 e^{-k_1 t} + a_2 e^{-k_2 t} + a_3 e^{-k_3 t}\,dt \tag{6}$$

Where $\tilde{A}$ denotes the time integral of the activity curve, t denotes time, a_i denotes the term coefficients and k_i denotes the exponent coefficients of the mono-, bi- and tri-exponential expressions. Beyond exponentials, multi-compartment models may even more accurately model the true kinetics of radioiodine transport to a tumour. A model with blood and tumour compartments is described with differential expressions in Equation 7 and 8:

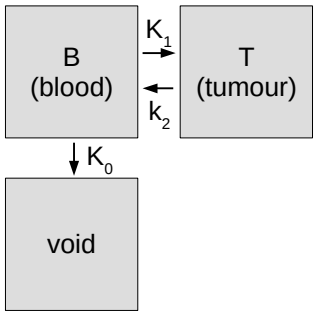

$$\frac{dB(t)}{dt} = -B(t)K_1 - B(t)K_0 + T(t)k_2 \quad (7)$$

$$\frac{dT(t)}{dt} = B(t)K_1 - T(t)k_2 \quad (8)$$

$$\tilde{A}_T = \int_0^\infty K_1 e^{-k_2 t} \otimes B(t)\,dt \quad (9)$$

Where $\tilde{A}_T$ denotes the time integral of the tumour activity curve, *B(t)* denotes the activity in blood, *T(t)* denotes the concentration in tumour, K_0 denotes the rate constant of clearance from blood, K_1 denotes the rate coefficient from blood to tumour and k_2 denotes the rate constant of clearance of iodine from tumour back into blood. The expression in Equation 9 describes the integral of the solution of the compartment model with regards to tumour iodine concentration.

In order to test the validity of the assumption of similar proportionality (i.e. that c_i in Equation 3 does not differ too much between plausible curve shapes) between the activity concentration at a given time point and the integral of the activity curve, previously published kinetic data was used. The effective half-live of thyroid remnants have been reported as means in the range 9 to 118 h, with a crude median of the mean effective half-lives in nine publications of 50 h [78,116,160–166]. The effective half-live of iodine in metastatic thyroid cancer tissue is less studied, with three studies reporting values for lymph note metastases of mean 17 h (8 patients) and 18 h (4 patients), and distant metastatic lesions at mean 52 h (4 patients) [118,167,168]. The effective half-life of iodine in blood in the therapeutic setting has been estimated to 15 h [169]. Based on these somewhat disparate published data, exponential functions in Equation 6 and solutions to the two-tissue compartment model described in Equation 9 were studied. The curves are shown in Figure 7. The compartment model rate coefficients were a range of values which spanned the previously published data.

The difference in the proportionality coefficients (c_i in Equation 3) between the tissue concentration at 36-60 hours and the time integral of the curve was found to be at most two-fold (for the curves corresponding to the most extreme two-tissue compartments), as shown in Figure 8. For 50% of the curve shapes shown in Figure 7, the difference of the proportionality constant was less than 10% from the mean value at 48 hours. A measurement point at 48 h was selected considering these results, given that multiple time-points was impossible.

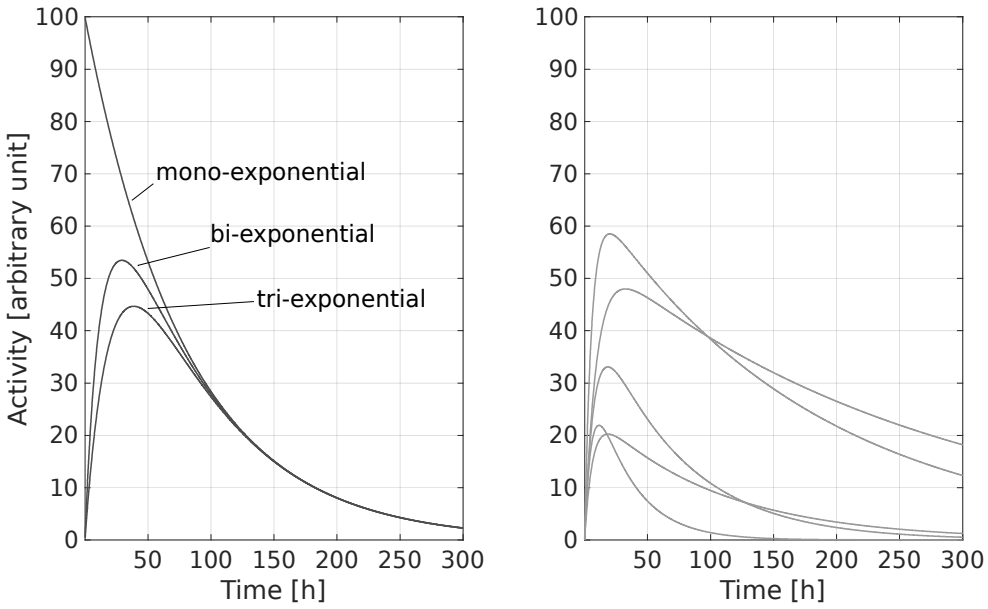

Figure 7: Time-activity curves for a set of (a) mono-, bi- and tri-exponential functions and (b) a range of solutions to a two-tissue compartment model. Only some of the curves in the analysis are shown to avoid clutter. The figure intends to show examples of plausible time-activity curves for different tumours. The curves were generated based on published kinetic data.

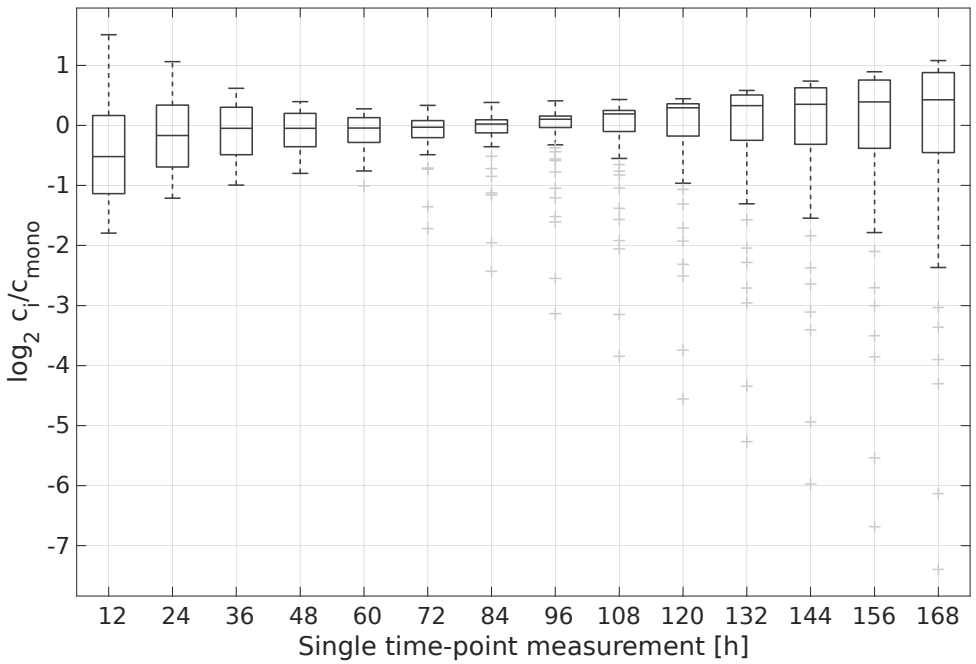

Figure 8: Relative error in proportionality for a specific curve compared to a mono-exponential curve (c_i/c_{mono}) measured at a specific time-point T (x-axis). Data for the functions described in Equation 6, and for solutions to the differential equations in Equation 9 for 60 permutations of kinetic parameters. Measurements on curves at 36-60 hours post injection had less than a two-fold difference to a mono-exponential curve.

Still, it is possible that a subgroup of tissue samples would exhibit very different curve shapes than another subgroup, which would then introduce a systematic bias in the estimation of avidity. Such a potential bias must be considered when interpreting the results of this thesis.

This limitation with single time-point measurements discussed here is present also in previously published research on iodine avidity, where uptake on single time-point nuclear imaging has been used. In such studies, images are usually acquired at a later time-point, where the variance in proportionality coefficients is much larger.

4.3 Monte Carlo Methods

Treatment effect and absorbed doses in radionuclide therapy are the cumulative result of some 10^{10}-10^{15} particle and photon emissions, depositing their energy in nearby tissues through a stochastic process. The underlying physics that govern the interactions of each emitted particle and photon is relatively well-known, and cross sections for interactions have been experimentally determined or theoretically modelled. Based on this knowledge, one could construct a mathematical expression for the radiation transport within tissue. However, similar to the deceptively simple equations describing three-body problems in classical mechanics, solving these equation systems analytically can be impossibly complex. Therefore, detailed dosimetric calculations may instead require a numerical approach. Because of the stochastic nature of nuclear interactions, the Monte Carlo method is often applied to these problems [170]. The method was developed by Stanisław Ulam and John von Neumann in the 1940's within the Manhattan Project [171]. First used to study neutron physics related to nuclear weapons, it was surreptitiously named "Monte Carlo" method after another stochastic process, casino gambling.

The Monte Carlo applications in Paper I used the Monte Carlo N-Particle (MCNP) code. Simulations were performed to study the particle (beta particles, conversion electrons and Auger electrons) and photon (gamma rays and X-rays) emissions from ^{131}I decay.

4.4 Molecular and Genetic Analysis of Tissue Specimen

An array of molecular and genetic analysis methods were used in this thesis. Immunohistochemistry was used in Paper II and III to assess the expression of Tg, Ki-67, mutant BRAF and NIS. For all primary tumours and the largest lymph node metastasis (in case of such metastases), at least one slide was stained.

Immunohistochemical staining of Tg was done using a 2H11 + 6E1 mouse monoclonal antibody (Ventana/Roche Diagnostics, Basel, Switzerland). Normal tissue adjacent to tumour tissue (in the same patient) and external tissue (unrelated anonymised reference material) were used as positive controls. Negative controls were anonymised references from lymph node, colon and kidney tissue. Tg staining was scored as a proportion of positive tumour cells in increments of 5%. Localisation was studied by separate scoring for luminal and cytoplasmic expression of Tg. The immunohistochemistry of Tg is established in clinical routine and was processed as such in the research project.

Ki-67 was stained for by use of the CONFIRM anti-Ki-67 clone 30-9 rabbit monoclonal antibody (Ventana/Roche Diagnostics, Basel, Switzerland). Positive controls consisted of healthy human lymph node, colon, kidney and pancreas tissue. The Ki-67 staining was scored as a proliferation index (percentage with one decimal precision) based on 2000 cells in hotspots. Immunohistochemistry of Ki-67 is in clinical routine and was processed as such in the research project.

NIS was stained using a mouse monoclonal FP5 antibody (ab242007, AbCam, Cambridge, UK) and scored for both cytoplasmic and membranous staining in increments of 10%. Positive controls of normal thyroid and Graves' disease was used to validate the staining and optimise the protocol with regards to pH, denaturation temperature and antibody concentration.

Mutation specific staining of BRAF V600E was performed in accordance with clinical routine using an anti-BRAF V600E (VE1) mouse monoclonal antibody (Roche, Basel, Switzerland). Genetic sequencing and detection of *BRAF* V600E was done by polymerase chain reaction (PCR) analysis. A Cobas z480 system was used for amplification and detection, together with Cobas 4800 *BRAF* V600 Mutation Test (Roche Diagnostics GmbH, Germany). Findings of *BRAF* mutations were verified by a parallel run of real-time PCR for hotspot mutations in *KRAS*, *NRAS* and *HRAS*

using the EntroGen Thyroid Cancer Mutation Analysis Panel Kit (EntroGen, Woodland Hills, CA). As *BRAF* and *RAS* mutations are mutually exclusive driver genes in thyroid cancer, absence of *RAS* would validate the *BRAF* results.

Screening for *TERT* promoter mutations in C228T and C250T was performed with a digital droplet PCR analysis system (QX200 Droplet Digital PCR system, Bio-Rad Laboratories, Hercules, CA) together with a mutation assay from the same company, specific for the *TERT* promoter region upstream positions for C228T (-124) and C250T (-146).

4.5 Determining Outcome in Thyroid Cancer

When trying to determine the outcome of patients with thyroid cancer, a few things are special compared to most other cancer types. One is that most patients have an excellent prognosis and will survive their cancers. This is mainly due to the indolent nature of most discovered tumours, but also because of effective treatment in the form of surgery, hormone suppression and radioiodine treatment. However, regional disease is common in PTC, both initially and as recurrent disease later on. Such metastases can arise many years later.

Due to the low proliferation rate of most thyroid cancers, it is likely that some metastases were present as macroscopic growths even at the time of diagnosis, only to be discovered later. This blurs the line between persistent disease (which is considered as disease present at initial therapy but does not go into complete remission) and recurrent disease (which is tumours that arise after a time period without any signs of disease).

In Paper IV, the follow-up period was relatively short for thyroid cancer (median 22 months). Therefore, all disease was considered as persistent disease, as the distinction between persistent and recurrent disease was not possible to make within the study period. While this was not pertinent to the study aims, which more focussed on the behaviour of any metastases in relation to the initial iodine avidity, it is an important aspect when studying treatment effect, such as progression- or recurrence-free survival.

4.6 Statistical Analysis

The statistical analysis in this work was done using R (version 3.6.3, R-project.org) and MATLAB (version R2018b, matlab.com). Many additional R packages and m-files created by the wider community of physicists, engineers and mathematicians were also used. Both the files and the helpful explanations and discussions on the respective online user forums were instrumental to the analyses in this work.

In order to apply statistical methods that enables accurate interpretation, the statistical distribution of iodine avidity is of great interest. The sample distribution was assessed through histogram and quantile-quantile plot inspection. The statistical distribution of the data on iodine avidity was found to be approximately log-normal after exploratory transformation, which influenced the choice of descriptive statistics. Due to the data being approximately log-normal, the geometric mean was used when calculating means for intra-patient measurements (e.g. for multiple samples of lymph node metastases in one patient). The geometric mean was chosen as it is robust to small sample sizes, and estimates the median of the log-normal distribution well. The log-normal distribution arises by multiplicative processes of independent variables and frequently occurs in observational data from the natural sciences [172].

The statistical tests used for differences between groups and correlations for continuous variables were Welch's t-test and Pearson's product-moment coefficient. They both require approximate normal sample distributions to be unbiased, which was considered to be fulfilled (after log-transform or calculation of means). Welch's t-test was used since it does not require the samples variances to be equal (as Student's t-test does), which was not the case in several of the datasets studied.

To find the underlying relation between tumoural iodine avidity and the other parameters studied in this work, regression modelling was used. The linear least-squares method with QR matrix decomposition (*lm* function in R) for linear regression was applied in both univariate and multivariate analysis. Multivariate analysis was performed to decrease the influence of confounding variables and find the best predictors. The model residuals were analysed for normality using quantile-quantile plots. Multicollinearity in the regression analysis was evaluated with variance inflation factors for each model (*VIF* function in R). Skedasticity was evaluated by the Goldfeld-Quandt test (*gqtest* function in R), with $p > 0.05$ considered

as no proven heteroskedasticity in the dataset. Multivariate model complexity was reduced, to avoid over-fitting and bias in variable selection, partly using a stepwise backwards Akaike information criterion (AIC) minimisation (*stepAIC* function in R).

Statistical power calculations were performed prior to study initiation. As the lack of quantitative data on avidity was the motivation for Paper II, III and IV, a rough approximative calculation had to be performed. The calculations were based on the expected number of occurrences of mutations and expression. The calculations showed that a study population of 42 would find a two-fold difference in avidity with statistical significance (α=0.05) in 90% (β=0.1) of trials. This was however based on assumptions on what a relevant avidity difference would be (a two-fold difference) and the variance of iodine avidity between different patients. As these factors were very uncertain ahead of study initiation, careful attention should be paid to the confidence intervals in the results, which reflect the actually observed effect sizes and sample variances.

Patient recruitment in Paper II, III and IV was done through continuous monitoring of surgical referrals for thyroid cancer to Karolinska University Hospital and subsequent inquiry for participation upon the referral visit. A large proportion of patients were able to be successfully inquired thanks to a tight-knit group of well-informed contact nurses managing thyroid cancer patients as well close communication with the surgeons meeting the patients.

The thyroid cancer catchment area of the hospital is the Stockholm and Gotland counties in their entirety (approximately 2.5 million inhabitants), and should therefore not introduce any bias in patient selection. However, age, gender and severity of disease may correlate with willingness to participate, potentially causing the distribution to be skewed.

Only patients with tumour diameters greater than 1 cm, as estimated by ultrasound, were considered for participation. This introduces some bias towards more aggressive disease, with potentially lower avidity than the general PTC population.

4.7 Ethical Considerations

The research in this thesis primarily involves two ethical considerations.

First, the radiation exposure to the 45 participants in Paper II, III and IV (which was the same cohort) associated with their participation in this research, incurs a risk of radiation induced cancer. The individual effective dose was low, estimated to between 2 and 3 mSv. This is equivalent to a diagnostic PET or SPECT scan (excluding any contributions from CT), or to the natural background radiation in Sweden during 3 years. The collective dose was approximately 0.1 man·Sv, associated with a statistical risk of detriment-adjusted radiation induced cancer in the cohort of 0.4% [173]. The amount of radioactivity used in the studies (5-10 MBq of ^{131}I) was minimised to a point where detector signal for weakly radioactive tissue samples (10^{-7} of injected activity) could still be measured adequately. The results in this thesis can possibly help guide treatment and better find patients that will not benefit from radioiodine therapy, and avoid treatment in those cases. This would by far offset the collective dose incurred by the project, as a standard radioiodine therapy for thyroid cancer can amount to 200-1300 mSv. The patients included in the project were thoroughly informed about the radiation exposure both in writing and verbally, and gave informed consent prior to participation. The surgeons and pathologists (15 persons) involved in the study were estimated to receive a collective dose of 0.4 man·mSv, approximately equivalent to one week of background radiation each.

Secondly, the results from study-related measurements in this thesis gave pre-therapeutic indications as to whether radioiodine therapy was likely to be beneficial to the patients that participated. It was decided to disregard any such information in clinical management of those patients, since there is no evidence published that such adaptations would improve the clinical outcome. In one case, a patient was analysed and imaged more extensively in connection to the radioiodine treatments following participation in the project. This was done with the dual purpose of research and to guide clinical management of the patient. The clinical guidance was not based on preliminary data from the project, but on tumour doses calculated in target lesions.

Ethical permits issued by the Swedish Ethical Review Authority relevant to this thesis are: (#1) 2017/2393-31/1 with amendment 2020-01222 and (#2) 2020-01541.

5 Results

5.1 Iodine Avidity Measurements

A major interest in this work was to study the true range of iodine avidity, expressed as normalised iodine concentration in thyroid cancer tissue. It was studied in quantitative detail as compared to a binary concept, in Paper II, III and IV. This included analysis of the distribution of iodine avidity within the studied cohort. Upon inspection, it was evident that the data had very large variance, across several orders of magnitude. Quantile-quantile plots of measured values and log-transformed values of iodine avidity are shown in Figure 9. The distribution appears log-normal over most of the range. The minimal detectable activity may distort the true distribution somewhat, as the lowest accurately quantified normalised iodine concentration was approximately $2{\cdot}10^{-6}$ IA·g^{-1}. Any real concentration values at or below that threshold would be expected to cluster around $2{\cdot}10^{-6}$ IA·g^{-1}, due to random detector noise. This effect can be noticed to the bottom left part of the log-transformed plot. Despite this minor effect, the distribution of iodine avidity in the cohort was considered to approximately log-normally distributed, for statistical analysis. The log-normal distribution of iodine avidity may be attributed to an underlying multiplicative pharmacokinetic process, as products of normally distributed stochastic variables, such as expression levels of specific proteins, are log-normal distributed [174].

The findings from Paper II on the complete range of iodine avidity are presented for subtypes of PTC and for PDTC in Figure 10. The iodine avidity in normal thyroid tissue was similar among patients (at most a 11-fold difference), while avidity in tumour tissue was found to differ more than a thousand-fold (from 6.4E-07 to 2.2E-03 IA·g^{-1}). The iodine concentrations in normal thyroid was multiplied by the weighed and estimated total gland masses, producing uptake values for the normal thyroid tissues. The uptake values were found to have a median of 40% (interquartile range: 29 – 54%) at a mean uptake time of 48 h, decay corrected to the time of injection.

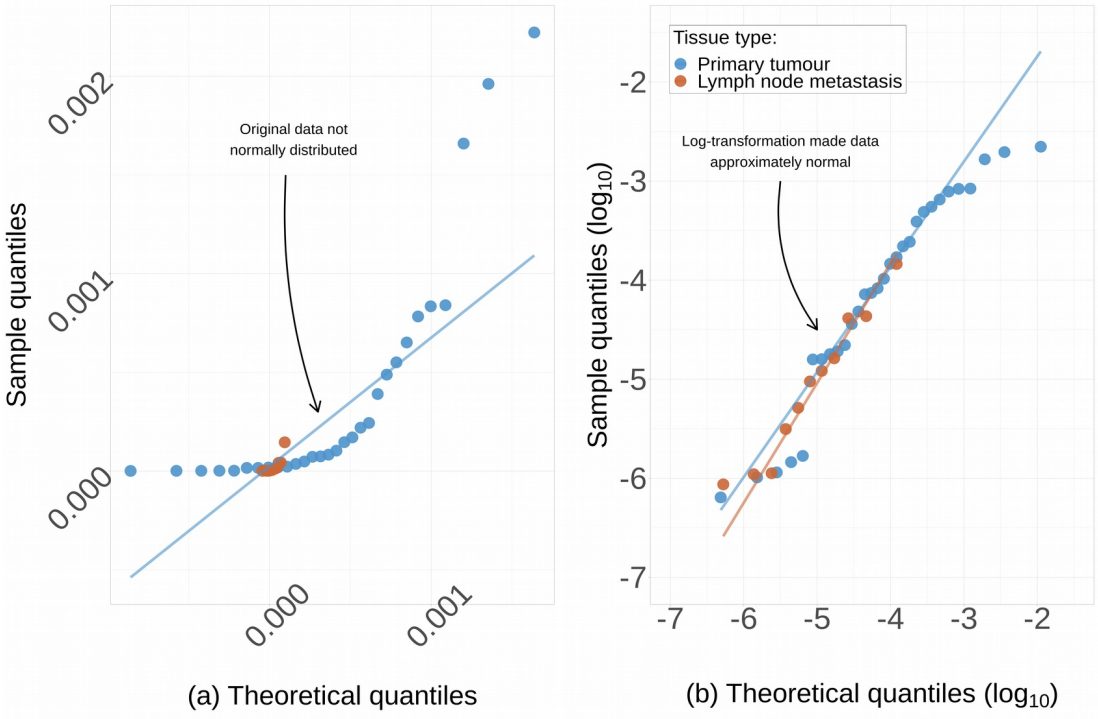

Figure 9: Normal quantile-quantile plots of iodine avidity for primary tumours and lymph node metastases. Multiple samples from the same patient are represented by their geometric mean. Both (a) original and (b) log-transformed data is shown.

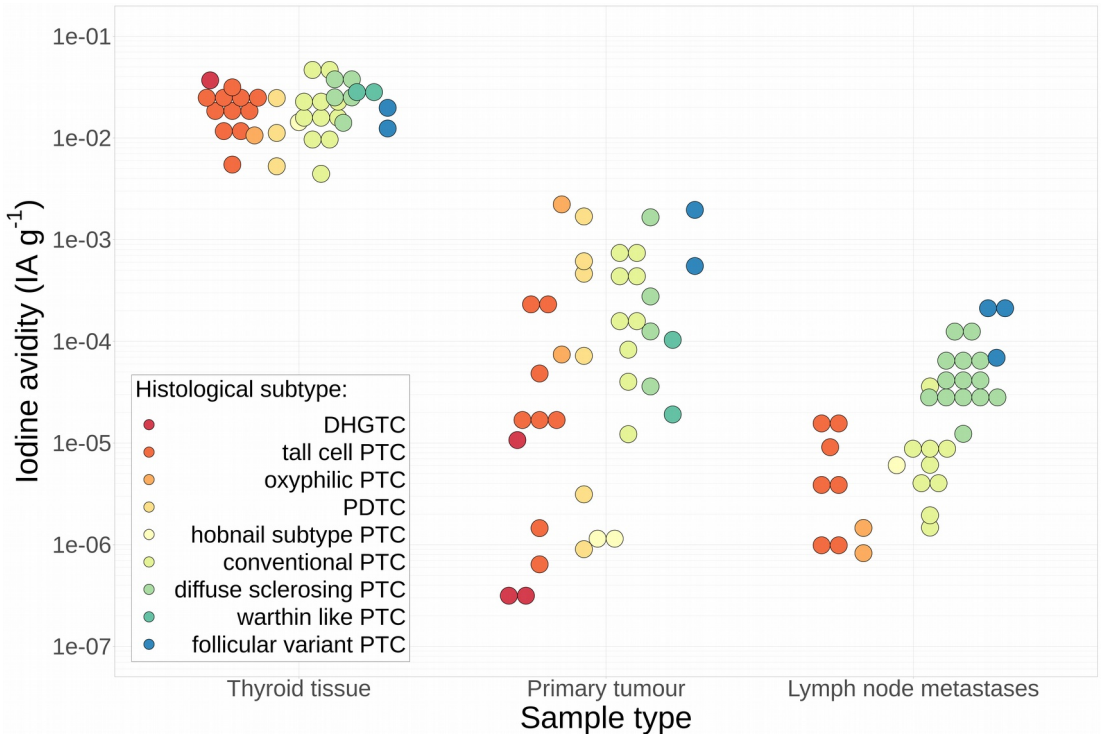

Figure 10: Iodine avidity in all samples collected from normal thyroid, primary tumour and lymph node metastases. DHGTC - differentiated high-grade thyroid cancer; PDTC - poorly differentiated thyroid cancer

The relationship between avidity in samples from primary tumour and lymph node metastases could be studied in 10 patients with synchronous metastases, and the results are shown in Figure 11. Overall, iodine concentrations were lower in lymph node metastases than in primary tumour samples but the difference was borderline non-significant (5.7-fold lower, CI 0.9–36). From samples taken in the same individual from either primary tumours or lymph node metastases, the intra-patient variation in avidity could be estimated. Such comparisons were possible in thirteen patients, in which the median of ratios between highest and lowest avidity in each patient was 3.3, indicating a much lower variance than observed between patients.

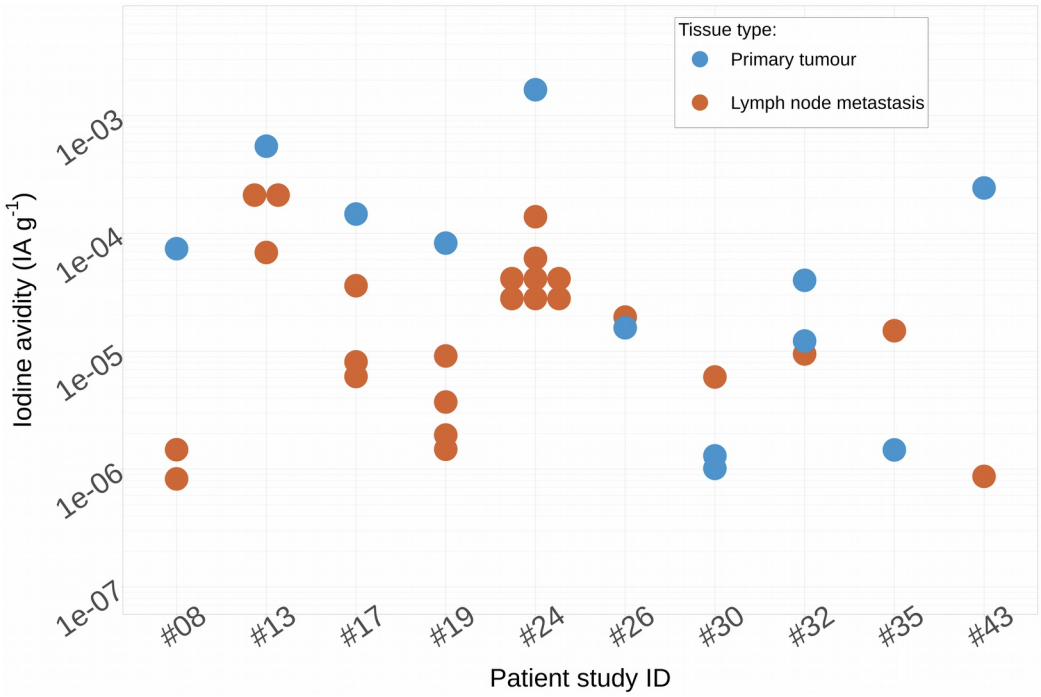

Figure 11: Iodine avidity in samples of primary tumour and lymph node metastases in the same patients (n=10). Multiple samples from the same patient are shown when available. Avidity was lower in metastases than in primary tumours for most patients, however, paired testing did not find a significantly lower avidity.

5.2 Iodine Avidity and Histopathological Markers

By analysis of the immunohistochemical data on Tg expression and Ki-67 index in Paper II, it was established that both had a strong correlation to iodine avidity, as can be seen in Figure 12. The data was log-transformed and the calculations of correlation coefficients showed r = 0.50 (CI 0.22 – 0.70) for Tg expression, and r = -0.49 (CI -0.70 – -0.21) for Ki-67 index. The measure of Tg that predicted avidity was the proportion of cells that expressed Tg. When analysed separately for samples

from primary tumour and lymph node metastatic samples, the significance and trends were still evident.

In addition to proportion, the localisation of Tg was studied, where cytoplasmic localisation was more common (33/37, 89%) than localisation in follicular lumen (13/37, 35%). Out of all samples, both Tg expression in both cytoplasm and lumen was present in a minority of samples (9/37, 24%). No statistical difference in avidity was found between the localisation of Tg expression. The spatial homogeneity of Tg expression in the tumour tissue was assessed, where heterogeneous expression was found in approximately half of the samples (19/37, 51%) and homogeneous in the other half (18/37, 49%). Similarly to Tg localisation, no significant difference in avidity was found for spatial homogeneity of expression.

High-risk histological subtypes (hobnail and tall cell subtype PTC, PDTC and differentiated high-grade thyroid cancer) had 7.1-fold lower avidity than other samples (CI 1.9–28).

The relation between size of the primary tumour and iodine avidity was studied in Paper II. Furthermore, the cancer staging according to the tumour, nodal and metastasis (TNM) classification in terms of pT and pN stage was analysed. The results of analyses for tumour size and pT stage are shown in Figure 13. There was no significant correlation between primary tumour size and iodine avidity (CI -0.52 – 0.18). Comparing the different pT stages and iodine avidity showed that there was a significantly higher avidity in pT1a/b and all others, by a factor of 5.9 (CI 1.2–29). However, tumours classified as pT1a/b+pT2 stage were not significantly more avid than pT3a/b (CI 0.11–5.1). Overall tumoural iodine avidity was not found to be significantly different according to pN stage, as pN0 was compared to pN1a/b or pNx/1a/1b. The avidity data with regards to pN stage is shown in Figure 14. The absence of difference in avidity between pN stages did not change upon separation of avidity in primary tumour and lymph node metastases.

The impact of the rate of renal clearance of iodine and the iodine concentrations in tumour and healthy thyroid was studied. No correlation was found between neither eGFR, blood iodine concentration at surgery nor the blood iodine concentration at surgery divided by the concentration at 5 min post injection. Patient age was found to be significantly correlated to iodine avidity with a correlation coefficient of r=-0.35 (CI -0.52 – -0.06).

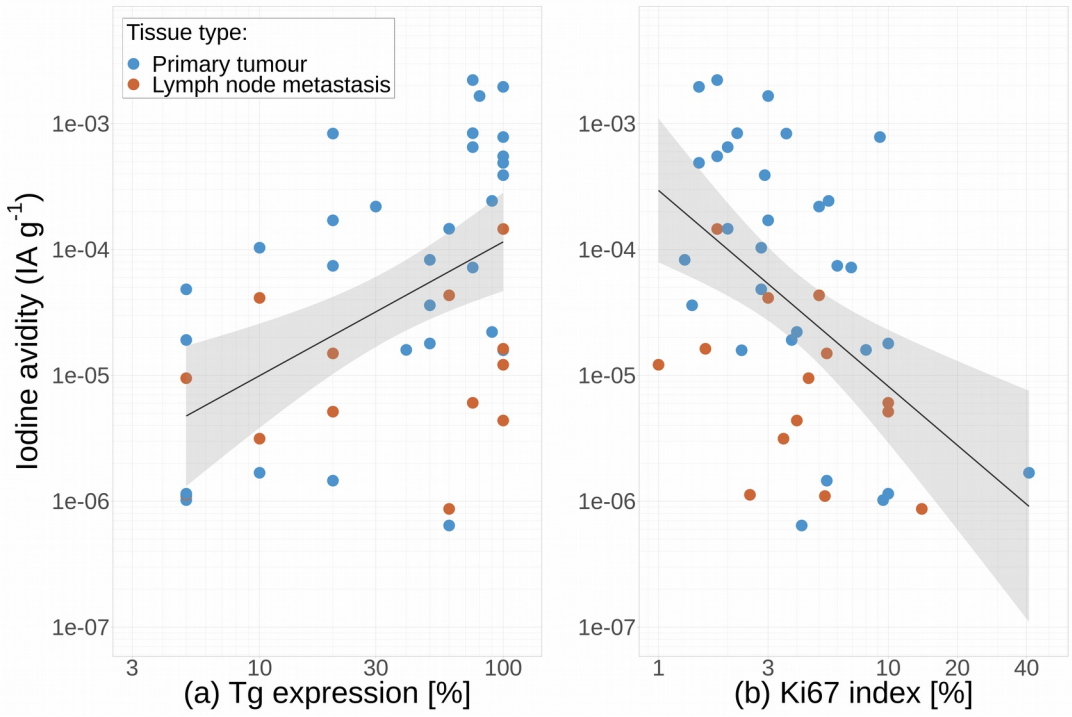

Figure 12: Iodine avidity for all cancer samples versus (a) Tg expression as a proportion of cells [%], and (b) Ki-67 index [%]. The display includes both primary tumour and metastases. The line and shaded area shows a linear fit and the 95% confidence intervals of the fit.

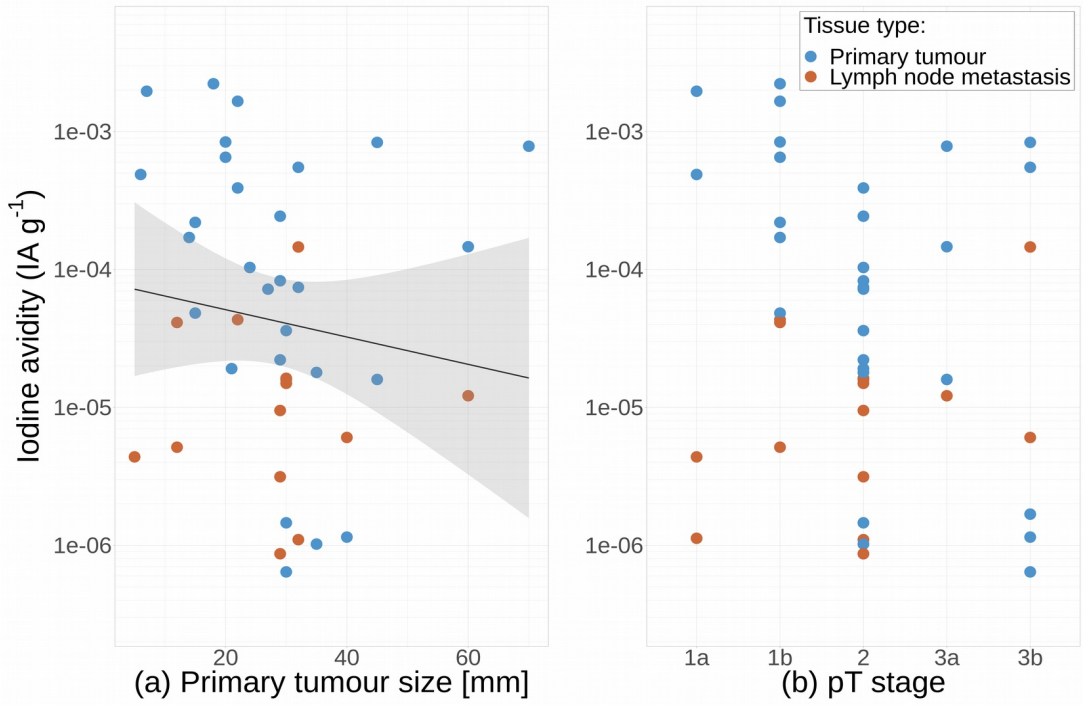

Figure 13: Iodine avidity for all samples depending on (a) tumour size and (b) pT stage. The line and shaded area shows a linear fit and the 95% confidence intervals of the fit.

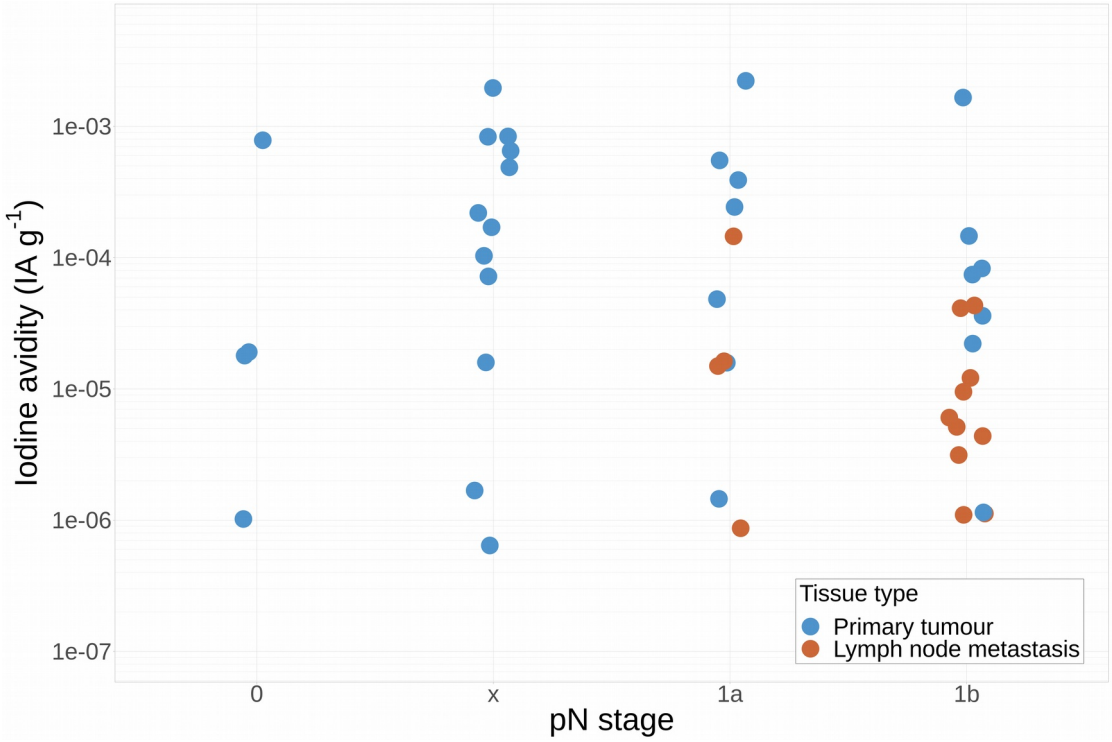

Figure 14: Iodine avidity for primary tumour and lymph node metastatic samples. The data is presented according to the pN stage and coloured according to sample tissue type.

Expression of NIS was studied with respect to both localisation and proportion of cells, similarly to Tg. It was found that cytoplasmic expression of NIS was widespread but highly variable in tumour tissue. An example of widespread membranous and cytoplasmic staining in tumour tissue is shown in Figure 15. Expression in ≥50% of cells was found in 17/35 (49%) samples. However, no significant correlation was observed between the proportion of cells with cytoplasmic expression and iodine avidity. NIS expression at the plasma membrane was rare, found only in 2/35 (6%) samples. The two samples were among those with highest avidity, with a statistically significant 40-fold higher avidity (CI 9.1-180) compared to those without membranous NIS staining. NIS expression was not found to be significantly lower in patients with neither *BRAF* (p=0.37) nor *TERT* (p=0.53) promoter mutations.

The occurrence of *BRAF* V600E mutations in the studied cohort was high, detected in 26/35 (74%) samples. It was found that iodine avidity was lower in the group with *BRAF* mutations, but only significantly in the case of lymph node metastases, where a 18-fold lower avidity was observed (CI 3.9–87). The avidity for lymph node metastases with and without *BRAF* mutations are shown in Figure 16a.

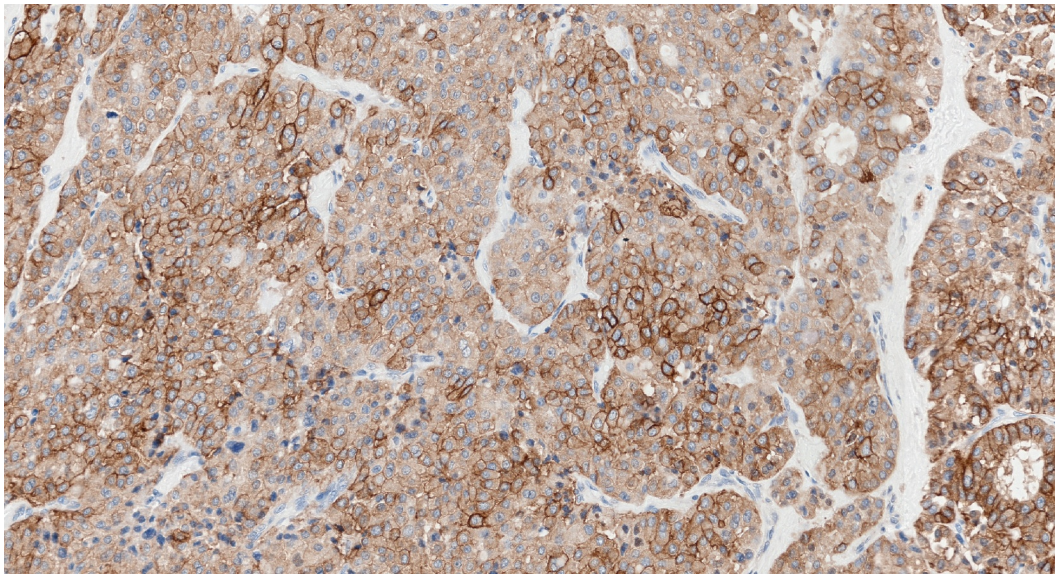

Figure 15: Both cytoplasmic and membranous NIS expression (brown) in primary tumour tissue. While the membranous expression in this sample was intense in most areas, there were some sections where only cytoplasmic localisation could be detected. The sample was scored as 100% cytoplasmic and 80% membranous NIS staining. Hematoxylin counter-stain (blue) shows cell nuclei.

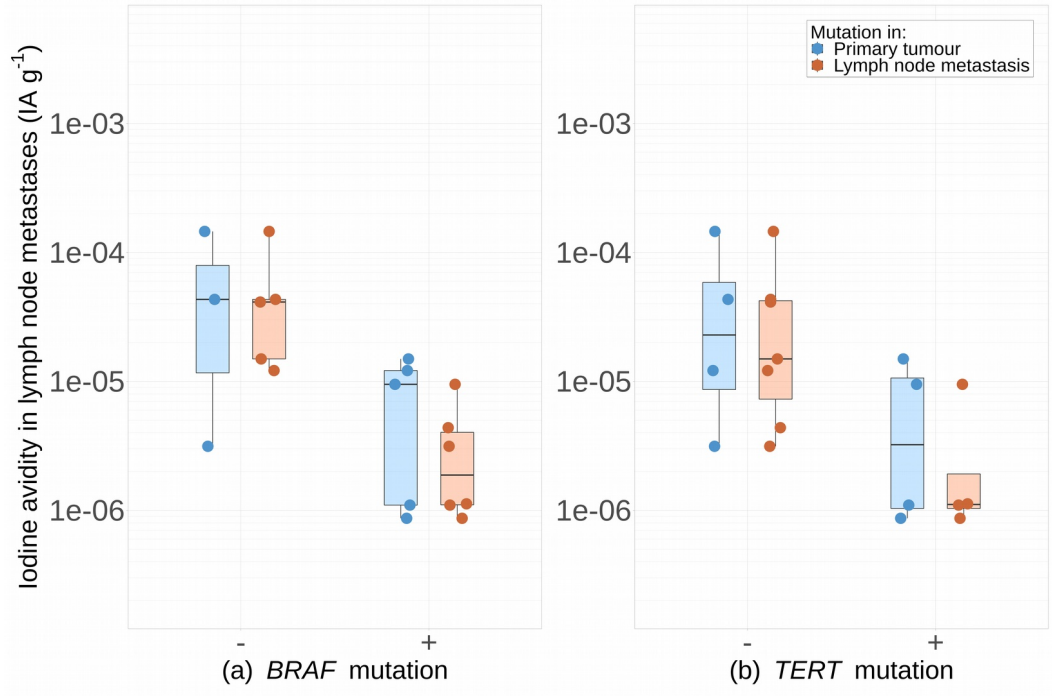

Figure 16: Iodine avidity in lymph node metastases depending on (a) *BRAF* V600E mutation or (b) *TERT* promoter (C228T) mutation. Data is shown according to mutational status in either the lymph node metastases themselves (orange) or the corresponding primary tumour (blue). The better separation between avidity in orange data points may suggest that mutational status in metastases better predict avidity in the adjuvant setting.

The detection of *BRAF* V600E mutations and the expression of BRAF V600E mutant protein was in strong agreement, with an accuracy of 0.91 (CI 0.76–0.98), allowing either method to be used.

TERT promoter mutations (C228T) were found in 12/35 (34%) samples. Similarly to *BRAF*, samples with mutations had lower avidity, but was only found to be significantly so in the case of lymph node metastases. Avidity in lymph node metastases with *TERT* promoter mutations was 10-fold lower (CI 1.7–60), as shown in Figure 16b. The slightly better separation of avidity for mutational status of both *BRAF* and *TERT* in lymph node metastases in the figure suggests an advantage in studying resected metastases when trying to predict avidity ahead of radioiodine treatment.

The iodine avidity in samples with combined *BRAF* and *TERT* promoter mutations was found to be lower than that in each of the separate groups, with a 19-fold lower avidity (CI 3.4–110) in lymph node metastases. Again, no significant difference was found in primary tumours alone.

5.3 Initial Iodine Avidity and Persistent Disease

The avidity data was studied with respect to the behaviour of persistent disease during follow-up in Paper IV. Out of data on 35 patients included in the study, 10 patients had persistent disease at the point of study conclusion (April 2022). The characteristics of those patients are shown in Table 1. Two patients died (#09 and #30) from distant metastases of their thyroid cancers. The two patients with distinct radioiodine uptake in distant metastases had PDTC and diffuse sclerosing subtype PTC, and the four patients with metastases without visible iodine accumulation had PDTC, diffuse sclerosing, tall cell and hobnail subtype PTC.

High iodine avidity in primary tumour and initial lymph node metastases correlated with high tumour-to-background signal ratio (log-log correlation coefficient r=0.69, CI 0.04-0.93), and the visual assessment of iodine avidity (56-fold higher avidity, CI 1.3-2400). The results suggest that tumoural avidity can be predictive of iodine avidity in metastases found during follow-up. The iodine avidity in primary tumour and lymph node metastases depending on the uptake status in persistent metastases is shown in Figure 17.

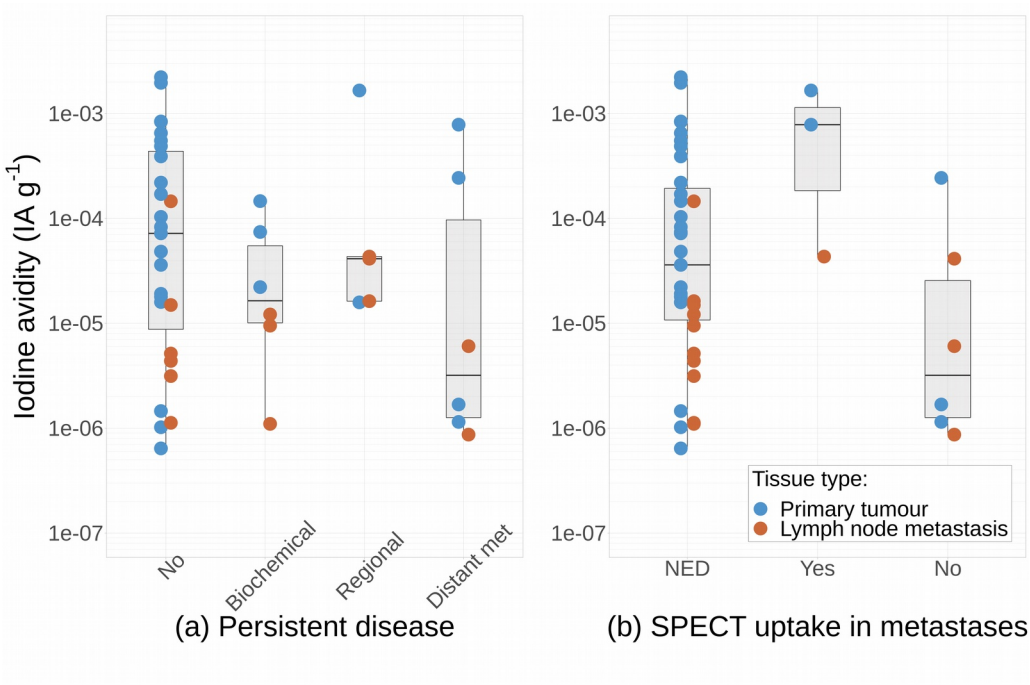

Figure 17: Iodine avidity in samples from patients (a) depending on localisation of persistent disease, or depending on (b) iodine uptake status on post-therapeutic SPECT imaging. The results show that peri-operative avidity as estimated in this thesis concurs well with uptake status in subsequent metastases. NED - no evidence of disease.

Table 1. All ten cases of persistent disease. Follow-up duration measured from cytological diagnosis.

dsPTC = diffuse sclerosing subtype of PTC; tcPTC = tall cell subtype of PTC; hPTC = hobnail subtype of PTC; cPTC = conventional subtype of PTC; NA = not available; T/B = tumour to background; † = death; * = not possible to assess due to no visible structural disease

Study ID	**Surgery**	**Macro/ micro radicality**	**Histol. subtype**	**pTNM**	**BRAF/ TERT mut**	**^{131}I activity 1st/2nd treatment [MBq]**	**Time to event after ^{131}I [months]**	**Type of presistent disease**	**Iodine uptake in metastases (T/B-ratio)**	**Serum Tg pre/post first ^{131}I**	**Follow-up duration [months]**
#08	Total +lgl central/dx	yes/yes	oncocy-tic PTC	T2N1b	yes/yes	7400	24	biochemical	* (*)	0.3/0.4	35
#09	Inoperable/ total	no/no	PDTC	T3bNx	no/no	7400	0	local/distant met	no (3)	251/587	18 †
#17	Total +lgl central/sin	no/yes	cPTC	T3aN1b	yes/no	5550	12	biochemical	* (*)	13/4.6	26
#24	Total + lgl central/ bilateral	yes/yo	dsPTC	T1bN1b	no/no	5550	4	regional	yes (1000)	19/6.4	23
#26	Total + lgl central	yes/yes	tcPTC	T2N1a	yes/NA	3700	9	regional	* (*)	0.3/0.6	22
#30	Total + lgl central	no/no	hPTC	T3bN1b	yes/NA	5550	7	regional/ distant met	no (1)	not detectable/ 15	17 †
#32	Total + lgl central/ bilateral	yes/yes	cPTC	T2N1b	yes/yes	5550	9	biochemical	* (*)	3.1/4.1	19
#40	Total + lgl central/dx	yes/yes	dsPTC	T1bN1b	no/no	5550	0	regional	no (2)	not detectable/ not detectable	15
#41	Total + lgl central	yes/yes	PDTC	T3aN0	no/no	3700/7400	0	distant met	yes (500)	3200/1800	14
#43	Total + lgl central	no/no	tcPTC	T2N1a	yes/yes	5550	0	distant met	no (1)	47/153	13

5.4 Dosimetric Impact of Target Geometry and Size

The Monte Carlo simulations on radiation transport from ^{131}I in Paper I showed that the target geometry is important on the scale of micrometastases (<2 mm diameter), at which a strongly oblate spheroid may receive up to 38% less absorbed dose per decay than a sphere. As target size increased, the effect of geometry diminished. The results from simulations of target geometry is shown in Table 2.

Similarly, the impact of target size was found to be more noticeable for smaller targets, where a small sphere of 0.005 g would receive 42% lower absorbed dose per decay than a sphere of 50 g. The effect of size is shown in Figure 18.

This means that the combined effect of a small target (micrometastases) and compressing the target into an oblate spheroid can translate to a three-fold lower absorbed dose per decay, compared to a large target growing freely in a spherical shape.

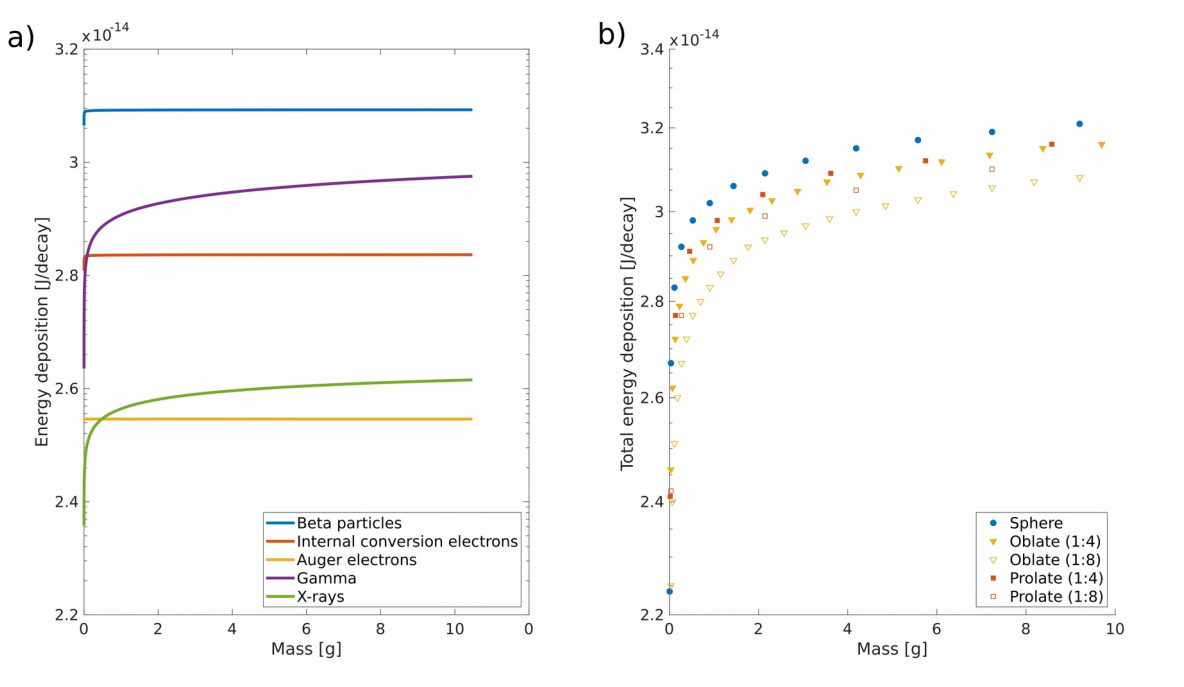

Figure 18: (a) Absolute energy deposition contributions per decay in a target sphere. (b) Total energy deposition in the smaller range of simulated masses for spheres and prolate and oblate spheroids.

Table 2. Normalised absorbed doses for different spheroids and spheres. Varying axis ratios horizontally, and different target masses vertically. Values are normalised to the absorbed dose to a sphere of the same mass.

	Axis ratio								
	Oblate				**Sphere**		**Prolate**		
Mass (g)	**1:16**	**1:8**	**1:4**	**1:2**	**1:1**	**1:2**	**1:4**	**1:8**	**1:16**
0.005	0.62	0.77	0.84	0.93	1.00	0.94	0.89	0.81	0.68
0.01	0.69	0.81	0.94	0.97	1.00	0.98	0.92	0.83	0.74
0.05	0.75	0.86	0.94	0.99	1.00	0.99	0.93	0.88	0.82
0.1	0.81	0.91	0.96	0.99	1.00	0.99	0.95	0.90	0.87
0.5	0.85	0.93	0.97	0.99	1.00	0.99	0.98	0.95	0.93
1.0	0.88	0.94	0.98	1.00	1.00	1.00	0.98	0.97	0.94
5.0	0.92	0.95	0.98	1.00	1.00	1.00	0.98	0.97	0.95
10	0.93	0.96	0.98	1.00	1.00	1.00	0.99	0.98	0.96

5.5 Multivariate Regression

The optimised multivariate regression model was built on the full cohort data. The initial iteration used the following variables: tissue type (primary tumour or lymph node metastasis), age, sex, Tg expression, Ki-67 index, size of primary tumour, number of metastases, extra-thyroidal extension, high-risk histological subtype (tall cell or hobnail variant PTC, differentiated high-grade thyroid cancer or PDTC), risk stratification according to the Swedish national guidelines, *BRAF* mutation, *TERT* promoter (C228T) mutation and membranous NIS expression.

Several multivariate models performed well, with low variance inflation factors, normally distributed residuals and moderately high adjusted R^2 values (in the range of 0.40 to 0.60). When restricting the number of predictive variables to four, a model containing Tg expression, *BRAF* mutation, tissue type and high-risk histology performed best. The resulting coefficient estimates, errors and confidence intervals are shown in Table 3.

Since the results showed that avidity is dependent on which tissue it is measured in, a model was also constructed for only primary tumour samples. When restricting the model to three prediction variables (to accommodate that the model had less data points to model), it was found that Tg expression, high-risk histology and patient age constructed a well-performing model in primary tumour tissue.

Table 3. Multivariate linear regression results for $\log_{10}(IA \cdot g^{-1})$ in all samples in the cohort. The model was constrained to four variables, had an adjusted R^2 of 0.55 and variance inflation factors were below 1.2 for all variables.

Predictive variable	**Estimate**	**Confidence intervals of estimate**	**Standard error**	**Variance inflation factor**
Intercept	-5.59	-6.62 – -4.57	0.51	-
$\log_{10}$(Tg expression [%])	0.80	0.30 – 1.31	0.25	1.11
BRAF mutation	-0.41	-1.00 – 0.18	0.29	1.12
Tissue = primary tumour*	0.96	0.44 – 1.49	0.26	1.07
High-risk histology**	-0.93	-1.40 – -0.47	0.23	1.03

* = compared to lymph node metastasis; ** = tall cell or hobnail subtype PTC, differentiated high-grade thyroid cancer or PDTC

6 Discussion

This thesis had one overarching purpose.

It involves the fact that despite requirements and recommendations to perform individualised dosimetry when optimising treatment in radionuclide therapy, most institutions do not [175–178]. This has many reasons: tradition, economy, convenience, lack of skills and knowledge, contradictions in regulation, and perhaps even negligence [179,180]. The most important reason is arguably the lack of established dose-response relationships in radionuclide therapy in general [181,182]. A case can be made that for thyroid cancer, individualised dosimetry may be unnecessary; most patients have excellent cure and disease control regardless of radioiodine treatment. Image-based tumour dosimetry is also near impossible in the majority of patients, where adjuvant treatment is given, with no visible metastases to perform dosimetry on at disease presentation. While radioiodine treatment is associated with improved outcome for more advanced disease, dosimetry-guided treatment studies have not clearly shown superior success rates compared to empirical activity schemes [25,88,183].

If an analogy of the current approach to radioiodine therapy to external beam radiotherapy can be afforded, it would entail the following: a fixed beam targetting one part of the body with a fixed photon output from the accelerator. The photon output would be adjusted according to the TNM stage of the cancer, in steps of 1.11, 1.85, 3.7, perhaps 5.55 or 7.4 (if for no other reason, in homage to Drs Curie) - a reasonable adaptation to risk of the individual patient, one might think. But similarly to how iodine avidity is usually not taken into account, the beam would be placed on the same body part, regardless of where the tumour was growing or how deep the tumour would be in the patient. To be sure, no radiation oncologist would expect a decent treatment response after missing the target tissue by 3 cm in external beam radiotherapy. Still, if the tumour was 3 cm outside the planning treatment volume that receives 68 Gy, it would receive perhaps 2 Gy, a 3% share of the intended dose. This is much higher than what can occur if the avidity data in this thesis is accurate, where more than thousand-fold differences between some patients were observed. In terms of magnitude, the equivalent situation in external beam radiotherapy would be irradiating the heart when the tumour was growing in the neck.

In absence of individualised dosimetry, the current choice of treatment activities is based mostly on primary tumour size and the presence of lymph node or distant metastases in guidelines [8–10]. As the staging of thyroid cancer is essentially a stratification by risk of persistent and recurrent disease, one might call this risk-guided therapy.

The purpose of this thesis was to find more relevant parameters related to expected treatment effect. Such knowledge can be incorporated into treatment decision making and thereby introduce the concept of *avidity-guided* therapy. Including pre-therapeutic avidity into management may bridge the schism between, on the one hand, requirements on individualised dosage and dosimetry, and on the other hand, very little dosimetry being done, even when occasionally feasible. Radionuclide therapy is unique in that the potency of the treatment in each patient can be estimated as it is given, using post-therapeutic imaging. In addition, pre-therapeutic knowledge of expected iodine avidity could potentially increase the precision of treatment selection. This is akin to how, for example, cancer treatment with trastuzumab and pembrolizumab is adapted to cellular expression of human epidermal growth receptor 2 (HER2) and programmed cell death protein 1 (PD-1), and therefore estimated treatment effect, in each tumour.

This discussion will argue that the findings of this thesis, in combination with other published research, support the concept of avidity-guided therapy in clinical practice and research. This concept is especially relevant if one wants to adapt adjuvant treatment for a smaller group of patients at high risk of their thyroid cancer impacting their lives. As the principle of "as low as reasonably achievable" of radiation protection applies, the definition of this sub-group has to be carefully constructed. Still, the patients at largest risk of recurrent disease or with distant metastases stand to benefit the greatest from individualised activity compensation, image-based dosimetry or future applications of redifferentiation therapy.

6.1 Determination of Tumoural Avidity

The importance of iodine avidity for successful radioiodine treatment was not in any doubt when these research projects were started. Our method of estimating avidity however, was unproven as a meaningful proxy in clinical practice. Two things had to be proven in order for it to be meaningful.

Firstly, it had to be shown that measurements in small sections of tissue were accurate in estimating the actual iodine content in the whole tumour or thyroid gland. This was assessed by calculating the uptake values of the entire healthy thyroid gland (interquartile range: 29 – 54%), which were found to be within expected values in euthyroid patients, considering they were on an iodine-restricted diet in study preparation [184]. These internal control measurements performed in each patient supports that the tissue segments measured can be considered representative of the whole tumour.

Secondly, the iodine concentration in primary tumour tissue would have to say something useful about any subsequent metastatic disease. This is important, as some data suggest that metastases can be very unlike their primary tumours [185]. To explore this, the measurements of primary tumour iodine avidity were compared to the follow-up of patients, primarily in Paper IV. The tumoural iodine avidity measured experimentally was found to have very good agreement with the avidity in the cases of clinically evident metastatic disease, as can be seen in Figure 17.

The data on tumoural iodine avidity produced in this thesis was found to span a wide range, with iodine concentrations differing more than a thousand-fold between patients. Relatively small variations were found between samples from primary tumours and lymph node metastases within the same patient. This refutes any simplistic view of iodine avidity as a binary parameter. While there must exist a critical level of iodine concentration under which no beneficial treatment effect may be achieved, it is currently unknown and is most certainly not what happens to be just noticeable with currently available SPECT/CT systems. Studies that have used detectable signal on imaging as a proxy for avidity add much to our understanding of thyroid cancer, but such classification should not be taken as the final verdict on whether treatment can be effective or not [186,187]. If one is uncertain if a certain lesion can receive therapeutical levels of absorbed dose from radioiodine treatment, image-based dosimetry is the most reliable option. While some hesitancy is warranted due to the lack of an established dose-effect relation [183] or uncertainties in dosimetric methods in thyroid cancer [188], image-based dosimetry should be considered the current best method of estimating avidity in visible metastases.

Iodine avidity as assessed by imaging in previously published studies have been performed in combination with TSH stimulation, either in preparation for a scan or

treatment. The studies have also been performed in patients who have already undergone thyroidectomy. This differs from the methodology in this work, where patients were euthyroid and had a functioning thyroid gland present. To minimise this difference, the competing uptake in normal thyroid tissue was corrected for (as detailed in Equation 1). The lack of TSH stimulation likely resulted in a bias toward lower iodine concentrations in this work than would have been observed in the therapeutic setting. This disarms any attempt to find exact cut-off values and limits any extrapolation of radiation doses to the therapeutic situation from the data obtained in this work. However, the results in Paper IV suggests that avidity in primary tumours and initial lymph node metastases assessed in a euthyroid state are good predictors of avidity in both lymph node and distant metastases under stimulation by high serum TSH levels.

Any method of estimating avidity with a single time-point measurement introduces some uncertainty. The assumption of mono-exponential activity curves and the use of a single time-point are sensitive to effective half-lives deviating far from the mean uptake time of 48 h used in this work. If effective half-lives were much shorter or longer than 48 h, that would lead to underestimation of the avidity as estimated in this work. The errors introduced by a mono-exponential curve shape assumption are complex to estimate. It depends on the true shape of the activity curve and the measurement time point on that curve, as discussed in section 4.2 in some detail. Bi-exponential curves with a positive and a negative component are common in pharmacokinetics, arising from a protracted uptake phase and a longer excretion or decay phase. A single measurement on such a curve will overestimate the integral if it is performed in the late stage when the decay component is dominant [158]. A potential systematic bias cannot be excluded, as some tumour subgroup may conceivably have consistently different activity curve shapes than another. However, the above is also true for single time-point imaging, which usually occurs later after radioiodine administration. This fact has cursorily been overlooked in previous research on iodine avidity.

The study population in this thesis had a higher proportion of men and older persons than might be representative for the total papillary thyroid cancer population. It was noted during recruitment that younger women were less likely to want to participate in the study. Since young women constitute a large group of patients with predominately low-risk disease, this explains the higher occurrence of high-risk persistent disease in the study cohort. This limits generalisations of iodine

avidity to the general thyroid cancer population, as the proportion of risk might be skewed. Furthermore, the studies in the thesis have not included any FTC or oxyphilic thyroid cancer tumours, which constitute a significant minority of thyroid cancers. Markers for avidity in FTC and oxyphilic thyroid cancer should be researched separately to test the validity of individual markers suggested to be useful in this thesis.

6.2 Markers for Iodine Avidity

This work has expanded the range of known markers for iodine avidity, with low Tg expression and high Ki-67 index both indicating low avidity. Histological subtype also showed promise in separating tumours of low avidity from others, in line with published data [189]. In the multivariate modelling, Tg expression turned out to be the most robust marker. It was significant in most iterations, especially when the model was constrained to only four predictive variables. As Tg immunohistochemistry can be set up and scored in most pathology labs, it could be a useful complement to predict iodine avidity in clinical practice.

The results from genetic analyses in this work are in line with published data on both *BRAF* and *TERT* promoter mutations [58–60,63,64]. *TERT* promoter mutations appears to have stronger correlation to low avidity in previously published data. The confidence intervals of the effect for the two mutations overlap heavily in this thesis. It is therefore not possible to determine which is the best in the current data. However, the results all point in the same direction (lower avidity for any of the mutations) as previous data. The fact that mutations in lymph node metastases predicted avidity better than in primary tumours may be worth exploring further.

The direct measurement of iodine concentration *ex vivo* in tumour tissue, as employed in this thesis, could also be considered as a way of determining iodine avidity ahead of radioiodine treatment. The method was shown to predict avidity in subsequent metastases well, and has a larger dynamic range and likely higher precision in low-avidity tumours than post-therapeutical nuclear imaging, as sub-Bq activity levels are detectable *ex vivo*. When measuring directly in surgical specimens of tumour tissue, only the actual tumour cells are measured and can be verified as such. It does however require the logistical coordination of pre-operative radioiodine administration with surgical planning and pathology grossing with the nuclear medicine department. Instruments that enable accurate measurement of low levels of radioactivity are also required. Arguably, it is mainly the logistical

requirements that makes such an implementation unlikely. The direct translation to therapy-setting tumoural avidity is also hindered by differences in TSH stimulation.

6.3 Avidity-guided Therapy

Treatment guidelines and classification systems like the American Joint Committee on Cancer (AJCC) TNM staging and the MACIS score aim to stratify patients according mainly to risk of recurrence and death [190]. Selection of therapeutic radioiodine approach has traditionally followed this line of thinking and radioiodine treatment effect has been found to be more pronounced, the higher the risk of recurrence. An avidity-guided approach would move away from this, and not focus only on pT, tumour size and pN, which were found to not correlate well with iodine avidity in this thesis.

How the results of this thesis would fit into an avidity-guided framework is shown in Table 4. The framework was in part inspired by a 2019 joint statement from the American and European associations for thyroidology and nuclear medicine [187]. In the statement, two principles (5 and 6) relates to unknown factors in radioiodine treatment selection and how decisions should be made, given that the evidence base is partially lacking. The framework in Table 4 should be seen as an attempt to put the findings of the current thesis into a greater context to amend the risk-based approach with avidity-based decision making.

A starting point would be to adjust the treatment based on both risk and expected avidity. Patients with very low risk of recurrence and the highest avidity can arguably be fully treated with lower activities. This is supported by randomised trials establishing that ablation treatments (studying low-risk patients) with 1.1 GBq are equal to 3.7 GBq with regards to both short term ablation success and long term recurrence rates [77,120,124,191]. Most pT1 patients are already treated this way, but the ability to distinguish patients with low risk using genetic profiling (e.g. for *TERT, TP53* or high tumour mutational burden) and histological sub-typing is further improving [3,192–194]. This may result in that more patients can safely be given only ablative treatment in the range of 1 GBq of ^{131}I, with less emphasis on tumour size.

For patients with a high risk of recurrent or persistent disease and lower avidity, radioiodine dosage could be increased, by activity compensation. This would aim to

at least in part compensate for the lower expected iodine concentration in any metastatic tissue. For such patients, it would be more motivated to initially administer higher activities with the aim to provide a successful treatment, considering that metastatic uptake and iodine kinetics seem to become less beneficial over the course of several treatments [195]. As an example: from the data collected in this thesis, a simple activity correction factor, e.g. the inverse of the proportion of cells expressing Tg, would mitigate the large variance in iodine avidity [196]. The results of such a compensation on absorbed doses to tumour tissue can be seen in Figure 19. It is evident that the absorbed doses relative to Tg expression would be equalised by such a compensation, but in Figure 19b it can be seen that the absorbed doses for intermediate risk patients (and the single high risk patient) increases more, and have lower variance in absorbed dose, after the compensation.

The interquartile ranges of overall absorbed doses decreased from 27-fold to 12-fold by the compensation, and from 33-fold to 16-fold for intermediate-risk tumours. Avidity compensation would increase administered activities in some patients by a substantial amount, but helps equalise the absorbed doses to tumours with poor avidity. The potential to improve treatment for patients with poor avidity has has to be weighed against increased risk of side effects from high activity radioiodine treatment, such as permanent xerostomia, bone marrow depression and risk of inducing secondary primary cancer. Further research should validate the span of iodine avidity and confirm the best markers for iodine avidity, to clarify which levels are likely to predict successful treatment. However, such compensation should not be applied below a threshold, where a low enough level of avidity would make any radioiodine treatment futile. This point of "too low avidity" is currently unknown and has to be established and clearly defined if treatment is to be withheld from patients at an initial stage.

For patients with distant metastatic disease, an avidity-guided approach may be supplanted by pre- or post-therapeutic dosimetry. Performing dosimetry adds some cost to a relatively cheap treatment, but can be valuable in patients with distant metastatic disease, as absorbed doses to metastases can guide treatment. The value of dosimetry-guided treatment in terms of improved survival of such approaches is disputed and only a few studies are published [197,198]. Regardless of survival advantages, dosimetry-guided treatment makes avoiding unnecessary treatments easier, as radioiodine refractoriness can be established early. This would reduce the risk of side effects impacting the quality of life for those patients. Further research

to resolve the question of optimal dosage in metastatic patients would fit well into an dosimetry-guided approach. The data in this thesis do not contribute to resolve the question of optimal dosage, as the data is pre-therapeutic, but the results can help in selecting which patients are likely to still have avid disease. Those patients can be routinely treated in a dosimetry-guided manner from the initial treatment onwards.

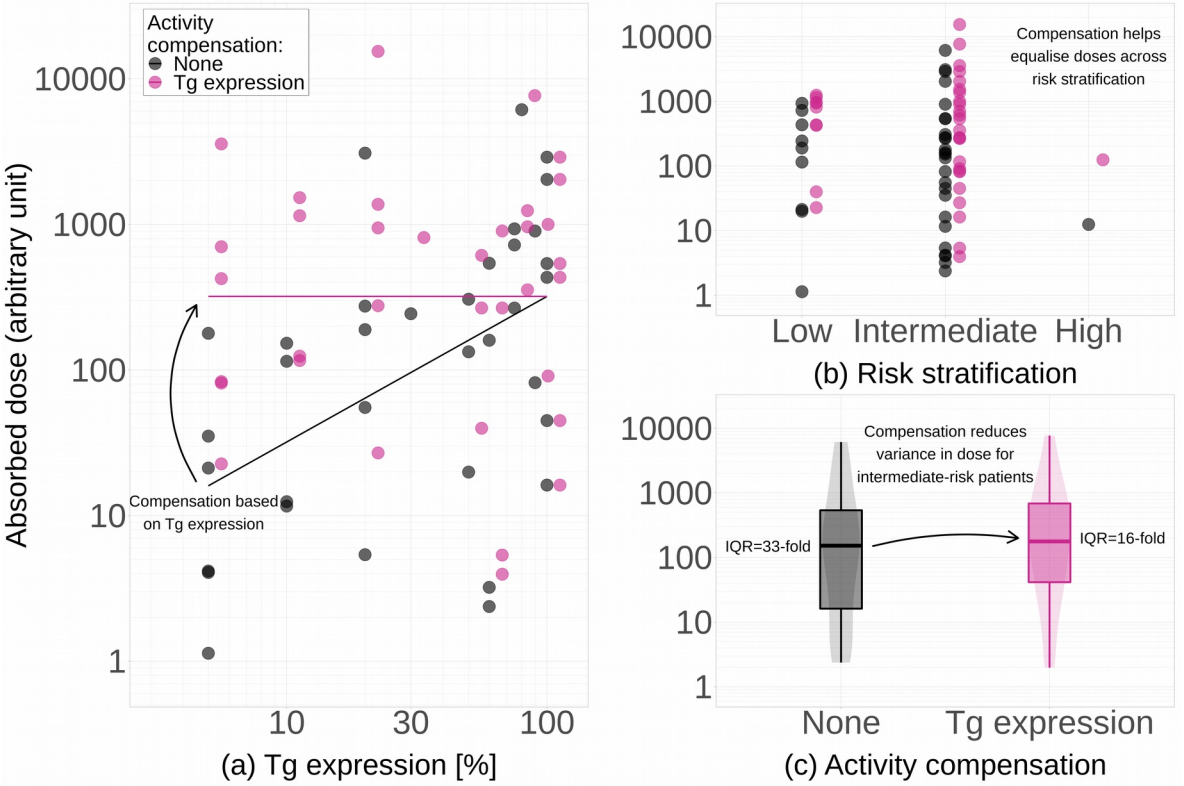

Figure 19: Illustration of how activity compensation according to (a) Tg expression would affect absorbed doses. The correction was done by multiplying the raw avidity values (grey) with the inverse of the proportion of tumour cells expressing thyroglobulin (pink). Data is shown for both primary tumour and lymph node metastasis samples, with linear fits of the data (solid lines). When comparing absorbed doses with respect to risk group (b) according to American Thyroid Association and Swedish national guidelines (same criteria), the compensation would help equalise absorbed doses across the spectrum. The interquartile range (IQR) of absorbed doses decreased from 33-fold to 16-fold in intermediate-risk tumours through this compensation, as shown in (c) with a combined box and violin plot.

Table 4. Suggested framework for radioiodine treatment of thyroid cancer that would include an avidity-guided approach. The avidity-guided approach is proposed for adjuvant treatment in patients with highest risk of aggressive and recurrent disease (shaded row). Examples of published evidence and specific needs for future research related to each approach is provided in the rightmost columns.

Risk of recurrent and persistent disease	**Risk stratification based on**	**Proposed approach**	**Evidence relevant to approach**	**Future research**
Low risk	Favourable TNM Favourable histological subtype of PTC/FTC Low Ki-67 index	Thyroid remnant ablation Low activities sufficient Activity range: 1 GBq	Efficacy of low activity ablation Mallick et al. 2012 [77] Schlumberger et al. 2012 [124] Lamartina et al. 2015 [82] Schlumberger et al. 2018 [191] Debhi et al. 2019 [120] Risk stratification Ho et al. 2020 [13]	Refined profiling of low-risk patients
High risk	Unfavourable TNM Unfavourable histological subtype of PTC/FTC; oncocytic thyroid cancer; differentiated high-grade thyroid cancer; PDTC TERT promoter mutation Recurrent lymph node metastases	Avidity-guided therapy Adapt activity to avidity markers: Lower amounts for highly avid tumours - compensate with higher activities when metastases likely have reduced avidity Activity range: 2-10 GBq	Risk stratification Rivera et al. 2008 [191] Kazaure et al. 2012 [14] Baloch et al. 2013 [16] Nath et al. 2018 [192] Avidity guidance Nilsson et al. 2021 [196] Yang et al. 2017 [194] Simões-Pereira et al. 2021 [189] Liu et al. 2020 [63]	Refined avidity markers Value of early redifferentiation in low-avidity tumours
Distant metastases	Visible metastases on SPECT, PET, CT or MRI	High-activity or dosimetry-guided therapy Target based (>40-80 Gy) or bone marrow based maximum tolerable activity (<2-3 Gy) Activity range: 5-25 GBq Other therapies if >40-80 Gy is not feasible Tyrosine kinase inhibitors EBRT	Absorbed dose targets Maxon et al. 1983 [79] Wierts et al 2016 [91] Dosimetric methods Dorn et al. 2003 [102] Sgouros et al. 2004 [94] Jentzen et al 2008 [96] Dosage regimen Deandreis et al. 2016 [198] Klubo-Gwiezdzinska et al. 2011 [197]	Value of dosimetry-guided vs. empirical activities Value of redifferentiation High initial dose vs. fractionated strategy

Another application made possible by this thesis and other detailed data on iodine avidity is patient selection for redifferentiation therapy. If patients are selected for redifferentiation treatment only if their tumours have low iodine avidity, it can potentially limit side-effects to those more likely to benefit from redifferentiation as well as reduce costs. Following the reports of small cohorts showing promising results for redifferentiation restoring radioiodine avidity, one large randomised clinical trial studied selumetinib given in addition to radioiodine therapy (NCT01843062, AstraZeneca). The trial was terminated because of presumably unfavourable primary analysis results. In this trial, any patient with high-risk disease was included, regardless of mutational or avidity status, and treatment was given as first line. A non-randomised trial in 40 patients is ongoing to explore if selective MEK and BRAF inhibitors combined with radioiodine are effective in metastatic radioiodine refractory disease, based on mutation status in *RAS* or *BRAF* (NCT03244956, Gustave Roussy), and has reported promising preliminary results with tumour control in 15/17 patients [199]. A more comprehensive review of preclinical evidence and listing of currently ongoing redifferentiation trials was published in 2021 [200].

Many aspects of redifferentiation are yet unknown and more research is warranted to evaluate in which patients it is feasible, how it should be optimally performed and to quantify the benefit patients might receive from it. There is now however convincing evidence supporting that redifferentiation increases absorbed doses per administered activity to a large proportion (40 to 80%) of radioiodine refractory patients [141–143,146–148]. From a clinical and dosimetric perspective, where it is always desirable to increase iodine uptake in the target, this body of data suggests a more substantial effect than that for, say, dietary restrictions [201]. Iodine diet restrictions are almost universally recommended for radioiodine therapy in thyroid cancer despite discordant results, albeit without any side effects except having to follow a strict diet. Furthermore, the data on dietary restriction effectiveness has been exclusively reported for success of thyroid remnant ablation and never studied in relation to tumour iodine uptake. The redifferentiation data suggests a complementary pathway that can increase iodine avidity in metastatic lesions for patients in need of better treatment options. So far, all published data comes from redifferentiation in progressive radioiodine refractory disease. A concerted research effort into this field should aim to find ways to select patients according to individual genetic profiling and pre-therapeutic knowledge of iodine avidity. Better effect may be achieved if redifferentiation is utilised before multiple radioiodine treatments

has forced clonal selection of only the cancer cells of lowest iodine avidity [195]. Considering the prominence of genetic aberrations in *BRAF* that cause up-regulation of the MAPK pathway in metastatic thyroid cancer, drugs targetting that pathway has potential to elevate iodine avidity earlier in many patients. Recent data also suggests ways to avoid resistance to redifferentiation [202]. As the field advances, an avidity-guided approach should aim to find low avidity tumours that are likely to respond to redifferentiation.

The results from Monte Carlo simulations in Paper I cannot be readily integrated in an avidity-guided approach, but rather support that avidity is the predominant factor in achieving high absorbed doses to the target. While lack of β^- particle coverage was found to diminish the absorbed dose per decay more than three-fold in very small targets, this effect was small compared to the thousand-fold differences in avidity found in Paper II, III and IV.

This thesis attempted to engage the research question of iodine avidity where radioiodine treatments originated: at the interface of nuclear physics and medicine. It has focussed on determining the activity concentrations in cancer tissue in advance of treatment, and makes inferences to the absorbed dose that would be delivered from a therapeutic administration of radioactivity. It is well known that the absorbed dose delivered is the best determinant of treatment success in radiation therapy. However, in radiotherapy in general and even more so in radionuclide therapy, it is also known that absorbed doses cannot fully explain the response and absence thereof in all patients [183]. The impact of other factors, both physical and biological, that are not encompassed by the amount of Gray delivered, remain subject to open scientific debate and dispute [203].

7 Epilogue

As it turns out, writing this thesis *was* surprisingly easy. At least, I enjoyed writing it and the text sprawled.

After some introspection I found that in "Why I Write", George Orwell describes the painful struggle of writing a book:

"One would never undertake such a thing if one were not driven on by some demon whom one can neither resist or understand. For all one knows that demon is simply the same instinct that makes a baby squall for attention."

That motivation, ever present at variable intensity, helped me tremendously in writing research articles and this thesis. Throughout, I have been confronted with many of my personal shortcomings; obstinacy, vanity, intellectual laziness, imprecise writing and a general fear of irrelevancy. These things stalled me and made me question the point of it.

But I was eventually urged forward by that demon, allowing me to delve deep into areas really out of my depth. Studying for a doctoral degree has honed my resistance against the worst motivations and shortcomings - I hope sufficiently. As Orwell continues:

"I cannot say with certainty which of my motives are the strongest, but I know which of them deserve to be followed."

While writing this text was made easy for me by whatever internal motivation, the virtues of it will now be judged by others.

As has been noted by other nuclear scientists, the fallout is the truly terrifying part.

8 Acknowledgements

I am grateful to many for aid throughout my doctoral studies:

Most essentially, to **all patients** for contributing your time, radiation burden and tissue specimen. Many of you participated selflessly in hope of advancing our common knowledge and to better alleviate the disease of your fellow patients and of coming generations. I hope my work honoured your trust.

My supervisors,

Cia Ihre Lundgren, for fiery enthusiasm and cold scrutiny. For encouragement, confidence and guidance above and beyond. For unflinchingly resisting better knowledge when adopting me as your doctoral student, which turned out to be an unlikely and indispensable match. In an alternate universe you might have also directed my hands into those of a skilled surgeon; I will instead have to content myself with acquired surgical focus, acuity and pace.

Jonathan Siikanen, for ample generosity in intellect and spirit. For knowing when to spur and when to rein in. For brilliant advice, which I often stubbornly neglected until too late. Forgive me for not fitting anything from your treasure trove of exotic nuclides into the thesis.

Christel Hedman, for clinical knowledge, sense and sensibility. For structure, diligence and emboldening comments throughout my writing. For sometimes being the singular, but crucial, cool-headed part of this constellation.

Per Grybäck, for enthusiasm, reassurance and quirky optimism. For now and then indulgently forgetting that I am not a nuclear medicine resident. Also, for the wild growth of our department in most dimensions.

My collaborators,

Christofer Juhlin, for effusive educational and scientific ambition, turning pathology reports, genetics and any odd stain into a mainstay joy throughout my doctoral studies. For forcefully demonstrating how research and clinical work can, and should, and absolutely must, be combined. You made me aim much higher.

Oscar Ardenfors, for lasting companionship, scientific rigour and for insight into the balance between pride and self-deprecation. For keeping our paper flying through several narrow passages. A sound comrade in adventures among electrons and stars.

Gabriella Bjerring, logistical mastermind, brilliant assessor of patients, surgeons and how to successfully combine the two. For untiring recruitment and assistance.

Anders Höög, for patience, encouraging praise and for detailed introduction to the fine art of surgical pathology.

Lisa Ånfalk, for skilful and instructive help with tissue specimens.

Ken Jatta and **Ravi Saini**, for an enthusiastic plunge into the mind-warping realm of molecular pathology.

Anna Malmerfelt, for nimble and educational help with immunohistochemistry.

The research group for Endocrine Surgery, for so generously adopting a stray physicist. Your reception sparked everything. I am exceptionally grateful to **Jan Zedenius** for bountiful wisdom, a jovial demeanour, prudent guidance, love of language and for convincingly pretending it was perfectly logical for me to join the group.

The research group for Medical Genetics, led by **Catharina Larsson**, for the bracing confrontation with thyroid cancer genetics. Thanks especially to fellow thyroid researchers **Martin Hysek**, **Johan Paulsson** and **Adam Stenman** for going out of your way in making me less out of place.

The staff att Molecular Medicine and Surgery, especially **Ann-Britt Wikström** and **Chatrin Lindahl**, for help with all practical and abstract matters that comes with PhD studies.

The Department of Breast, Endocrine Tumours and Sarcoma, for promoting research and high ambition. All endocrine surgeons, endocrinologists and oncologists, for clinical tutoring, extensive co-operation and for eagerly recruiting patients. Warm thanks especially to **Inga-Lena Nilsson** and **Ivan Shabo** for extraordinary encouragement and interest. **Hanna Pettersson**, for assistance with recruitment. **Robert Bränström** and **Liselotte Karlsson** for a generous welcome to a clinic replete with talent. The surgical planning team, who always shuffled operation schedules in my favour. **Per Mattsson**, for momentum at crucial starting points and for insisting I observe my first thyroidectomy.

The Department of Medical Radiation Physics and Nuclear Medicine, for providing academic freedom and fertile proving grounds. I am grateful to our nurses for assistance throughout my projects and to our radiologists for interest and clinical tutoring. **Åsa Rådemark Oldner**, for being a wise friend, a reliable lightning rod and for skilfully steering the ship.

I am further obliged to my colleagues in the nuclear medicine physics group, for during these years achieving criticality and turning into the best place I know where to do physics. **Daniel Thor**, for natural and statistical philosophy, and for your expansive rationality - always extreme and always reasonable. **Cornelia Held**, for help and criticism, laced in sarcasm and a hint of joy. **Disa Åstrand**, for still trying to save me from my own handling of radioactivity, and frequent contagious laughter. **Staffan Jacobsson Svärd**, for natural calm and for your incorruptible intellectual clarity. **Alejandro Sanchez Crespo**, for genuine and sprawling discussions about anything interesting, including these projects. **Cecilia Hindorf**, for ambitious engagement and discussions.

Mikael Skorpil, mentor, for peculiar yet inspirational lunches.

Johanna Svensson, for scrutinising my work at half-time. The gutsy cool with which you confront physics has inspired me to mimic it on medicine.

NatiOn V, led by **Daria Glaessgren**, **Svetlana Bajalica Lagercrantz**, **Ingemar Ernberg** and **Karin Lindberg**, for high quality PhD courses and fine tutoring. For a class full of inspiring clinicians and aspiring researchers. This was probably the last time I went to school. I will miss it.

Henric Rydén, for your fearless impetus, our relentless dialectic and my closest friendship. My world would be sparse without you insisting on expanding, inverting and supersampling it. **Nathalie Thomé**, for your generosity and friendly attempts to understand ourselves and the world.

Martin Bolin, for friendly companionship and perpetual intellectual stimulation. For our mutual joy and frustration that comes with knowing things.

Fredrik Johansson, for lasting friendship and for nurturing a steamrolling rationality during our childhood. For your regular calls to make sure I am not wasting your taxes on anything pointless.

Martin Olofsson, **Hanna Thorold Klingspor**, **Linn Johansson** and **Linnea Ekström** for being warm and happy friends throughout my life. Time and distance can cause even the best friendships to fade, I just wish I was less complicit in it.

Filip Weidenmo, for calling me *doktorand* prematurely, perhaps setting things in motion long before I noticed. **Niclas Magnusson**, **Marcus Rehnman**, **Anders Garberg Löfving**, **Joachim Hedberg, Rufus Björk** and **Jonas Pettersson**, for friendly adventures, fun and games.

Carina Nilsson, my mother. You never doubted, not that I was taught to ever listen if you did. Somehow, it is *all* because of you.

Marina Ahllund, my sister, disciplined companion and cordial critic. With age, I begin to fully see your true merits. In the end, even I might get it. Despite the intensity, being with you, **Jesper Ahllund** and your sons these years have been like coming up for air.

Mikael Karlsson, my father. For proving that an iron will can conquer mountains and intellectual climbs alike.

Mikael Yang, my bundle of joy, hope and ambition. For shifting gears up and down according to my pace, above all others. For dimples and dumplings whenever I needed them. 我爱你.

9 References

1. Keston, A.S.; Ball, R.P.; Frantz, V.K.; Palmer, W.W. Storage of Radioactive Iodine in Metastasis from Thyroid Carcinoma. *Science* **1942**, *95*, 362–363, doi:10.1126/science.95.2466.362.

2. Seidlin, S.M.; Marinelli, L.D.; Oshry, E. Radioactive Iodine Therapy; Effect on Functioning Metastases of Adenocarcinoma of the Thyroid. *J Am Med Assoc* **1946**, *132*, 838–847, doi:10.1001/jama.1946.02870490016004.

3. Baloch, Z.W.; Asa, S.L.; Barletta, J.A.; Ghossein, R.A.; Juhlin, C.C.; Jung, C.K.; LiVolsi, V.A.; Papotti, M.G.; Sobrinho-Simões, M.; Tallini, G.; et al. Overview of the 2022 WHO Classification of Thyroid Neoplasms. *Endocr Pathol* **2022**, *33*, 27–63, doi:10.1007/s12022-022-09707-3.

4. Lundgren, C.I.; Hall, P.; Ekbom, A.; Frisell, J.; Zedenius, J.; Dickman, P.W. Incidence and Survival of Swedish Patients with Differentiated Thyroid Cancer. *Int. J. Cancer* **2003**, *106*, 569–573, doi:10.1002/ijc.11275.

5. Mazzaferri, E.L. An Overview of the Management of Papillary and Follicular Thyroid Carcinoma. *Thyroid* **1999**, *9*, 421–427, doi:10.1089/thy.1999.9.421.

6. Lundgren, C.I.; Hall, P.; Dickman, P.W.; Zedenius, J. Clinically Significant Prognostic Factors for Differentiated Thyroid Carcinoma: A Population-Based, Nested Case-Control Study. *Cancer* **2006**, *106*, 524–531, doi:10.1002/cncr.21653.

7. Shaha, A.R.; Shah, J.P.; Loree, T.R. Risk Group Stratification and Prognostic Factors in Papillary Carcinoma of Thyroid. *Ann Surg Oncol* **1996**, *3*, 534–538, doi:10.1007/BF02306085.

8. Haugen, B.R.; Alexander, E.K.; Bible, K.C.; Doherty, G.M.; Mandel, S.J.; Nikiforov, Y.E.; Pacini, F.; Randolph, G.W.; Sawka, A.M.; Schlumberger, M.; et al. 2015 American Thyroid Association Management Guidelines for Adult Patients with Thyroid Nodules and Differentiated Thyroid Cancer: The American Thyroid Association Guidelines Task Force on Thyroid Nodules and Differentiated Thyroid Cancer. *Thyroid* **2016**, *26*, 1–133, doi:10.1089/thy.2015.0020.

9. Pacini, F.; Schlumberger, M.; Dralle, H.; Elisei, R.; Smit, J.W.A.; Wiersinga, W.; European Thyroid Cancer Taskforce European Consensus for the Management of Patients with Differentiated Thyroid Carcinoma of the Follicular Epithelium. *Eur J Endocrinol* **2006**, *154*, 787–803, doi:10.1530/eje.1.02158.

10. Jansson, S.; Bergenfelz, A.; Hennings, J.; Gimm, O. Sköldkörtelcancer, Nationellt vårdprogram Available online: https://kunskapsbanken.cancercentrum.se/diagnoser/skoldkortelcancer/ (accessed on 4 April 2022).

11. Perros, P.; Boelaert, K.; Colley, S.; Evans, C.; Evans, R.M.; Gerrard Ba, G.; Gilbert, J.; Harrison, B.; Johnson, S.J.; Giles, T.E.; et al. Guidelines for the Management of Thyroid Cancer. *Clin Endocrinol (Oxf)* **2014**, *81 Suppl 1*, 1–122, doi:10.1111/cen.12515.

12. Coca-Pelaz, A.; Shah, J.P.; Hernandez-Prera, J.C.; Ghossein, R.A.; Rodrigo, J.P.; Hartl, D.M.; Olsen, K.D.; Shaha, A.R.; Zafereo, M.; Suarez, C.; et al. Papillary Thyroid Cancer-Aggressive Variants and Impact on Management: A Narrative Review. *Adv Ther* **2020**, *37*, 3112–3128, doi:10.1007/s12325-020-01391-1.

13. Ho, A.S.; Luu, M.; Barrios, L.; Chen, I.; Melany, M.; Ali, N.; Patio, C.; Chen, Y.; Bose, S.; Fan, X.; et al. Incidence and Mortality Risk Spectrum Across Aggressive Variants of Papillary Thyroid Carcinoma. *JAMA Oncol* **2020**, *6*, 706, doi:10.1001/jamaoncol.2019.6851.

14. Kazaure, H.S.; Roman, S.A.; Sosa, J.A. Aggressive Variants of Papillary Thyroid Cancer: Incidence, Characteristics and Predictors of Survival among 43,738 Patients. *Ann Surg Oncol* **2012**, *19*, 1874–1880, doi:10.1245/s10434-011-2129-x.

15. Wenter, V.; Jellinek, A.; Unterrainer, M.; Ahmaddy, F.; Lehner, S.; Albert, N.L.; Bartenstein, P.; Knösel, T.; Spitzweg, C.; Ilhan, H.; et al. Long-Term Outcome of Rare Oncocytic Papillary (Hürthle Cell) Thyroid Carcinoma Following (Adjuvant) Initial Radioiodine Therapy. *Eur J Nucl Med Mol Imaging* **2019**, *46*, 2526–2535, doi:10.1007/s00259-019-04456-8.

16. Baloch, Z.; LiVolsi, V.A.; Tondon, R. Aggressive Variants of Follicular Cell Derived Thyroid Carcinoma; the so Called "Real Thyroid Carcinomas." *J Clin Pathol* **2013**, *66*, 733–743, doi:10.1136/jclinpath-2013-201626.

17. Liu, F.-H.; Kuo, S.-F.; Hsueh, C.; Chao, T.-C.; Lin, J.-D. Postoperative Recurrence of Papillary Thyroid Carcinoma with Lymph Node Metastasis. *J Surg Oncol* **2015**, *112*, 149–154, doi:10.1002/jso.23967.

18. Londero, S.C.; Krogdahl, A.; Bastholt, L.; Overgaard, J.; Pedersen, H.B.; Hahn, C.H.; Bentzen, J.; Schytte, S.; Christiansen, P.; Gerke, O.; et al. Papillary Thyroid Carcinoma in Denmark, 1996–2008: Outcome and Evaluation of Established Prognostic Scoring Systems in a Prospective National Cohort. *Thyroid* **2015**, *25*, 78–84, doi:10.1089/thy.2014.0294.

19. Hay, I.D.; Thompson, G.B.; Grant, C.S.; Bergstralh, E.J.; Dvorak, C.E.; Gorman, C.A.; Maurer, M.S.; McIver, B.; Mullan, B.P.; Oberg, A.L.; et al. Papillary Thyroid Carcinoma Managed at the Mayo Clinic during Six Decades (1940-1999): Temporal Trends in Initial Therapy and Long-Term Outcome in 2444 Consecutively Treated Patients. *World Journal of Surgery* **2002**, *26*, 879–885, doi:10.1007/s00268-002-6612-1.

20. Bates, M.F.; Lamas, M.R.; Randle, R.W.; Long, K.L.; Pitt, S.C.; Schneider, D.F.; Sippel, R.S. Back so Soon? Is Early Recurrence of Papillary Thyroid Cancer Really Just Persistent Disease? *Surgery* **2018**, *163*, 118–123, doi:10.1016/j.surg.2017.05.028.

21. Guo, K.; Wang, Z. Risk Factors Influencing the Recurrence of Papillary Thyroid Carcinoma: A Systematic Review and Meta-Analysis. *Int J Clin Exp Pathol* **2014**, *7*, 5393–5403.

22. Grogan, R.H.; Kaplan, S.P.; Cao, H.; Weiss, R.E.; Degroot, L.J.; Simon, C.A.; Embia, O.M.A.; Angelos, P.; Kaplan, E.L.; Schechter, R.B. A Study of Recurrence and Death from Papillary Thyroid Cancer with 27 Years of Median Follow-Up. *Surgery* **2013**, *154*, 1436–1446; discussion 1446-1447, doi:10.1016/j.surg.2013.07.008.

23. Wang, F.; Yu, X.; Shen, X.; Zhu, G.; Huang, Y.; Liu, R.; Viola, D.; Elisei, R.; Puxeddu, E.; Fugazzola, L.; et al. The Prognostic Value of Tumor Multifocality in Clinical Outcomes of Papillary Thyroid Cancer. *J Clin Endocrinol Metab* **2017**, *102*, 3241–3250, doi:10.1210/jc.2017-00277.

24. Vuong, H.G.; Duong, U.N.P.; Pham, T.Q.; Tran, H.M.; Oishi, N.; Mochizuki, K.; Nakazawa, T.; Hassell, L.; Katoh, R.; Kondo, T. Clinicopathological Risk Factors for Distant Metastasis in Differentiated Thyroid Carcinoma: A Meta-Analysis. *World J Surg* **2018**, *42*, 1005–1017, doi:10.1007/s00268-017-4206-1.

25. Mazzaferri, E.L.; Jhiang, S.M. Long-Term Impact of Initial Surgical and Medical Therapy on Papillary and Follicular Thyroid Cancer. *The American Journal of Medicine* **1994**, *97*, 418–428, doi:10.1016/0002-9343(94)90321-2.

26. Lukovic, J.; Petrovic, I.; Liu, Z.; Armstrong, S.M.; Brierley, J.D.; Tsang, R.; Pasternak, J.D.; Gomez-Hernandez, K.; Liu, A.; Asa, S.L.; et al. Oncocytic Papillary Thyroid Carcinoma and Oncocytic Poorly Differentiated Thyroid Carcinoma: Clinical Features, Uptake, and Response to Radioactive Iodine Therapy, and Outcome. *Front Endocrinol (Lausanne)* **2021**, *12*, 795184, doi:10.3389/fendo.2021.795184.

27. Wong, K.S.; Dong, F.; Telatar, M.; Lorch, J.H.; Alexander, E.K.; Marqusee, E.; Cho, N.L.; Nehs, M.A.; Doherty, G.M.; Afkhami, M.; et al. Papillary Thyroid Carcinoma with High-Grade Features Versus Poorly Differentiated Thyroid Carcinoma: An Analysis of Clinicopathologic and Molecular Features and Outcome. *Thyroid* **2021**, *31*, 933–940, doi:10.1089/thy.2020.0668.

28. Ibrahimpasic, T.; Ghossein, R.; Carlson, D.L.; Nixon, I.; Palmer, F.L.; Shaha, A.R.; Patel, S.G.; Tuttle, R.M.; Shah, J.P.; Ganly, I. Outcomes in Patients With Poorly Differentiated Thyroid Carcinoma. *The Journal of Clinical Endocrinology & Metabolism* **2014**, *99*, 1245–1252, doi:10.1210/jc.2013-3842.

29. Ibrahimpasic, T.; Ghossein, R.; Shah, J.P.; Ganly, I. Poorly Differentiated Carcinoma of the Thyroid Gland: Current Status and Future Prospects. *Thyroid* **2019**, *29*, 311–321, doi:10.1089/thy.2018.0509.

30. Kebebew, E.; Greenspan, F.S.; Clark, O.H.; Woeber, K.A.; McMillan, A. Anaplastic Thyroid Carcinoma. Treatment Outcome and Prognostic Factors. *Cancer* **2005**, *103*, 1330–1335, doi:10.1002/cncr.20936.

31. Bible, K.C.; Kebebew, E.; Brierley, J.; Brito, J.P.; Cabanillas, M.E.; Clark, T.J.; Di Cristofano, A.; Foote, R.; Giordano, T.; Kasperbauer, J.; et al. 2021 American Thyroid Association Guidelines for Management of Patients with Anaplastic Thyroid Cancer: American Thyroid Association Anaplastic Thyroid Cancer Guidelines Task Force. *Thyroid* **2021**, *31*, 337–386, doi:10.1089/thy.2020.0944.

32. Molinaro, E.; Romei, C.; Biagini, A.; Sabini, E.; Agate, L.; Mazzeo, S.; Materazzi, G.; Sellari-Franceschini, S.; Ribechini, A.; Torregrossa, L.; et al. Anaplastic Thyroid Carcinoma: From Clinicopathology to Genetics and Advanced Therapies. *Nat Rev Endocrinol* **2017**, *13*, 644–660, doi:10.1038/nrendo.2017.76.

33. Evans, C.; Tennant, S.; Perros, P. Thyroglobulin in Differentiated Thyroid Cancer. *Clinica Chimica Acta* **2015**, *444*, 310–317, doi:10.1016/j.cca.2014.10.035.

34. Patell, R.; Mikhael, A.; Tabet, M.; Bena, J.; Berber, E.; Nasr, C. Assessing the Utility of Preoperative Serum Thyroglobulin in Differentiated Thyroid Cancer: A Retrospective Cohort Study. *Endocrine* **2018**, *61*, 506–510, doi:10.1007/s12020-018-1643-z.

35. Piccardo, A.; Arecco, F.; Puntoni, M.; Foppiani, L.; Cabria, M.; Corvisieri, S.; Arlandini, A.; Altrinetti, V.; Bandelloni, R.; Orlandi, F. Focus on High-Risk DTC Patients: High Postoperative Serum Thyroglobulin Level Is a Strong Predictor of Disease Persistence and Is Associated to Progression-Free Survival and Overall Survival. *Clin Nucl Med* **2013**, *38*, 18–24, doi:10.1097/RLU.0b013e318266d4d8.

36. Pelttari, H.; Välimäki, M.J.; Löyttyniemi, E.; Schalin-Jäntti, C. Post-Ablative Serum Thyroglobulin Is an Independent Predictor of Recurrence in Low-Risk Differentiated Thyroid Carcinoma: A 16-Year Follow-up Study. *Eur J Endocrinol* **2010**, *163*, 757–763, doi:10.1530/EJE-10-0553.

37. Pacini, F.; Mariotti, S.; Formica, N.; Elisei, R.; Anelli, S.; Capotorti, E.; Pinchera, A. Thyroid Autoantibodies in Thyroid Cancer: Incidence and Relationship with Tumour Outcome. *Acta Endocrinol (Copenh)* **1988**, *119*, 373–380, doi:10.1530/acta.0.1190373.

38. Hsieh, C.-J.; Wang, P.-W. Sequential Changes of Serum Antithyroglobulin Antibody Levels Are a Good Predictor of Disease Activity in Thyroglobulin-Negative Patients with Papillary Thyroid Carcinoma. *Thyroid* **2014**, *24*, 488–493, doi:10.1089/thy.2012.0611.

39. Bueno, F.; Falcone, M.G.G.; Peñaloza, M.A.; Abelleira, E.; Pitoia, F. Dynamics of Serum Antithyroglobulin Antibodies in Patients with Differentiated Thyroid Cancer. *Endocrine* **2020**, *67*, 387–396, doi:10.1007/s12020-019-02112-7.

40. O'Connell, K.; Yen, T.W.; Quiroz, F.; Evans, D.B.; Wang, T.S. The Utility of Routine Preoperative Cervical Ultrasonography in Patients Undergoing Thyroidectomy for Differentiated Thyroid Cancer. *Surgery* **2013**, *154*, 697–701; discussion 701-703, doi:10.1016/j.surg.2013.06.040.

41. Pacini, F.; Molinaro, E.; Castagna, M.G.; Agate, L.; Elisei, R.; Ceccarelli, C.; Lippi, F.; Taddei, D.; Grasso, L.; Pinchera, A. Recombinant Human

Thyrotropin-Stimulated Serum Thyroglobulin Combined with Neck Ultrasonography Has the Highest Sensitivity in Monitoring Differentiated Thyroid Carcinoma. *J Clin Endocrinol Metab* **2003**, *88*, 3668–3673, doi:10.1210/jc.2002-021925.

42. Carmeci, C.; Jeffrey, R.B.; McDougall, I.R.; Nowels, K.W.; Weigel, R.J. Ultrasound-Guided Fine-Needle Aspiration Biopsy of Thyroid Masses. *Thyroid* **1998**, *8*, 283–289, doi:10.1089/thy.1998.8.283.

43. Fatourechi, V.; Hay, I.D.; Mullan, B.P.; Wiseman, G.A.; Eghbali-Fatourechi, G.Z.; Thorson, L.M.; Gorman, C.A. Are Posttherapy Radioiodine Scans Informative and Do They Influence Subsequent Therapy of Patients with Differentiated Thyroid Cancer? *Thyroid* **2000**, *10*, 573–577, doi:10.1089/thy.2000.10.573.

44. Kohlfuerst, S.; Igerc, I.; Lobnig, M.; Gallowitsch, H.J.; Gomez-Segovia, I.; Matschnig, S.; Mayr, J.; Mikosch, P.; Beheshti, M.; Lind, P. Posttherapeutic (131)I SPECT-CT Offers High Diagnostic Accuracy When the Findings on Conventional Planar Imaging Are Inconclusive and Allows a Tailored Patient Treatment Regimen. *Eur J Nucl Med Mol Imaging* **2009**, *36*, 886–893, doi:10.1007/s00259-008-1044-2.

45. Grewal, R.K.; Tuttle, R.M.; Fox, J.; Borkar, S.; Chou, J.F.; Gonen, M.; Strauss, H.W.; Larson, S.M.; Schöder, H. The Effect of Posttherapy 131I SPECT/CT on Risk Classification and Management of Patients with Differentiated Thyroid Cancer. *J Nucl Med* **2010**, *51*, 1361–1367, doi:10.2967/jnumed.110.075960.

46. Dotinga, M.; Vriens, D.; van Velden, F.; Heijmen, L.; Nagarajah, J.; Hicks, R.; Kapiteijn, E.; de Geus-Oei, L.-F. Managing Radioiodine Refractory Thyroid Cancer: The Role of Dosimetry and Redifferentiation on Subsequent I-131 Therapy. *Q J Nucl Med Mol Imaging* **2020**, *64*, 250–264, doi:10.23736/S1824-4785.20.03264-1.

47. Lassmann, M.; Reiners, C.; Luster, M. Dosimetry and Thyroid Cancer: The Individual Dosage of Radioiodine. *Endocrine-Related Cancer* **2010**, *17*, R161–R172, doi:10.1677/ERC-10-0071.

48. Mandel, S.J.; Shankar, L.K.; Benard, F.; Yamamoto, A.; Alavi, A. Superiority of Iodine-123 Compared with Iodine-131 Scanning for Thyroid Remnants in Patients with Differentiated Thyroid Cancer. *Clin Nucl Med* **2001**, *26*, 6–9, doi:10.1097/00003072-200101000-00002.

49. Wu, D.; Ylli, D.; Heimlich, S.L.; Burman, K.D.; Wartofsky, L.; Van Nostrand, D. 124I Positron Emission Tomography/Computed Tomography Versus Conventional Radioiodine Imaging in Differentiated Thyroid Cancer: A Review. *Thyroid* **2019**, *29*, 1523–1535, doi:10.1089/thy.2018.0598.

50. Piccardo, A.; Trimboli, P.; Foppiani, L.; Treglia, G.; Ferrarazzo, G.; Massollo, M.; Bottoni, G.; Giovanella, L. PET/CT in Thyroid Nodule and Differentiated Thyroid Cancer Patients. The Evidence-Based State of the Art. *Rev Endocr Metab Disord* **2019**, *20*, 47–64, doi:10.1007/s11154-019-09491-2.

51. Dai, G.; Levy, O.; Carrasco, N. Cloning and Characterization of the Thyroid Iodide Transporter. *Nature* **1996**, *379*, 458–460, doi:10.1038/379458a0.

52. Ravera, S.; Reyna-Neyra, A.; Ferrandino, G.; Amzel, L.M.; Carrasco, N. The Sodium/Iodide Symporter (NIS): Molecular Physiology and Preclinical and Clinical Applications. *Annu Rev Physiol* **2017**, *79*, 261–289, doi:10.1146/annurev-physiol-022516-034125.

53. Fernández, L.P.; López-Márquez, A.; Santisteban, P. Thyroid Transcription Factors in Development, Differentiation and Disease. *Nat Rev Endocrinol* **2015**, *11*, 29–42, doi:10.1038/nrendo.2014.186.

54. Cancer Genome Atlas Research Network Integrated Genomic Characterization of Papillary Thyroid Carcinoma. *Cell* **2014**, *159*, 676–690, doi:10.1016/j.cell.2014.09.050.

55. Yip, L.; Nikiforova, M.N.; Yoo, J.Y.; McCoy, K.L.; Stang, M.T.; Armstrong, M.J.; Nicholson, K.J.; Ohori, N.P.; Coyne, C.; Hodak, S.P.; et al. Tumor Genotype Determines Phenotype and Disease-Related Outcomes in Thyroid Cancer: A Study of 1510 Patients. *Ann Surg* **2015**, *262*, 519–525; discussion 524-525, doi:10.1097/SLA.0000000000001420.

56. Crispo, F.; Notarangelo, T.; Pietrafesa, M.; Lettini, G.; Storto, G.; Sgambato, A.; Maddalena, F.; Landriscina, M. BRAF Inhibitors in Thyroid Cancer: Clinical Impact, Mechanisms of Resistance and Future Perspectives. *Cancers (Basel)* **2019**, *11*, E1388, doi:10.3390/cancers11091388.

57. Mitsutake, N.; Miyagishi, M.; Mitsutake, S.; Akeno, N.; Mesa, C.; Knauf, J.A.; Zhang, L.; Taira, K.; Fagin, J.A. BRAF Mediates RET/PTC-Induced Mitogen-Activated Protein Kinase Activation in Thyroid Cells: Functional Support for Requirement of the RET/PTC-RAS-BRAF Pathway in Papillary Thyroid Carcinogenesis. *Endocrinology* **2006**, *147*, 1014–1019, doi:10.1210/en.2005-0280.

58. Sabra, M.M.; Dominguez, J.M.; Grewal, R.K.; Larson, S.M.; Ghossein, R.A.; Tuttle, R.M.; Fagin, J.A. Clinical Outcomes and Molecular Profile of Differentiated Thyroid Cancers With Radioiodine-Avid Distant Metastases. *The Journal of Clinical Endocrinology & Metabolism* **2013**, *98*, E829–E836, doi:10.1210/jc.2012-3933.

59. Yang, K.; Wang, H.; Liang, Z.; Lin, Y. BRAFV600E Mutation Associated With Non-Radioiodine-Avid Status in Distant Metastatic Papillary Thyroid Carcinoma. *Clinical Nuclear Medicine* **2014**, *39*, 5.

60. Xing, M.; Haugen, B.R.; Schlumberger, M. Progress in Molecular-Based Management of Differentiated Thyroid Cancer. *Lancet* **2013**, *381*, 1058–1069, doi:10.1016/S0140-6736(13)60109-9.

61. Henke, L.E.; Pfeifer, J.D.; Ma, C.; Perkins, S.M.; DeWees, T.; El-Mofty, S.; Moley, J.F.; Nussenbaum, B.; Haughey, B.H.; Baranski, T.J.; et al. BRAF Mutation Is Not Predictive of Long-Term Outcome in Papillary Thyroid Carcinoma. *Cancer Med* **2015**, *4*, 791–799, doi:10.1002/cam4.417.

62. McKelvey, B.A.; Umbricht, C.B.; Zeiger, M.A. Telomerase Reverse Transcriptase (TERT) Regulation in Thyroid Cancer: A Review. *Front Endocrinol (Lausanne)* **2020**, *11*, 485, doi:10.3389/fendo.2020.00485.

63. Liu, J.; Liu, R.; Shen, X.; Zhu, G.; Li, B.; Xing, M. The Genetic Duet of *BRAF* V600E and *TERT* Promoter Mutations Robustly Predicts Loss of Radioiodine Avidity in Recurrent Papillary Thyroid Cancer. *J Nucl Med* **2020**, *61*, 177–182, doi:10.2967/jnumed.119.227652.

64. Xing, M.; Liu, R.; Liu, X.; Murugan, A.K.; Zhu, G.; Zeiger, M.A.; Pai, S.; Bishop, J. *BRAF* V600E and *TERT* Promoter Mutations Cooperatively Identify the Most Aggressive Papillary Thyroid Cancer With Highest Recurrence. *JCO* **2014**, *32*, 2718–2726, doi:10.1200/JCO.2014.55.5094.

65. Paulsson, J.O.; Mu, N.; Shabo, I.; Wang, N.; Zedenius, J.; Larsson, C.; Juhlin, C.C. TERT Aberrancies: A Screening Tool for Malignancy in Follicular Thyroid Tumours. *Endocr Relat Cancer* **2018**, *25*, 723–733, doi:10.1530/ERC-18-0050.

66. Xing, M. Molecular Pathogenesis and Mechanisms of Thyroid Cancer. *Nat Rev Cancer* **2013**, *13*, 184–199, doi:10.1038/nrc3431.

67. Romei, C.; Ciampi, R.; Elisei, R. A Comprehensive Overview of the Role of the RET Proto-Oncogene in Thyroid Carcinoma. *Nat Rev Endocrinol* **2016**, *12*, 192–202, doi:10.1038/nrendo.2016.11.

68. Romei, C.; Ciampi, R.; Faviana, P.; Agate, L.; Molinaro, E.; Bottici, V.; Basolo, F.; Miccoli, P.; Pacini, F.; Pinchera, A.; et al. BRAFV600E Mutation, but Not RET/PTC Rearrangements, Is Correlated with a Lower Expression of Both Thyroperoxidase and Sodium Iodide Symporter Genes in Papillary Thyroid Cancer. *Endocr Relat Cancer* **2008**, *15*, 511–520, doi:10.1677/ERC-07-0130.

69. Ricarte-Filho, J.C.; Li, S.; Garcia-Rendueles, M.E.R.; Montero-Conde, C.; Voza, F.; Knauf, J.A.; Heguy, A.; Viale, A.; Bogdanova, T.; Thomas, G.A.; et al. Identification of Kinase Fusion Oncogenes in Post-Chernobyl Radiation-Induced Thyroid Cancers. *J Clin Invest* **2013**, *123*, 4935–4944, doi:10.1172/JCI69766.

70. Gregory Powell, J.; Wang, X.; Allard, B.L.; Sahin, M.; Wang, X.-L.; Hay, I.D.; Hiddinga, H.J.; Deshpande, S.S.; Kroll, T.G.; Grebe, S.K.; et al. The PAX8/PPARγ Fusion Oncoprotein Transforms Immortalized Human Thyrocytes through a Mechanism Probably Involving Wild-Type PPARγ Inhibition. *Oncogene* **2004**, *23*, 3634–3641, doi:10.1038/sj.onc.1207399.

71. Howell, G.M.; Hodak, S.P.; Yip, L. RAS Mutations in Thyroid Cancer. *Oncologist* **2013**, *18*, 926–932, doi:10.1634/theoncologist.2013-0072.

72. Prete, A.; Borges de Souza, P.; Censi, S.; Muzza, M.; Nucci, N.; Sponziello, M. Update on Fundamental Mechanisms of Thyroid Cancer. *Front. Endocrinol.* **2020**, *11*, 102, doi:10.3389/fendo.2020.00102.

73. Landa, I.; Ibrahimpasic, T.; Boucai, L.; Sinha, R.; Knauf, J.A.; Shah, R.H.; Dogan, S.; Ricarte-Filho, J.C.; Krishnamoorthy, G.P.; Xu, B.; et al. Genomic and Transcriptomic Hallmarks of Poorly Differentiated and Anaplastic Thyroid Cancers. *J Clin Invest* **2016**, *126*, 1052–1066, doi:10.1172/JCI85271.

74. Orosco, R.K.; Hussain, T.; Noel, J.E.; Chang, D.C.; Dosiou, C.; Mittra, E.; Divi, V.; Orloff, L.A. Radioactive Iodine in Differentiated Thyroid Cancer: A National Database Perspective. *Endocr Relat Cancer* **2019**, *26*, 795–802, doi:10.1530/ERC-19-0292.

75. Eustatia-Rutten, C.F.A.; Smit, J.W.A.; Romijn, J.A.; van der Kleij-Corssmit, E.P.M.; Pereira, A.M.; Stokkel, M.P.; Kievit, J. Diagnostic Value of Serum Thyroglobulin Measurements in the Follow-up of Differentiated Thyroid Carcinoma, a Structured Meta-Analysis. *Clin Endocrinol* **2004**, *61*, 61–74, doi:10.1111/j.1365-2265.2004.02060.x.

76. Carhill, A.A.; Litofsky, D.R.; Ross, D.S.; Jonklaas, J.; Cooper, D.S.; Brierley, J.D.; Ladenson, P.W.; Ain, K.B.; Fein, H.G.; Haugen, B.R.; et al. Long-Term Outcomes Following Therapy in Differentiated Thyroid Carcinoma: NTCTCS Registry Analysis 1987–2012. *The Journal of Clinical Endocrinology & Metabolism* **2015**, *100*, 3270–3279, doi:10.1210/JC.2015-1346.

77. Mallick, U.; Harmer, C.; Yap, B.; Wadsley, J.; Clarke, S.; Moss, L.; Nicol, A.; Clark, P.M.; Farnell, K.; McCready, R.; et al. Ablation with Low-Dose Radioiodine and Thyrotropin Alfa in Thyroid Cancer. *N Engl J Med* **2012**, *366*, 1674–1685, doi:10.1056/NEJMoa1109589.

78. Flux, G.D.; Haq, M.; Chittenden, S.J.; Buckley, S.; Hindorf, C.; Newbold, K.; Harmer, C.L. A Dose-Effect Correlation for Radioiodine Ablation in Differentiated Thyroid Cancer. *Eur J Nucl Med Mol Imaging* **2010**, *37*, 270–275, doi:10.1007/s00259-009-1261-3.

79. Maxon, H.R.; Thomas, S.R.; Hertzberg, V.S.; Kereiakes, J.G.; Chen, I.W.; Sperling, M.I.; Saenger, E.L. Relation between Effective Radiation Dose and Outcome of Radioiodine Therapy for Thyroid Cancer. *N. Engl. J. Med.* **1983**, *309*, 937–941, doi:10.1056/NEJM198310203091601.

80. Yap, B.K.; Homer, J.; Parrott, N.; Loughran, S.; Murby, B.; Swindell, R.; Gandhi, A. Use of Pre-Ablation Radioiodine-131 Scan to Assess the Impact of Surgical Volume and Specialisation Following Thyroidectomy for Differentiated Thyroid Carcinoma. *Eur Thyroid J* **2013**, *2*, 275–281, doi:10.1159/000355911.

81. Oltmann, S.C.; Schneider, D.F.; Leverson, G.; Sivashanmugam, T.; Chen, H.; Sippel, R.S. Radioactive Iodine Remnant Uptake After Completion Thyroidectomy: Not Such a Complete Cancer Operation. *Ann Surg Oncol* **2014**, *21*, 1379–1383, doi:10.1245/s10434-013-3450-3.

82. Lamartina, L.; Durante, C.; Filetti, S.; Cooper, D.S. Low-Risk Differentiated Thyroid Cancer and Radioiodine Remnant Ablation: A Systematic Review of the

Literature. *The Journal of Clinical Endocrinology & Metabolism* **2015**, *100*, 1748–1761, doi:10.1210/jc.2014-3882.

83. Chow, S.-M.; Yau, S.; Kwan, C.-K.; Poon, P.C.M.; Law, S.C.K. Local and Regional Control in Patients with Papillary Thyroid Carcinoma: Specific Indications of External Radiotherapy and Radioactive Iodine According to T and N Categories in AJCC 6th Edition. *Endocr Relat Cancer* **2006**, *13*, 1159–1172, doi:10.1677/erc.1.01320.

84. Ruel, E.; Thomas, S.; Dinan, M.; Perkins, J.M.; Roman, S.A.; Sosa, J.A. Adjuvant Radioactive Iodine Therapy Is Associated with Improved Survival for Patients with Intermediate-Risk Papillary Thyroid Cancer. *J. Clin. Endocrinol. Metab.* **2015**, *100*, 1529–1536, doi:10.1210/jc.2014-4332.

85. Verburg, F.A.; Flux, G.; Giovanella, L.; van Nostrand, D.; Muylle, K.; Luster, M. Differentiated Thyroid Cancer Patients Potentially Benefitting from Postoperative I-131 Therapy: A Review of the Literature of the Past Decade. *Eur J Nucl Med Mol Imaging* **2020**, *47*, 78–83, doi:10.1007/s00259-019-04479-1.

86. Jonklaas, J.; Sarlis, N.J.; Litofsky, D.; Ain, K.B.; Bigos, S.T.; Brierley, J.D.; Cooper, D.S.; Haugen, B.R.; Ladenson, P.W.; Magner, J.; et al. Outcomes of Patients with Differentiated Thyroid Carcinoma Following Initial Therapy. *Thyroid* **2006**, *16*, 1229–1242, doi:10.1089/thy.2006.16.1229.

87. Podnos, Y.D.; Smith, D.D.; Wagman, L.D.; Ellenhorn, J.D.I. Survival in Patients with Papillary Thyroid Cancer Is Not Affected by the Use of Radioactive Isotope. *J. Surg. Oncol.* **2007**, *96*, 3–7, doi:10.1002/jso.20656.

88. Durante, C.; Haddy, N.; Baudin, E.; Leboulleux, S.; Hartl, D.; Travagli, J.P.; Caillou, B.; Ricard, M.; Lumbroso, J.D.; De Vathaire, F.; et al. Long-Term Outcome of 444 Patients with Distant Metastases from Papillary and Follicular Thyroid Carcinoma: Benefits and Limits of Radioiodine Therapy. *The Journal of Clinical Endocrinology & Metabolism* **2006**, *91*, 2892–2899, doi:10.1210/jc.2005-2838.

89. Schlumberger, M.; Challeton, C.; De Vathaire, F.; Travagli, J.P.; Gardet, P.; Lumbroso, J.D.; Francese, C.; Fontaine, F.; Ricard, M.; Parmentier, C. Radioactive Iodine Treatment and External Radiotherapy for Lung and Bone Metastases from Thyroid Carcinoma. *J. Nucl. Med.* **1996**, *37*, 598–605.

90. Qiu, Z.-L.; Shen, C.-T.; Sun, Z.-K.; Song, H.-J.; Zhang, G.-Q.; Luo, Q.-Y. Lung Metastases From Papillary Thyroid Cancer With Persistently Negative Thyroglobulin and Elevated Thyroglobulin Antibody Levels During Radioactive Iodine Treatment and Follow-Up: Long-Term Outcomes and Prognostic Indicators. *Front Endocrinol (Lausanne)* **2019**, *10*, 903, doi:10.3389/fendo.2019.00903.

91. Wierts, R.; Brans, B.; Havekes, B.; Kemerink, G.J.; Halders, S.G.; Schaper, N.N.; Backes, W.H.; Mottaghy, F.M.; Jentzen, W. Dose-Response Relationship in Differentiated Thyroid Cancer Patients Undergoing Radioiodine Treatment

Assessed by Means of 124I PET/CT. *J Nucl Med* **2016**, *57*, 1027–1032, doi:10.2967/jnumed.115.168799.

92. Flux, G.; Leek, F.; Gape, P.; Gear, J.; Taprogge, J. Iodine-131 and Iodine-131-Meta-Iodobenzylguanidine Dosimetry in Cancer Therapy. *Seminars in Nuclear Medicine* **2022**, *52*, 167–177, doi:10.1053/j.semnuclmed.2021.11.002.

93. Wierts, R.; Jentzen, W.; Quick, H.H.; Wisselink, H.J.; Pooters, I.N.A.; Wildberger, J.E.; Herrmann, K.; Kemerink, G.J.; Backes, W.H.; Mottaghy, F.M. Quantitative Performance Evaluation of ^{124} I PET/MRI Lesion Dosimetry in Differentiated Thyroid Cancer. *Phys. Med. Biol.* **2017**, *63*, 015014, doi:10.1088/1361-6560/aa990b.

94. Sgouros, G.; Kolbert, K.S.; Sheikh, A.; Pentlow, K.S.; Mun, E.F.; Barth, A.; Robbins, R.J.; Larson, S.M. Patient-Specific Dosimetry for 131I Thyroid Cancer Therapy Using 124I PET and 3-Dimensional-Internal Dosimetry (3D-ID) Software. *J. Nucl. Med.* **2004**, *45*, 1366–1372.

95. Gregory, R.A.; Murray, I.; Gear, J.; Leek, F.; Chittenden, S.; Fenwick, A.; Wevrett, J.; Scuffham, J.; Tipping, J.; Murby, B.; et al. Standardised Quantitative Radioiodine SPECT/CT Imaging for Multicentre Dosimetry Trials in Molecular Radiotherapy. *Phys Med Biol* **2019**, *64*, 245013, doi:10.1088/1361-6560/ab5b6c.

96. Jentzen, W.; Freudenberg, L.; Eising, E.G.; Sonnenschein, W.; Knust, J.; Bockisch, A. Optimized 124I PET Dosimetry Protocol for Radioiodine Therapy of Differentiated Thyroid Cancer. *Journal of Nuclear Medicine* **2008**, *49*, 1017–1023, doi:10.2967/jnumed.107.047159.

97. Eckerman, K.; Endo, A. ICRP Publication 107. Nuclear Decay Data for Dosimetric Calculations. *Ann ICRP* **2008**, *38*, 7–96, doi:10.1016/j.icrp.2008.10.004.

98. Ferris, T.; Carroll, L.; Jenner, S.; Aboagye, E.O. Use of Radioiodine in Nuclear Medicine-A Brief Overview. *J Labelled Comp Radiopharm* **2021**, *64*, 92–108, doi:10.1002/jlcr.3891.

99. International Atomic Energy Agency Cumulative Fission Yields Available online: https://www-nds.iaea.org/sgnucdat/c3.htm (accessed on 28 June 2022).

100. Benua, R.S.; Cicale, N.R.; Sonenberg, M.; Rawson, R.W. The Relation of Radioiodine Dosimetry to Results and Complications in the Treatment of Metastatic Thyroid Cancer. *Am J Roentgenol Radium Ther Nucl Med* **1962**, *87*, 171–182.

101. Tuttle, R.M.; Leboeuf, R.; Robbins, R.J.; Qualey, R.; Pentlow, K.; Larson, S.M.; Chan, C.Y. Empiric Radioactive Iodine Dosing Regimens Frequently Exceed Maximum Tolerated Activity Levels in Elderly Patients with Thyroid Cancer. *J Nucl Med* **2006**, *47*, 1587–1591.

102. Dorn, R.; Kopp, J.; Vogt, H.; Heidenreich, P.; Carroll, R.G.; Gulec, S.A. Dosimetry-Guided Radioactive Iodine Treatment in Patients with Metastatic

Differentiated Thyroid Cancer: Largest Safe Dose Using a Risk-Adapted Approach. *J. Nucl. Med.* **2003**, *44*, 451–456.

103. Clement, S.C.; Peeters, R.P.; Ronckers, C.M.; Links, T.P.; van den Heuvel-Eibrink, M.M.; Nieveen van Dijkum, E.J.M.; van Rijn, R.R.; van der Pal, H.J.H.; Neggers, S.J.; Kremer, L.C.M.; et al. Intermediate and Long-Term Adverse Effects of Radioiodine Therapy for Differentiated Thyroid Carcinoma – A Systematic Review. *Cancer Treatment Reviews* **2015**, *41*, 925–934, doi:10.1016/j.ctrv.2015.09.001.

104. Vini, L. Prognosis for Fertility and Ovarian Function after Treatment with Radioiodine for Thyroid Cancer. *Postgraduate Medical Journal* **2002**, *78*, 92–93, doi:10.1136/pmj.78.916.92.

105. Hieu, T.T.; Russell, A.W.; Cuneo, R.; Clark, J.; Kron, T.; Hall, P.; Doi, S.A.R. Cancer Risk after Medical Exposure to Radioactive Iodine in Benign Thyroid Diseases: A Meta-Analysis. *Endocr. Relat. Cancer* **2012**, *19*, 645–655, doi:10.1530/ERC-12-0176.

106. Dickman, P.W.; Holm, L.-E.; Lundell, G.; Boice, J.D.; Hall, P. Thyroid Cancer Risk after Thyroid Examination with 131I: A Population-Based Cohort Study in Sweden. *Int. J. Cancer* **2003**, *106*, 580–587, doi:10.1002/ijc.11258.

107. Hakala, T.T.; Sand, J.A.; Jukkola, A.; Huhtala, H.S.; Metso, S.; Kellokumpu-Lehtinen, P.-L. Increased Risk of Certain Second Primary Malignancies in Patients Treated for Well-Differentiated Thyroid Cancer. *Int J Clin Oncol* **2016**, *21*, 231–239, doi:10.1007/s10147-015-0904-6.

108. Lamartina, L.; Handkiewicz-Junak, D. Follow-up of Low Risk Thyroid Cancer Patients: Can We Stop Follow-up after 5 Years of Complete Remission? *European Journal of Endocrinology* **2020**, *182*, D1–D16, doi:10.1530/EJE-19-0960.

109. Subramanian, S.; Goldstein, D.P.; Parlea, L.; Thabane, L.; Ezzat, S.; Ibrahim-Zada, I.; Straus, S.; Brierley, J.D.; Tsang, R.W.; Gafni, A.; et al. Second Primary Malignancy Risk in Thyroid Cancer Survivors: A Systematic Review and Meta-Analysis. *Thyroid* **2007**, *17*, 1277–1288, doi:10.1089/thy.2007.0171.

110. Weiss, W. Chernobyl Thyroid Cancer: 30 Years of Follow-up Overview. *Radiat Prot Dosimetry* **2018**, *182*, 58–61, doi:10.1093/rpd/ncy147.

111. Rabinowitch, I.M.; Frith, A.B. IODINE STUDIES. *J. Clin. Invest.* **1925**, *1*, 473–481, doi:10.1172/JCI100025.

112. Dohán, O.; De la Vieja, A.; Paroder, V.; Riedel, C.; Artani, M.; Reed, M.; Ginter, C.S.; Carrasco, N. The Sodium/Iodide Symporter (NIS): Characterization, Regulation, and Medical Significance. *Endocr Rev* **2003**, *24*, 48–77, doi:10.1210/er.2001-0029.

113. Wapnir, I.L.; van de Rijn, M.; Nowels, K.; Amenta, P.S.; Walton, K.; Montgomery, K.; Greco, R.S.; Dohán, O.; Carrasco, N. Immunohistochemical Profile of the Sodium/Iodide Symporter in Thyroid, Breast, and Other

Carcinomas Using High Density Tissue Microarrays and Conventional Sections. *The Journal of Clinical Endocrinology & Metabolism* **2003**, *88*, 1880–1888, doi:10.1210/jc.2002-021544.

114. Goldman, J.M.; Line, B.R.; Aamodt, R.L.; Robbins, J. Influence of Triiodothyronine Withdrawal Time on 131I Uptake Postthyroidectomy for Thyroid Cancer. *J. Clin. Endocrinol. Metab.* **1980**, *50*, 734–739, doi:10.1210/jcem-50-4-734.

115. Ladenson, P.W.; Braverman, L.E.; Mazzaferri, E.L.; Brucker-Davis, F.; Cooper, D.S.; Garber, J.R.; Wondisford, F.E.; Davies, T.F.; DeGroot, L.J.; Daniels, G.H.; et al. Comparison of Administration of Recombinant Human Thyrotropin with Withdrawal of Thyroid Hormone for Radioactive Iodine Scanning in Patients with Thyroid Carcinoma. *N Engl J Med* **1997**, *337*, 888–896, doi:10.1056/NEJM199709253371304.

116. Hänscheid, H.; Lassmann, M.; Luster, M.; Thomas, S.R.; Pacini, F.; Ceccarelli, C.; Ladenson, P.W.; Wahl, R.L.; Schlumberger, M.; Ricard, M.; et al. Iodine Biokinetics and Dosimetry in Radioiodine Therapy of Thyroid Cancer: Procedures and Results of a Prospective International Controlled Study of Ablation after RhTSH or Hormone Withdrawal. *J. Nucl. Med.* **2006**, *47*, 648–654.

117. Coura-Filho, G.B.; Willegaignon, J.; Buchpiguel, C.A.; Sapienza, M.T. Effects of Thyroid Hormone Withdrawal and Recombinant Human Thyrotropin on Glomerular Filtration Rate During Radioiodine Therapy for Well-Differentiated Thyroid Cancer. *Thyroid* **2015**, *25*, 1291–1296, doi:10.1089/thy.2015.0173.

118. Pötzi, C.; Moameni, A.; Karanikas, G.; Preitfellner, J.; Becherer, A.; Pirich, C.; Dudczak, R. Comparison of Iodine Uptake in Tumour and Nontumour Tissue under Thyroid Hormone Deprivation and with Recombinant Human Thyrotropin in Thyroid Cancer Patients. *Clin Endocrinol* **2006**, *65*, 519–523, doi:10.1111/j.1365-2265.2006.02626.x.

119. Simões-Pereira, J.; C. Ferreira, T.; Limbert, E.; Cavaco, B.M.; Leite, V. Outcomes of Thyrotropin Alfa Versus Levothyroxine Withdrawal-Aided Radioiodine Therapy for Distant Metastasis of Papillary Thyroid Cancer. *Thyroid* **2021**, thy.2021.0013, doi:10.1089/thy.2021.0013.

120. Dehbi, H.-M.; Mallick, U.; Wadsley, J.; Newbold, K.; Harmer, C.; Hackshaw, A. Recurrence after Low-Dose Radioiodine Ablation and Recombinant Human Thyroid-Stimulating Hormone for Differentiated Thyroid Cancer (HiLo): Long-Term Results of an Open-Label, Non-Inferiority Randomised Controlled Trial. *The Lancet Diabetes & Endocrinology* **2019**, *7*, 44–51, doi:10.1016/S2213-8587(18)30306-1.

121. Handkiewicz-Junak, D.; Gawlik, T.; Rozkosz, J.; Puch, Z.; Michalik, B.; Gubala, E.; Krajewska, J.; Kluczewska, A.; Jarzab, B. Recombinant Human Thyrotropin Preparation for Adjuvant Radioiodine Treatment in Children and Adolescents with Differentiated Thyroid Cancer. *European Journal of Endocrinology* **2015**, *173*, 873–881, doi:10.1530/EJE-15-0562.

122. Ma, C.; Xie, J.; Liu, W.; Wang, G.; Zuo, S.; Wang, X.; Wu, F. Recombinant Human Thyrotropin (RhTSH) Aided Radioiodine Treatment for Residual or Metastatic Differentiated Thyroid Cancer. *Cochrane Database of Systematic Reviews* **2010**, doi:10.1002/14651858.CD008302.pub2.

123. Molinaro, E.; Giani, C.; Agate, L.; Biagini, A.; Pieruzzi, L.; Bianchi, F.; Brozzi, F.; Ceccarelli, C.; Viola, D.; Piaggi, P.; et al. Patients With Differentiated Thyroid Cancer Who Underwent Radioiodine Thyroid Remnant Ablation With Low-Activity 131I After Either Recombinant Human TSH or Thyroid Hormone Therapy Withdrawal Showed the Same Outcome After a 10-Year Follow-Up. *The Journal of Clinical Endocrinology & Metabolism* **2013**, *98*, 2693–2700, doi:10.1210/jc.2012-4137.

124. Schlumberger, M.; Catargi, B.; Borget, I.; Deandreis, D.; Zerdoud, S.; Bridji, B.; Bardet, S.; Leenhardt, L.; Bastie, D.; Schvartz, C.; et al. Strategies of Radioiodine Ablation in Patients with Low-Risk Thyroid Cancer. *N. Engl. J. Med.* **2012**, *366*, 1663–1673, doi:10.1056/NEJMoa1108586.

125. Wolff, J.; Chaikoff, I.L. Plasma Inorganic Iodide as a Homeostatic Regulator of Thyroid Function. *J. Biol. Chem.* **1948**, *174*, 555–564.

126. Sawka, A.M.; Ibrahim-Zada, I.; Galacgac, P.; Tsang, R.W.; Brierley, J.D.; Ezzat, S.; Goldstein, D.P. Dietary Iodine Restriction in Preparation for Radioactive Iodine Treatment or Scanning in Well-Differentiated Thyroid Cancer: A Systematic Review. *Thyroid* **2010**, *20*, 1129–1138, doi:10.1089/thy.2010.0055.

127. Pluijmen, M.J.H.M.; Eustatia-Rutten, C.; Goslings, B.M.; Stokkel, M.P.; Arias, A.M.P.; Diamant, M.; Romijn, J.A.; Smit, J.W.A. Effects of Low-Iodide Diet on Postsurgical Radioiodide Ablation Therapy in Patients with Differentiated Thyroid Carcinoma. *Clin. Endocrinol. (Oxf)* **2003**, *58*, 428–435, doi:10.1046/j.1365-2265.2003.01735.x.

128. Sohn, S.Y.; Choi, J.Y.; Jang, H.W.; Kim, H.J.; Jin, S.M.; Kim, S.W.; Suh, S.; Hur, K.Y.; Kim, J.H.; Chung, J.H.; et al. Association between Excessive Urinary Iodine Excretion and Failure of Radioactive Iodine Thyroid Ablation in Patients with Papillary Thyroid Cancer. *Thyroid* **2013**, *23*, 741–747, doi:10.1089/thy.2012.0136.

129. Padovani, R.P.; Kasamatsu, T.S.; Nakabashi, C.C.D.; Camacho, C.P.; Andreoni, D.M.; Malouf, E.Z.; Marone, M.M.S.; Maciel, R.M.B.; Biscolla, R.P.M. One Month Is Sufficient for Urinary Iodine to Return to Its Baseline Value After the Use of Water-Soluble Iodinated Contrast Agents in Post-Thyroidectomy Patients Requiring Radioiodine Therapy. *Thyroid* **2012**, *22*, 926–930, doi:10.1089/thy.2012.0099.

130. Sohn, S.Y.; Choi, J.H.; Kim, N.K.; Joung, J.Y.; Cho, Y.Y.; Park, S.M.; Kim, T.H.; Jin, S.M.; Bae, J.C.; Lee, S.Y.; et al. The Impact of Iodinated Contrast Agent Administered during Preoperative Computed Tomography Scan on Body Iodine Pool in Patients with Differentiated Thyroid Cancer Preparing for Radioactive Iodine Treatment. *Thyroid* **2014**, *24*, 872–877, doi:10.1089/thy.2013.0238.

131. Lee, S.Y.; Chang, D.L.F.; He, X.; Pearce, E.N.; Braverman, L.E.; Leung, A.M. Urinary Iodine Excretion and Serum Thyroid Function in Adults after Iodinated Contrast Administration. *Thyroid* **2015**, *25*, 471–477, doi:10.1089/thy.2015.0024.

132. Vassaux, G.; Zwarthoed, C.; Signetti, L.; Guglielmi, J.; Compin, C.; Guigonis, J.-M.; Juhel, T.; Humbert, O.; Benisvy, D.; Pourcher, T.; et al. Iodinated Contrast Agents Perturb Iodide Uptake by the Thyroid Independently of Free Iodide. *J Nucl Med* **2018**, *59*, 121–126, doi:10.2967/jnumed.117.195685.

133. Hichri, M.; Vassaux, G.; Guigonis, J.-M.; Juhel, T.; Graslin, F.; Guglielmi, J.; Pourcher, T.; Cambien, B. Proteomic Analysis of Iodinated Contrast Agent-Induced Perturbation of Thyroid Iodide Uptake. *J Clin Med* **2020**, *9*, doi:10.3390/jcm9020329.

134. McDougall, I.R.; Iagaru, A. Thyroid Stunning: Fact or Fiction? *Seminars in Nuclear Medicine* **2011**, *41*, 105–112, doi:10.1053/j.semnuclmed.2010.10.004.

135. Verburg, F.A.; Verkooijen, R.B.T.; Stokkel, M.P.M.; van Isselt, J.W. The Success of 131I Ablation in Thyroid Cancer Patients Is Significantly Reduced after a Diagnostic Activity of 40 MBq 131I. *Nuklearmedizin* **2009**, *48*, 138–142, doi:10.3413/nukmed-0225.

136. Lundh, C.; Lindencrona, U.; Postgard, P.; Carlsson, T.; Nilsson, M.; Forssell-Aronsson, E. Radiation-Induced Thyroid Stunning: Differential Effects of 123I, 131I, 99mTc, and 211At on Iodide Transport and NIS MRNA Expression in Cultured Thyroid Cells. *Journal of Nuclear Medicine* **2009**, *50*, 1161–1167, doi:10.2967/jnumed.108.061150.

137. Hilditch, T.E.; Dempsey, M.F.; Bolster, A.A.; McMenemin, R.M.; Reed, N.S. Self-Stunning in Thyroid Ablation: Evidence from Comparative Studies of Diagnostic 131I and 123I. *Eur J Nucl Med* **2002**, *29*, 783–788, doi:10.1007/s00259-002-0785-6.

138. Fugazzola, L.; Elisei, R.; Fuhrer, D.; Jarzab, B.; Leboulleux, S.; Newbold, K.; Smit, J. 2019 European Thyroid Association Guidelines for the Treatment and Follow-Up of Advanced Radioiodine-Refractory Thyroid Cancer. *Eur Thyroid J* **2019**, *8*, 227–245, doi:10.1159/000502229.

139. Brose, M.S.; Nutting, C.M.; Jarzab, B.; Elisei, R.; Siena, S.; Bastholt, L.; de la Fouchardiere, C.; Pacini, F.; Paschke, R.; Shong, Y.K.; et al. Sorafenib in Radioactive Iodine-Refractory, Locally Advanced or Metastatic Differentiated Thyroid Cancer: A Randomised, Double-Blind, Phase 3 Trial. *The Lancet* **2014**, *384*, 319–328, doi:10.1016/S0140-6736(14)60421-9.

140. Schlumberger, M.; Tahara, M.; Wirth, L.J.; Robinson, B.; Brose, M.S.; Elisei, R.; Habra, M.A.; Newbold, K.; Shah, M.H.; Hoff, A.O.; et al. Lenvatinib versus Placebo in Radioiodine-Refractory Thyroid Cancer. *N Engl J Med* **2015**, *372*, 621–630, doi:10.1056/NEJMoa1406470.

141. Ho, A.L.; Grewal, R.K.; Leboeuf, R.; Sherman, E.J.; Pfister, D.G.; Deandreis, D.; Pentlow, K.S.; Zanzonico, P.B.; Haque, S.; Gavane, S.; et al. Selumetinib-

Enhanced Radioiodine Uptake in Advanced Thyroid Cancer. *N Engl J Med* **2013**, *368*, 623–632, doi:10.1056/NEJMoa1209288.

142. Rothenberg, S.M.; McFadden, D.G.; Palmer, E.L.; Daniels, G.H.; Wirth, L.J. Redifferentiation of Iodine-Refractory *BRAF* V600E-Mutant Metastatic Papillary Thyroid Cancer with Dabrafenib. *Clin Cancer Res* **2015**, *21*, 1028–1035, doi:10.1158/1078-0432.CCR-14-2915.

143. Groussin, L.; Clerc, J.; Huillard, O. Larotrectinib-Enhanced Radioactive Iodine Uptake in Advanced Thyroid Cancer. *N Engl J Med* **2020**, *383*, 1686–1687, doi:10.1056/NEJMc2023094.

144. Groussin, L.; Theodon, H.; Bessiene, L.; Bricaire, L.; Bonnet-Serrano, F.; Cochand-Priollet, B.; Leroy, K.; Garinet, S.; Pasmant, E.; Zerbit, J.; et al. Redifferentiating Effect of Larotrectinib in NTRK-Rearranged Advanced Radioactive-Iodine Refractory Thyroid Cancer. *Thyroid* **2022**, doi:10.1089/thy.2021.0524.

145. Chu, Y.-H.; Dias-Santagata, D.; Farahani, A.A.; Boyraz, B.; Faquin, W.C.; Nosé, V.; Sadow, P.M. Clinicopathologic and Molecular Characterization of NTRK-Rearranged Thyroid Carcinoma (NRTC). *Mod Pathol* **2020**, *33*, 2186–2197, doi:10.1038/s41379-020-0574-4.

146. Iravani, A.; Solomon, B.; Pattison, D.A.; Jackson, P.; Ravi Kumar, A.; Kong, G.; Hofman, M.S.; Akhurst, T.; Hicks, R.J. Mitogen-Activated Protein Kinase Pathway Inhibition for Redifferentiation of Radioiodine Refractory Differentiated Thyroid Cancer: An Evolving Protocol. *Thyroid* **2019**, *29*, 1634–1645, doi:10.1089/thy.2019.0143.

147. Buffet, C.; Wassermann, J.; Hecht, F.; Leenhardt, L.; Dupuy, C.; Groussin, L.; Lussey-Lepoutre, C. Redifferentiation of Radioiodine-Refractory Thyroid Cancers. *Endocrine-Related Cancer* **2020**, *27*, R113–R132, doi:10.1530/ERC-19-0491.

148. Dunn, L.A.; Sherman, E.J.; Baxi, S.S.; Tchekmedyian, V.; Grewal, R.K.; Larson, S.M.; Pentlow, K.S.; Haque, S.; Tuttle, R.M.; Sabra, M.M.; et al. Vemurafenib Redifferentiation of *BRAF* Mutant, RAI-Refractory Thyroid Cancers. *The Journal of Clinical Endocrinology & Metabolism* **2019**, *104*, 1417–1428, doi:10.1210/jc.2018-01478.

149. Postgård, P.; Himmelman, J.; Lindencrona, U.; Bhogal, N.; Wiberg, D.; Berg, G.; Jansson, S.; Nyström, E.; Forssell-Aronsson, E.; Nilsson, M. Stunning of Iodide Transport by (131)I Irradiation in Cultured Thyroid Epithelial Cells. *J Nucl Med* **2002**, *43*, 828–834.

150. Yap, B.K.; Murby, B. No Adverse Affect in Clinical Outcome Using Low Preablation Diagnostic 131I Activity in Differentiated Thyroid Cancer: Refuting Thyroid-Stunning Effect. *The Journal of Clinical Endocrinology & Metabolism* **2014**, *99*, 2433–2440, doi:10.1210/jc.2014-1405.

151. Knoll, G.F. *Radiation Detection and Measurement*; Wiley, 2010; ISBN 978-0-470-13148-0.

152. Blue, P.W.; Brownt, P.H.; Manier, S.M.; Ghaed, N. Calculation of Minimal Detectable Activity for Scintillation Detection Systems. *Journal of Nuclear Medicine Technology* **1987**, *15*, 4.

153. Kogai, T.; Brent, G.A. The Sodium Iodide Symporter (NIS): Regulation and Approaches to Targeting for Cancer Therapeutics. *Pharmacology & Therapeutics* **2012**, *135*, 355–370, doi:10.1016/j.pharmthera.2012.06.007.

154. Riedel, C.; Levy, O.; Carrasco, N. Post-Transcriptional Regulation of the Sodium/Iodide Symporter by Thyrotropin. *J Biol Chem* **2001**, *276*, 21458–21463, doi:10.1074/jbc.M100561200.

155. Kleiman, D.A.; Buitrago, D.; Crowley, M.J.; Beninato, T.; Veach, A.J.; Zanzonico, P.B.; Jin, M.; Fahey, T.J.; Zarnegar, R. Thyroid Stimulating Hormone Increases Iodine Uptake by Thyroid Cancer Cells during BRAF Silencing. *J Surg Res* **2013**, *182*, 85–93, doi:10.1016/j.jss.2012.08.053.

156. Rowe, C.W.; Paul, J.W.; Gedye, C.; Tolosa, J.M.; Bendinelli, C.; McGrath, S.; Smith, R. Targeting the TSH Receptor in Thyroid Cancer. *Endocr Relat Cancer* **2017**, *24*, R191–R202, doi:10.1530/ERC-17-0010.

157. Edmonds, C.J.; Hayes, S.; Kermode, J.C.; Thompson, B.D. Measurement of Serum TSH and Thyroid Hormones in the Management of Treatment of Thyroid Carcinoma with Radioiodine. *Br J Radiol* **1977**, *50*, 799–807, doi:10.1259/0007-1285-50-599-799.

158. Hänscheid, H.; Lapa, C.; Buck, A.K.; Lassmann, M.; Werner, R.A. Dose Mapping After Endoradiotherapy with 177Lu-DOTATATE/DOTATOC by a Single Measurement After 4 Days. *J Nucl Med* **2018**, *59*, 75–81, doi:10.2967/jnumed.117.193706.

159. Madsen, M.T.; Menda, Y.; O'Dorisio, T.M.; O'Dorisio, M.S. Technical Note: Single Time Point Dose Estimate for Exponential Clearance. *Med Phys* **2018**, *45*, 2318–2324, doi:10.1002/mp.12886.

160. Bacher, R.; Hohberg, M.; Dietlein, M.; Wild, M.; Kobe, C.; Drzezga, A.; Schmidt, M. Thyroid Uptake and Effective Half-Life of Radioiodine in Thyroid Cancer Patients at Radioiodine Therapy and Follow-Up Whole-Body Scintigraphy Either in Hypothyroidism or Under RhTSH. *J Nucl Med* **2019**, *60*, 631–637, doi:10.2967/jnumed.118.217638.

161. Pacini, F.; Ladenson, P.W.; Schlumberger, M.; Driedger, A.; Luster, M.; Kloos, R.T.; Sherman, S.; Haugen, B.; Corone, C.; Molinaro, E.; et al. Radioiodine Ablation of Thyroid Remnants after Preparation with Recombinant Human Thyrotropin in Differentiated Thyroid Carcinoma: Results of an International, Randomized, Controlled Study. *The Journal of Clinical Endocrinology & Metabolism* **2006**, *91*, 926–932, doi:10.1210/jc.2005-1651.

162. Luster, M.; Sherman, S.I.; Skarulis, M.C.; Reynolds, J.R.; Lassmann, M.; Hänscheid, H.; Reiners, C. Comparison of Radioiodine Biokinetics Following the Administration of Recombinant Human Thyroid Stimulating Hormone and after Thyroid Hormone Withdrawal in Thyroid Carcinoma. *European Journal of Nuclear Medicine and Molecular Imaging* **2003**, *30*, 1371–1377, doi:10.1007/s00259-003-1230-1.

163. Mínguez, P.; Flux, G.; Genollá, J.; Delgado, A.; Rodeño, E.; Sjögreen Gleisner, K. Whole-Remnant and Maximum-Voxel SPECT/CT Dosimetry in 131I-NaI Treatments of Differentiated Thyroid Cancer. *Med Phys* **2016**, *43*, 5279, doi:10.1118/1.4961742.

164. Lassmann, M.; Luster, M.; Hänscheid, H.; Reiners, C. Impact of 131I Diagnostic Activities on the Biokinetics of Thyroid Remnants. *J Nucl Med* **2004**, *45*, 619–625.

165. Samuel, A.M.; Rajashekharrao, B. Radioiodine Therapy for Well-Differentiated Thyroid Cancer: A Quantitative Dosimetric Evaluation for Remnant Thyroid Ablation after Surgery. *J. Nucl. Med.* **1994**, *35*, 1944–1950.

166. Bal, C.S.; Kumar, A.; Pant, G.S. Radioiodine Dose for Remnant Ablation in Differentiated Thyroid Carcinoma: A Randomized Clinical Trial in 509 Patients. *J Clin Endocrinol Metab* **2004**, *89*, 1666–1673, doi:10.1210/jc.2003-031152.

167. Hong, C.M.; Kim, C.-Y.; Son, S.H.; Jung, J.; Lee, C.-H.; Jeong, J.H.; Jeong, S.Y.; Lee, S.-W.; Lee, J.; Ahn, B.-C. I-131 Biokinetics of Remnant Normal Thyroid Tissue and Residual Thyroid Cancer in Patients with Differentiated Thyroid Cancer: Comparison between Recombinant Human TSH Administration and Thyroid Hormone Withdrawal. *Ann Nucl Med* **2017**, *31*, 582–589, doi:10.1007/s12149-017-1188-x.

168. Koral, K.F.; Adler, R.S.; Carey, J.E.; Beierwaltes, W.H. Iodine-131 Treatment of Thyroid Cancer: Absorbed Dose Calculated from Post-Therapy Scans. *J Nucl Med* **1986**, *27*, 1207–1211.

169. Ruhlmann, M.; Sonnenschein, W.; Nagarajah, J.; Binse, I.; Herrmann, K.; Jentzen, W. Pretherapeutic 124I Dosimetry Reliably Predicts Intratherapeutic Blood Kinetics of 131I in Patients with Differentiated Thyroid Carcinoma Receiving High Therapeutic Activities. *Nucl Med Commun* **2018**, *39*, 457–464, doi:10.1097/MNM.0000000000000817.

170. Rogers, D.W.O. Fifty Years of Monte Carlo Simulations for Medical Physics. *Phys. Med. Biol.* **2006**, *51*, R287–R301, doi:10.1088/0031-9155/51/13/R17.

171. Metropolis, N. The Beginning of the Monte Carlo Method. *Los Alamos Science* **1987**, *15*, 131–137.

172. Limpert, E.; Stahel, W.A.; Abbt, M. Log-Normal Distributions across the Sciences: Keys and Clues. *BioScience* **2001**, *51*, 341, doi:10.1641/0006-3568(2001)051[0341:LNDATS]2.0.CO;2.

173. The 2007 Recommendations of the International Commission on Radiological Protection. ICRP Publication 103. *Ann ICRP* **2007**, *37*, 1–332, doi:10.1016/j.icrp.2007.10.003.

174. Julious, S.A.; Debarnot, C.A. Why Are Pharmacokinetic Data Summarized by Arithmetic Means? *J Biopharm Stat* **2000**, *10*, 55–71, doi:10.1081/BIP-100101013.

175. Directive, C. 59/Euratom of 5 December 2013 Laying down Basic Safety Standards for Protection against the Dangers Arising from Exposure to Ionising Radiation, and Repealing Directives 89/618/Euratom, 90/641/Euratom, 96/29/Euratom, 97/43/Euratom and 2003/122/Euratom 2013.

176. Konijnenberg, M.; Herrmann, K.; Kobe, C.; Verburg, F.; Hindorf, C.; Hustinx, R.; Lassmann, M. EANM Position Paper on Article 56 of the Council Directive 2013/59/Euratom (Basic Safety Standards) for Nuclear Medicine Therapy. *Eur J Nucl Med Mol Imaging* **2021**, *48*, 67–72, doi:10.1007/s00259-020-05038-9.

177. Sjögreen Gleisner, K.; Spezi, E.; Solny, P.; Gabina, P.M.; Cicone, F.; Stokke, C.; Chiesa, C.; Paphiti, M.; Brans, B.; Sandström, M.; et al. Variations in the Practice of Molecular Radiotherapy and Implementation of Dosimetry: Results from a European Survey. *EJNMMI Phys* **2017**, *4*, 28, doi:10.1186/s40658-017-0193-4.

178. McGowan, D.R.; Guy, M.J. Time to Demand Dosimetry for Molecular Radiotherapy? *BJR* **2015**, *88*, 20140720, doi:10.1259/bjr.20140720.

179. Flux, G.D.; Sjogreen Gleisner, K.; Chiesa, C.; Lassmann, M.; Chouin, N.; Gear, J.; Bardiès, M.; Walrand, S.; Bacher, K.; Eberlein, U.; et al. From Fixed Activities to Personalized Treatments in Radionuclide Therapy: Lost in Translation? *Eur J Nucl Med Mol Imaging* **2018**, *45*, 152–154, doi:10.1007/s00259-017-3859-1.

180. Chiesa, C.; Sjogreen Gleisner, K.; Flux, G.; Gear, J.; Walrand, S.; Bacher, K.; Eberlein, U.; Visser, E.P.; Chouin, N.; Ljungberg, M.; et al. The Conflict between Treatment Optimization and Registration of Radiopharmaceuticals with Fixed Activity Posology in Oncological Nuclear Medicine Therapy. *Eur J Nucl Med Mol Imaging* **2017**, *44*, 1783–1786, doi:10.1007/s00259-017-3707-3.

181. Sgouros, G.; Dewaraja, Y.K.; Escorcia, F.; Graves, S.A.; Hope, T.A.; Iravani, A.; Pandit-Taskar, N.; Saboury, B.; James, S.S.; Zanzonico, P.B. Tumor Response to Radiopharmaceutical Therapies: The Knowns and the Unknowns. *J Nucl Med* **2021**, *62*, 12S-22S, doi:10.2967/jnumed.121.262750.

182. Lawhn-Heath, C.; Hope, T.A.; Martinez, J.; Fung, E.K.; Shin, J.; Seo, Y.; Flavell, R.R. Dosimetry in Radionuclide Therapy: The Clinical Role of Measuring Radiation Dose. *Lancet Oncol* **2022**, *23*, e75–e87, doi:10.1016/S1470-2045(21)00657-4.

183. Strigari, L.; Konijnenberg, M.; Chiesa, C.; Bardies, M.; Du, Y.; Gleisner, K.S.; Lassmann, M.; Flux, G. The Evidence Base for the Use of Internal Dosimetry in the Clinical Practice of Molecular Radiotherapy. *Eur J Nucl Med Mol Imaging* **2014**, *41*, 1976–1988, doi:10.1007/s00259-014-2824-5.

184. Pittman, J.A.; Dailey, G.E.; Beschi, R.J. Changing Normal Values for Thyroidal Radioiodine Uptake. *N Engl J Med* **1969**, *280*, 1431–1434, doi:10.1056/NEJM196906262802602.

185. Paulsson, J.O.; Backman, S.; Wang, N.; Stenman, A.; Crona, J.; Thutkawkorapin, J.; Ghaderi, M.; Tham, E.; Stålberg, P.; Zedenius, J.; et al. Whole-genome Sequencing of Synchronous Thyroid Carcinomas Identifies Aberrant DNA Repair in Thyroid Cancer Dedifferentiation. *J. Pathol.* **2020**, *250*, 183–194, doi:10.1002/path.5359.

186. Van Nostrand, D. Radioiodine Refractory Differentiated Thyroid Cancer: Time to Update the Classifications. *Thyroid* **2018**, *28*, 1083–1093, doi:10.1089/thy.2018.0048.

187. Tuttle, R.M.; Ahuja, S.; Avram, A.M.; Bernet, V.J.; Bourguet, P.; Daniels, G.H.; Dillehay, G.; Draganescu, C.; Flux, G.; Führer, D.; et al. Controversies, Consensus, and Collaboration in the Use of ^{131}I Therapy in Differentiated Thyroid Cancer: A Joint Statement from the American Thyroid Association, the European Association of Nuclear Medicine, the Society of Nuclear Medicine and Molecular Imaging, and the European Thyroid Association. *Thyroid* **2019**, *29*, 461–470, doi:10.1089/thy.2018.0597.

188. Finocchiaro, D.; Gear, J.I.; Fioroni, F.; Flux, G.D.; Murray, I.; Castellani, G.; Versari, A.; Iori, M.; Grassi, E. Uncertainty Analysis of Tumour Absorbed Dose Calculations in Molecular Radiotherapy. *EJNMMI Phys* **2020**, *7*, 63, doi:10.1186/s40658-020-00328-5.

189. Simões-Pereira, J.; Mourinho, N.; Ferreira, T.C.; Limbert, E.; Cavaco, B.M.; Leite, V. Avidity and Outcomes of Radioiodine Therapy for Distant Metastasis of Distinct Types of Differentiated Thyroid Cancer. *J Clin Endocrinol Metab* **2021**, *106*, e3911–e3922, doi:10.1210/clinem/dgab436.

190. Dwamena, S.; Patel, N.; Egan, R.; Stechman, M.; Scott-Coombes, D. Impact of the Change from the Seventh to Eighth Edition of the AJCC TNM Classification of Malignant Tumours and Comparison with the MACIS Prognostic Scoring System in Non-Medullary Thyroid Cancer. *BJS Open* **2019**, *3*, 623–628, doi:10.1002/bjs5.50182.

191. Schlumberger, M.; Leboulleux, S.; Catargi, B.; Deandreis, D.; Zerdoud, S.; Bardet, S.; Rusu, D.; Godbert, Y.; Buffet, C.; Schvartz, C.; et al. Outcome after Ablation in Patients with Low-Risk Thyroid Cancer (ESTIMABL1): 5-Year Follow-up Results of a Randomised, Phase 3, Equivalence Trial. *Lancet Diabetes Endocrinol* **2018**, *6*, 618–626, doi:10.1016/S2213-8587(18)30113-X.

192. Rivera, M.; Ghossein, R.A.; Schoder, H.; Gomez, D.; Larson, S.M.; Tuttle, R.M. Histopathologic Characterization of Radioactive Iodine-refractory Fluorodeoxyglucose-positron Emission Tomography-positive Thyroid Carcinoma. *Cancer* **2008**, *113*, 48–56, doi:10.1002/cncr.23515.

193. Nath, M.C.; Erickson, L.A. Aggressive Variants of Papillary Thyroid Carcinoma: Hobnail, Tall Cell, Columnar, and Solid. *Adv Anat Pathol* **2018**, *25*, 8.

194. Yang, X.; Li, J.; Li, X.; Liang, Z.; Gao, W.; Liang, J.; Cheng, S.; Lin, Y. TERT Promoter Mutation Predicts Radioiodine-Refractory Character in Distant Metastatic Differentiated Thyroid Cancer. *J Nucl Med* **2017**, *58*, 258–265, doi:10.2967/jnumed.116.180240.

195. Kumar, P.; Bal, C.; Damle, N.A.; Ballal, S.; Dwivedi, S.N.; Agarwala, S. Lesion-Wise Comparison of Pre-Therapy and Post-Therapy Effective Half-Life of Iodine-131 in Pediatric and Young Adult Patients with Differentiated Thyroid Cancer Undergoing Radioiodine Therapy. *Nucl Med Mol Imaging* **2019**, *53*, 199–207, doi:10.1007/s13139-019-00592-z.

196. Nilsson, J.N.; Siikanen, J.; Hedman, C.; Juhlin, C.C.; Ihre Lundgren, C. Pre-Therapeutic Measurements of Iodine Avidity in Papillary and Poorly Differentiated Thyroid Cancer Reveal Associations with Thyroglobulin Expression, Histological Variants and Ki-67 Index. *Cancers (Basel)* **2021**, *13*, 3627, doi:10.3390/cancers13143627.

197. Klubo-Gwiezdzinska, J.; Van Nostrand, D.; Atkins, F.; Burman, K.; Jonklaas, J.; Mete, M.; Wartofsky, L. Efficacy of Dosimetric *Versus* Empiric Prescribed Activity of ^{131}I for Therapy of Differentiated Thyroid Cancer. *The Journal of Clinical Endocrinology & Metabolism* **2011**, *96*, 3217–3225, doi:10.1210/jc.2011-0494.

198. Deandreis, D.; Rubino, C.; Tala, H.; Leboulleux, S.; Terroir, M.; Baudin, E.; Larson, S.; Fagin, J.A.; Schlumberger, M.; Tuttle, R.M. Comparison of Empiric Versus Whole-Body/-Blood Clearance Dosimetry–Based Approach to Radioactive Iodine Treatment in Patients with Metastases from Differentiated Thyroid Cancer. *J Nucl Med* **2017**, *58*, 717–722, doi:10.2967/jnumed.116.179606.

199. Leboulleux, S.; Cao, C.D.; Zerdoud, S.; Attard, M.; Bournaud, C.; Benisvy, D.; Taieb, D.; Bardet, S.; Terroir-Cassou-Mounat, M.; Betrian, S.; et al. MERAIODE: A Redifferentiation Phase II Trial With Trametinib and Dabrafenib Followed by Radioactive Iodine Administration for Metastatic Radioactive Iodine Refractory Differentiated Thyroid Cancer Patients With a BRAFV600E Mutation (NCT 03244956). *Journal of the Endocrine Society* **2021**, *5*, A876–A876, doi:10.1210/jendso/bvab048.1789.

200. Oh, J.M.; Ahn, B.-C. Molecular Mechanisms of Radioactive Iodine Refractoriness in Differentiated Thyroid Cancer: Impaired Sodium Iodide Symporter (NIS) Expression Owing to Altered Signaling Pathway Activity and Intracellular Localization of NIS. *Theranostics* **2021**, *11*, 6251–6277, doi:10.7150/thno.57689.

201. Li, J.H.; He, Z.H.; Bansal, V.; Hennessey, J.V. Low Iodine Diet in Differentiated Thyroid Cancer: A Review. *Clin Endocrinol (Oxf)* **2016**, *84*, 3–12, doi:10.1111/cen.12846.

202. Tchekmedyian, V.; Dunn, L.; Sherman, E.; Baxi, S.S.; Grewal, R.K.; Larson, S.M.; Pentlow, K.S.; Haque, S.; Tuttle, R.M.; Sabra, M.M.; et al. Enhancing Radioiodine Incorporation in BRAF-Mutant, Radioiodine-Refractory Thyroid Cancers with Vemurafenib and the Anti-ErbB3 Monoclonal Antibody CDX-3379: Results of a Pilot Clinical Trial. *Thyroid* **2022**, *32*, 273–282, doi:10.1089/thy.2021.0565.

203. Verburg, F.A.; Nonnekens, J.; Konijnenberg, M.W.; de Jong, M. To Go Where No One Has Gone before: The Necessity of Radiobiology Studies for Exploration beyond the Limits of the "Holy Gray" in Radionuclide Therapy. *Eur J Nucl Med Mol Imaging* **2021**, *48*, 2680–2682, doi:10.1007/s00259-020-05147-5.